ABSTRACT

Human Kinematic Responses to Walking and Riding Camels and Horses

“Benny” Buqing Ni, M.S.B.M.E.

Mentor: Brian A. Garner, Ph.D.

Hippotherapy is a novel and promising therapeutic method. The prevailing rationale for hippotherapy is that the motion of a horse can provide movement patterns that mimic those of walking. The purpose of this study is to measure and compare human pelvic kinematics during natural walking, horse riding, and camel riding. Motion capture of three human subjects walking, riding on three horses, and riding on two camels was recorded. Pelvic trajectories exhibit many similar features between walking, horse-riding, and camel-riding, including distorted infinity-shape patterns in the transverse and frontal planes. In the sagittal plane, pelvic trajectories display an oval pattern during walking and camel-riding and a more diagonal pattern during horse riding. This study shows that many features of human pelvic kinematics during walking can be reproduced when riding on a horse or camel. To date, this is the first and only study that compared pelvic movement during camel-riding to walking.

Human Kinematic Responses to Walking and to Riding Camels and Horses

by

"Benny" Buqing Ni, M.S.B.M.E.

A Thesis

Approved by the Department of Mechanical Engineering

Paul I. Ro, Ph.D., Chairperson

Submitted to the Graduate Faculty of
Baylor University in Partial Fulfillment of the
Requirements for the Degree
of

Master of Science in Biomedical Engineering

Approved by the Thesis Committee

Brian A. Garner, Ph.D., Chairperson

Jonathan H. Rylander, Ph.D.

Beth A. Lanning, Ph.D.

Accepted by the Graduate School

May 2020

J. Larry Lyon, Ph.D., Dean

*Page bearing signatures is kept on file in the Graduate School.*

TABLE OF CONTENTS

LIST OF FIGURES

LIST OF TABLES

# ACKNOWLEDGMENTS

I would like to thank Dr. Brian Garner and Dr. Jonathan Rylander for all their guidance during the past two years. I am very grateful for the opportunity they gave me to work on this thesis project and all the advice they provided along the way. I would like to thank Dr. Beth Lanning for joining my thesis committee and providing valuable insights about horses and hippotherapy. A special thank you to Mr. Doug Baum, Ms. Malin Larsson, and Ms. Mie Meiner for their interest in therapeutic camel riding and initiating the camel riding study. Thank you to Heart of Texas Therapeutic Riding Center that provided the facility for the horse and camel riding studies.

Thank you to my friends and family who helped and encouraged me. I would like to thank my parents for their love and support. A special thank you to my church family, Brad, Beth, Jerry, and Glenda for their continuous encouragement and fostering my spiritual growth. I would like to thank the wonderful professors I had at Baylor University – Dr. Baker, Dr. Johns, Dr. Jonklaas, Dr. Kearney, and others for not only teaching me knowledge but also helping me to become a better person. Thank you to my fellow graduate students, Bradley, Forrest, and Amanda, for helping me with research and coursework. Finally, I would like to thank all my friends, David, Evan, Hannah, Jeff, Sarah, Griffin, and many others for always being there for me. A special thank you to David for being my roommate and putting up with me for the past five years.

# DEDICATION

To all my family, mentors, and friends,
Thank you for your unending support, guidance, and encouragement.
Words cannot express how grateful I am for all of you.

# LIST OF ABBREVIATIONS

ASIS: Anterior Superior Iliac Spine

CAI: Camel Assisted Interventions

HPOT: Hippotherapy

LASI: Left Anterior Superior Iliac Spine Marker

LPSI: Left Posterior Superior Iliac Spine Marker

PSIS: Posterior Superior Iliac Spine

RASI: Right Anterior Superior Iliac Spine Marker

RPSI: Right Posterior Superior Iliac Spine Marker

SD: Standard Deviation

# CHAPTER ONE

## Introduction

Walking is the basic form of human locomotion. It is the most natural and economical way of movement at short distances. However, a number of musculoskeletal and neurological conditions, including cerebral palsy, stroke, and spinal cord injuries, can impair walking. For those impaired, there are multiple therapeutic methods to help individuals improve walking function. One of the more interesting methods is called hippotherapy (HPOT), which involves time riding on a horse. Recently, camels have also been suggested for therapeutic uses. Aiming to better understand how hippotherapy and camel assisted interventions (CAI) may be beneficial, the focus of this thesis is to characterize the movement patterns of the human pelvis during walking gait and trials of riding on horses and on camels, with a view toward gaining insights relevant to therapeutic benefits. Before discussing how riding may benefit patients, a thorough understanding of pelvic anatomy and the biomechanics of walking is warranted.

### *Human Pelvis*

The human pelvis plays a central role in many critical biological processes, including bipedal locomotion (walking), thermoregulation, and parturition (childbirth) [1]. The human pelvis includes the pelvic girdle and the coccyx. The pelvic girdle is made up of the right and left hipbones (*ossa coxae*) that join each other anteriorly and the sacrum posteriorly. Each hipbone consists of the ischium, the ilium, and the pubis, as shown in Figure 1.1. The superior portion of the ilium is called the iliac crest. The

anterior end of the crest is the anterior superior iliac spine (ASIS), and the posterior end is the posterior superior iliac spine (PSIS). Portions of the ilium, ischium, and pubis form the acetabulum, where the articulation between the pelvis and the femur occurs [2].

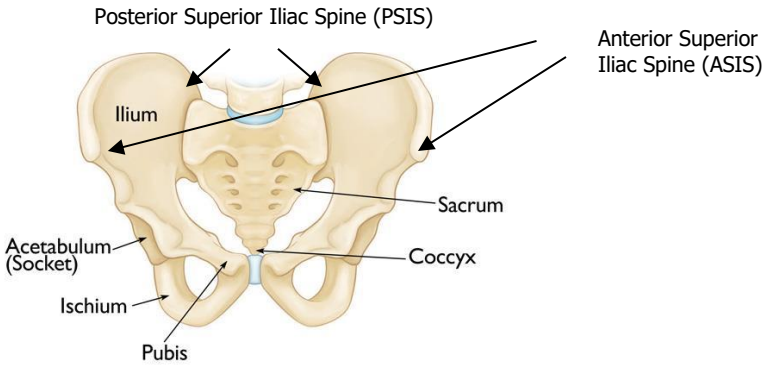


Figure 1.1: Skeleton diagram of human pelvis [3]

Several hip muscles originate on the hip bone and insert onto the femur. The anterior hip muscles, the iliacus and the psoas major, flex the hip (Figure 1.2). The gluteus maximus functions to extend the hip. The deep hip muscles, including the gluteus medius, gluteus minimus, and tensor fasciae latae medially rotate the hip [4]. During walking, the gluteus medius and minimus tilt the pelvis and maintain the trunk in an upright posture, as the foot of the opposite limb is raised from the ground. The improper function of these two muscles leads to pelvis sagging downward on the unsupported side (Trendelenburg gait) [5].

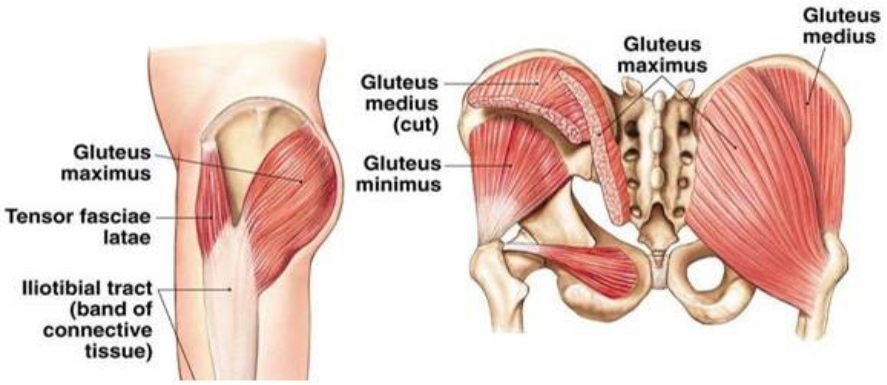


Figure 1.2: A diagram of key pelvic muscles [6]

There are sex-specific differences in the overall structure of the human pelvis. The female pelvis tends to be wider and broader with less prominent ischial spines. The male pelvis typically has a narrower sub-pubic arch and a longer, more curved sacrum. The differences in the pelvis allow for a wider pelvic aperture in females which functions as the birth canal [7,8]. As a result of a wider female pelvis, kinematic differences in pelvic motion between males and females have been observed [9].

*Pelvic Motions*

Motions of the pelvis may be described as rotations about one of the three cardinal axes (XYZ). Pelvis tilt (Figure 1.3A) occurs when the pelvis rotates about a mediolateral axis (Z-axis) that produces motion within the sagittal plane. With anterior pelvic tilt (negative pelvic tilt angle), the ASIS each move anteriorly and inferiorly while the PSIS each move anteriorly and superiorly. Posterior pelvic tilt occurs when the ASIS move posteriorly and superiorly while the PSIS move posteriorly and inferiorly [7].

Pelvic list (Figure 1.3B) refers to the motion that occurs about the anterior-posterior axis (X-axis) in the frontal plane when one side of the pelvis moves inferiorly as the other side moves superiorly. This motion is controlled by the stance hip abductor

muscles, including the gluteus medius and gluteus minimus [10]. When the pelvis is supported by only one weight-bearing lower extremity, the hip abductors activate on the contralateral side of the pelvis to keep the pelvis level [11]. Pelvic drop refers the lowering of one side of the pelvis, while pelvic hike refers to the raising of one side of the pelvis [7].

Pelvic twist (or rotation) (Figure 1.3C) is the pelvic motion about a vertical axis (Y-axis) in the transverse plane. When standing on one side of lower extremities, forward rotation is when the contralateral side is moving forward or anteriorly. Backward rotation is when the contralateral side is moving backward or posteriorly [7].

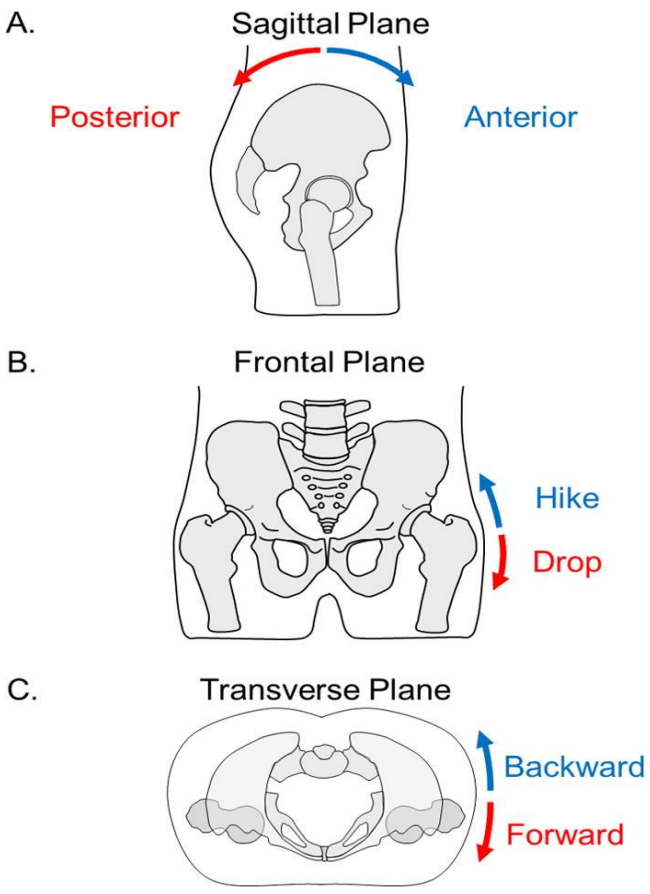


Figure 1.3: Illustration of pelvic tilt (A), list (B) and twist(C) [7]

*Human Walking*

Walking is one of the principal movements of the human body. It is a procedure completed by sequential steps. A step is defined as the pendulum movement of one leg around the pelvis, which is made between the time that foot leaves the contacted surface and touches again [12].

*The Gait Cycle*

The gait cycle can be broken down into two phases, the stance phase and the swing phase. The phases alternate for each lower limb (Figure 1.4). The stance phase consists of the entire time that a foot is on the ground, while the swing phase consists of the entire time the foot is in the air [13].

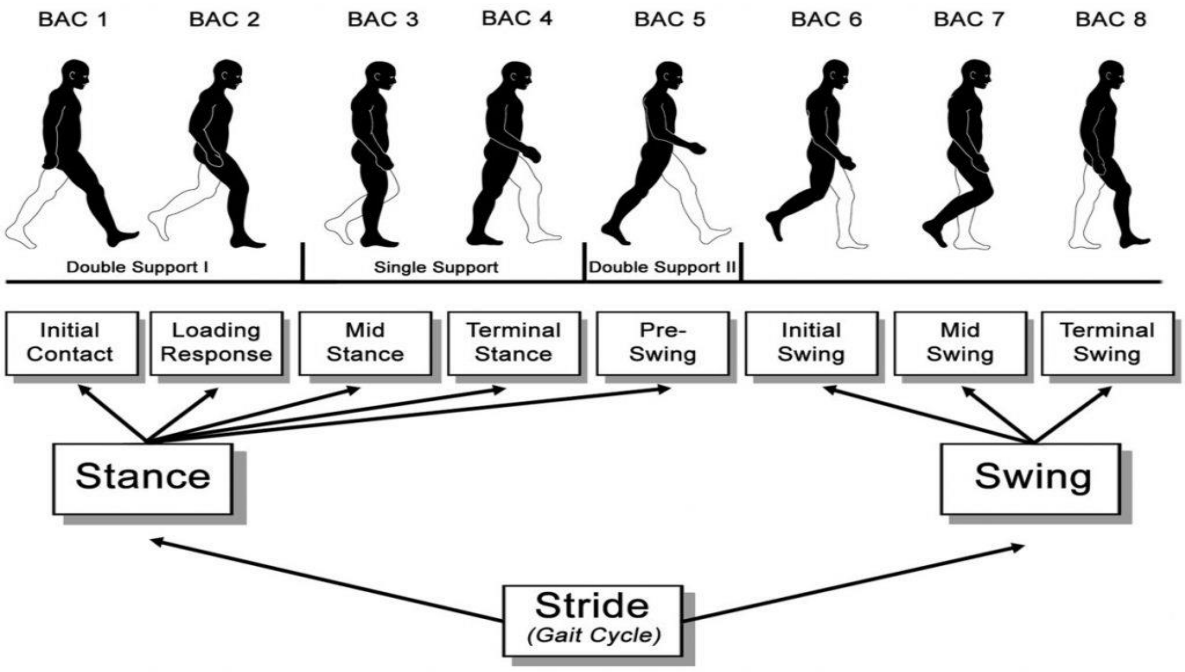


Figure 1.4: Diagram of a complete human gait cycle [14]

*Stance phase.* The stance phase of the human gait can be further broken down into four sub-phases: initial contact, loading response, mid-stance, and terminal stance. Initial contact consists of the first 3% of the gait cycle, during which the heel strikes the ground and initiates the rotation over the heel to foot flat on the ground. Loading response goes from 3-12% of the gait cycle. The knee flexes slightly to absorb shock as the foot falls flat on the ground, stabilizing the body in advance of single-limb support. The midstance takes place during 12-31% of the gait cycle. In this subphase, the shank rotates forward over the supporting foot. Finally, during the terminal stance which lasts from 31-50% of the gait cycle, the heel raises off the ground as one rolls onto the ball of the foot [13].

*Swing phase.* The swing phase is also divided into four subphases, including pre-swing, initial swing, mid-swing, and terminal swing. Pre-swing goes from 50-62% of the gait cycle. This subphase is the transition phase between stance and swing, in which the body is supported by both limbs while one foot is pushed and lifted off the ground. The initial swing takes place during 62-75% of the gait cycle. The hip, knee, and ankle are flexed to begin the advancement of limb forward and create clearance of the foot over the ground. Mid-swing goes from 75-87% of the gait cycle, during which limb advancement continues and the thigh reaches its peak advancement. Terminal swing is the final phase lasting from 87-100% of the gait cycle. The foot is positioned for initial foot contact to start the next gait cycle [13].

*Pelvic Parameters during Walking*

The pelvis moves in three planes to produce smooth and efficient motion during normal walking gait. The pelvic motion has been well studied and documented in previous literature [7,15,16]. Lewis et al. collected pelvic motion data on 44 healthy individuals (22 males and 22 females) while walking on an instrumented force treadmill [7]. Each subject was tested walking at both self-selected (~1.27 m/s) and prescribed speeds (1.25 m/s) [7]. They observed that, in the sagittal plane, the pelvis maintained an anterior pelvic tilt throughout gait and completed two full cycles of a sinusoidal wave for each gait cycle [7]. The mean total excursion of pelvic tilt was 4.3 degrees with a SD of 1.1 degrees and a range of 2.6 to 7.3 degrees at the preferred walking speed [7]. In the frontal plane, the pelvis completed one cycle of motion throughout each gait cycle [7]. The mean total excursion of the pelvic list was 7.4 degrees with a SD of 2.5 degrees and a range of 1.9 to 12.5 degrees at the preferred walking speed [7]. In the transverse plane, the pelvis completed one cycle of motion as well. The mean total excursion of pelvic twist was 9.5 degrees with a SD of 2.9 degrees and a range of 4.0 to 16.8 degrees at the preferred walking speed [7]. While gait motion was measured and studied by many others [15,16], the study by Lewis et al. was a recent walking study with a strong emphasis on pelvic motion [7]. Their results will serve as the reference data for this thesis study.

*Motor Impairment and Therapies*

Normal walking gait requires musculoskeletal and neurological systems to provide strength, sensation, and coordination in an integrated function [17]. As a result, a wide range of musculoskeletal or neurological conditions can negatively impact the normal gait and impair a person's ability to walk properly [18-21]. Gait impairment is a large contributor to long-term disability and ambulatory function in daily living [21]. In the youth population, Cerebral palsy and Autism spectrum disorder are two of the main conditions that alter a child's gait [18,19]. For the elderly population, Cerebrovascular accidents (stroke) and Parkinson are common causes of difficulty with walking [17].

A number of physical therapies aim to help patients improve walking function [21-23]. Bodyweight supported treadmill training is a direct approach to gait training and rehabilitation. The patient walks on a treadmill with his or her body weight partially supported while the therapist(s) guide the patient's limbs where required [22]. For stroke patients, neuro-developmental training that targets emotional, social, and functional problems in addition to the main sensory-motor deficits, aims to suppress abnormal movement synergies and move towards normal motor patterns [23]. Robot-driven therapy was also purposed for the neurologically impaired where robotic actuators aid the patient while measuring his/her output [24]. One additional interesting and unique gait training and rehabilitation method is equine-assisted therapy.

## *Hippotherapy (HPOT)*

Hippotherapy is a treatment strategy utilizing the movement of the horse. HPOT was first used by therapists in Europe in the 1960s for increasing strength, balance, posture, and function of patients [25]. Since then, HPOT has been employed in physical therapies for the trHPOTment of a variety of conditions, including autism, cerebral palsy, stroke, spinal cord injury, multiple sclerosis, and many more. HPOT has the potential to provide physical, cognitive, emotional, and social benefits to patients [26-33].

### *HPOT Practice*

HPOT sessions are usually conducted with one or more therapists and staff members (Figure 1.5). The HPOT licensed therapist conducts activities and exercises with a patient [30], such as identifying shapes and colors, catching objects, or balance and coordination exercises [31]. The therapist often walks behind or beside the horse to observe the movement of a patient and implements adjustments in the speed, gait, and direction of the horse. An experienced horse handler is often on the therapy team to lead the horse and put into effect any requests by the therapist for change in motion of the horse [31].

Figure 1.5: A sample HPOT therapy session [34]

Therapy horses are selected for their gentle temperament, symmetrical gait, obedience, health, girth, and height. The horses are subject to extensive training, during which they are schooled to tolerate unbalanced riders, sudden distraction, and to perform smooth gait transitions [32,33]. The height, girth, breed, and gait mechanics of the selected horse can have a significant impact on the frequency, amplitude, and magnitude of stimuli received by the patient [32].

*Rationale*

Although many studies have demonstrated the therapeutic benefits of HPOT, the underlying mechanisms are not well understood [26-34]. One theory suggests the horse induces in the rider's body a repetitive and cyclic pattern of motion that is similar to that of natural human walking [26-29]. The movement of the horse's back and pelvis during horseback riding provides motor and sensory inputs to the human body. Because the rider sits on the horse's back near the pelvis, and the horse's pelvis is driven by the movement of its hind limbs when walking, this movement propagates to produce pelvic movement in the rider's body that resembles human walking [26,27,30].

Several previous studies aimed to quantify similarities between walking and horse riding motions. Fleck studied the body motions of 24 healthy children while walking on a treadmill and while riding on a horse walking on an equine treadmill. She reported measurement ranges of lateral pelvic displacement in the sagittal and frontal planes, lateral pelvic list angle and the vertical displacement of the estimated body center of mass. Her results showed similarities between walking and horse riding for the pelvic tilt angle, timing sequences of stride [35].

Uchiyama et al. used acceleration sensors to analyze the acceleration patterns of walking in 50 healthy humans and 11 horses. They reported that the acceleration curves of human walking overlapped with that of horse walking. They also measured the exercise intensity by comparing heart rate, breathing rate, and blood pressure of 127 healthy individuals before and after walking and horse riding. Exercise intensity was not significantly different between horse riding and human walking [26].

Garner and Rigby quantitatively compared human pelvis motions when walking to those when riding a horse. They measured anteroposterior, superoinferior, and mediolateral translations as well as list angle about the anteroposterior axis and twist angle about the superoinferior axis. They observed similar features of pelvic trajectories between walking and riding, including distorted lemniscate patterns in the transverse and frontal planes. They also reported some differences in pelvic trajectories in the sagittal plane. The pelvic trajectory during walking exhibited a circular pattern whereas in riding it exhibited a more diagonal pattern [27].

In summary, previous studies suggested that riding on a horse can generate kinematics in the human pelvis that mimic many characteristics of those during natural human walking [26,27,35], indicating a reasonable rationale behind HPOT.

*Camel Assisted Interventions (CAI)*

Camel (genus *Camelus*) is the most important livestock animal in the semiarid areas of Northern and Eastern Africa as well as in the Arabian Peninsula and Iran. The one-humped Arabian camel (*Camelus dromedarius*) and the two-humped Bactrian camel (*Camelus bactrianus,* Figure 1.6) are two of the domesticated species of camel. The camel is a multipurpose animal that can be used for milk, meat, hides, and transport [36]. Because camels are well adapted to dehydration for a relatively long period in harsh conditions, they are ridden by humans as a means of transportation across deserts [37]. Today a number of Sub-Saharan countries still use camels for military campaigns and transportation of industrial or agricultural goods [38].

Figure 1.6: A two-humped Bactrian camel

The camel has a unique pacing gait due to its leg morphology. The distinctive features of the camel's locomotor apparatus include divergence of the third and fourth digits of its feet, lack of hooves, broad footpads, and lack of the interdigital ligaments [38-40]. These features permit the camel to walk on shifting sand, in the desert, on rough

rock, and up steep inclines [39]. A number of previous studies on camel gait focused on the interaction between the camel foot and sand. The results of these studies were used to improve traction control of desert vehicles [40-42].

*Rational*

Like HPOT, Camel-assisted interventions (CAI) have potential therapeutic benefits. Therapeutic camels fill similar functions as horses. Camel riding, like HPOT, provides sensory, motor, and vestibular stimulation. In contrast to HPOT, camels have different locomotion and may provide different motor stimuli for riders. Meanwhile, the humps of two-humped camels may provide tactile stimulus and support [43].

CAI has been experimented at places such as Oasis Camel Dairy in San Diego, USA [44]. However, there is no previous study on CAI or biomechanics of camel riding. Therefore, one goal of this study is to measure the motion experienced by the camel riders and compare the motion to that of horse riding, and that of walking.

*Motivation*

While the kinematics of walking have been well documented, only three studies have quantitatively compared walking and horse riding [26,27,35]. Each of these three studies have limitations that can be improved. The Fleck study presented only the ranges of a few kinematic measures and did not look at the temporal characteristics or phase sequencing of the kinematics measures. Only a single horse was included in the riding trials, and these trials were performed on an equine treadmill [35]. Uchiyama et al. included a significant number of subjects (50 humans and 11 horses). However, this study used acceleration sensors to measure the kinetics of walking and riding movement

instead of the kinematics of these motions [26]. Finally, the Garner and Rigby study only included posterior pelvic markers. Therefore, pelvic tilt angle in the sagittal plane was not reported [27].

Since there is a similarity between the kinematics of walking and horse riding, studies that quantitatively measure the pelvic movement during walking and horse riding should be conducted. Furthermore, there is no existing camel riding study, and CAI research is needed to compare HPOT with CAI. This thesis advances the body of knowledge on the characteristics and relationships of human pelvis kinematics during walking, horse riding, and camel riding, towards a better holistic understanding of the mechanism of how Hippotherapy and Camel-Assisted Interventions may provide physical benefits to patients. It is the first known study using motion capture data to compare human pelvis motions while riding a camel, horse and while walking.

### *Objective*

The objective of this study is to measure and compare human kinematics during natural walking, horse riding, and camel riding. The specific focus will be on the kinematics of the human pelvis because of its key role in maintaining a smooth and efficient gait [7]. Motion capture of human pelvis kinematics from three human subjects walking, riding on three horses, and riding on two camels was recorded. Since it is known that horses with different height, girth, and gait may produce different magnitude of stimuli and movement received by riders [32], kinematic measurements of each human subject of each horse and camel were analyzed and compared first. An overall average of kinematic measurements of all human subjects on all horses was then computed and compared with camel riding average data and human walking average data.

Six main variables of interest were identified that have been previously measured in similar studies [27]:

1) Pelvic Displacements
    a) Frontal (X) Displacement
    b) Vertical (Y) Displacement
    c) Lateral (Z) Displacement
2) Pelvic Angles
    a) Tilt
    b) List
    c) Twist

# CHAPTER TWO

## Methods Validation Study

The objective of the current study is to quantitatively measure and compare the human pelvic motion when walking and when riding a horse or camel. Optical motion capture of human and animal (horses/camels) subjects is the primary method used to record and measure the movement generated and experienced by all subjects. While optical motion capture systems are widely utilized in clinical and research applications [45,46], they are rarely used in outdoor animal motion studies [47]. Therefore, the motion capture methods planned for the thesis study were first validated in a separate study comparing the motion patterns of a live steer to those of two popular mechanical training devices. This chapter will present this unique study of team roping.

### *Motion Capture Methods of Human Kinematic Studies*

Team roping is a premiere and longstanding rodeo event that involves two ropers and two horses working together in a finely trained pattern to rope the head and hind legs of an escaping steer (Figure 2.1) [48,49]. The header ropes the head or horns of the steer first, then pulls the steer into position for the heeler. As the steer is constrained at the head, it typically enters into a hopping gait in which both hooves leave the ground roughly together, thereby providing the opportunity for the heeler to rope the hind legs. The heeler in chase must time the rope's throw to arrive at both hooves while they are off the ground so as to loop under and around them for a successful roping. All of this is done with the goal of completing the task as quickly as possible, while riding and guiding

a galloping horse, and while the steer is running and hopping to escape. This event requires great skill and coordination to complete successfully. Team ropers spend many years, and many long hours of training and practice to excel in their sport.

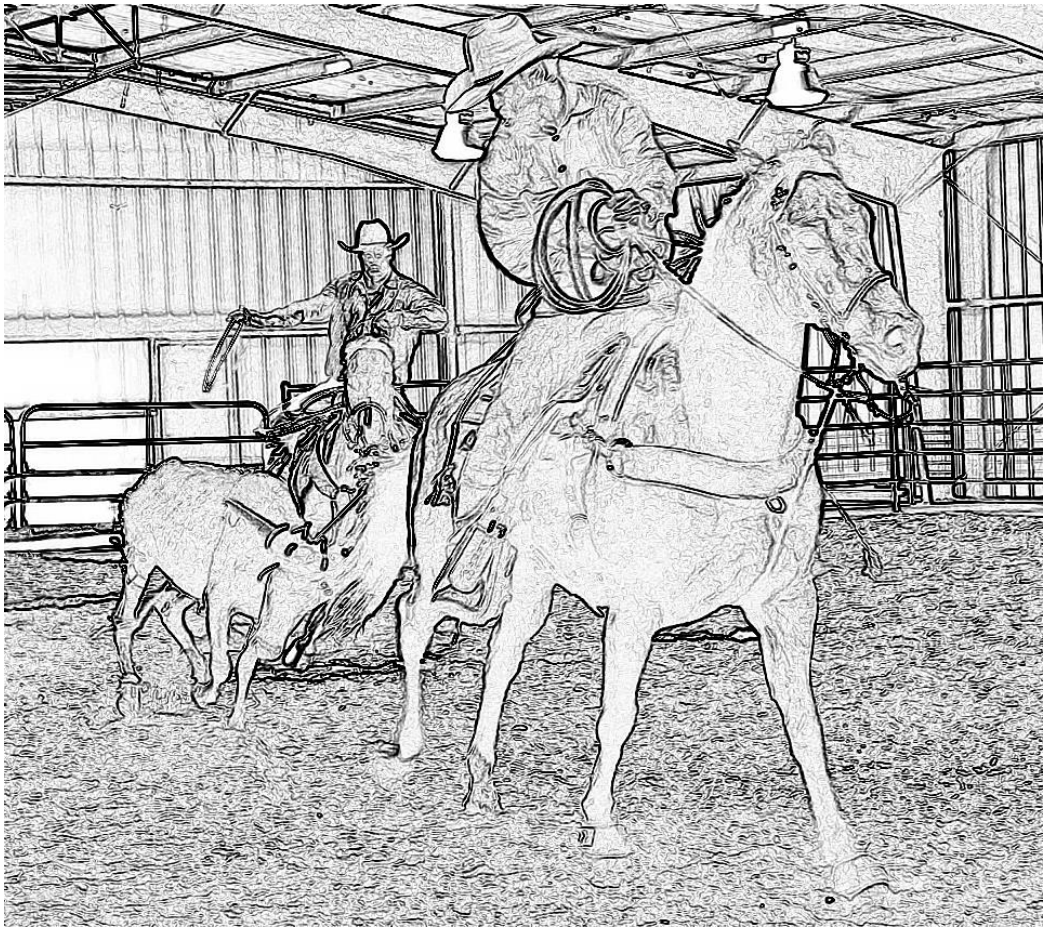

Figure 2.1: Representation of the team roping rodeo event where two ropers and two horses work together to rope first the head or horns of an escaping steer, and then the hind hooves or heels. The heeler must time the rope's throw to arrive on target in the short time window during which the steer hooves are off the ground.

One of the greatest challenges for this sport is that persistent training with live steer can be cumbersome and limiting since it requires access to facilities to constrain, release, and corral the steer, coordination of practice by both ropers, management of the horses, and risk of fatigue or injury to the live animals [50]. As a result, a number of

mechanical team roping trainers have been developed. Some popular examples are marketed by Heel-O-Matic Training Systems (Longmont, Colorado, USA) – an older model called *The Pro*, and a newer model called *The Trainer* (Figure 2.2). These training devices are designed to be pulled behind small off-road utility vehicles in the practice arena. The devices have wheels that roll along the ground and drive motion of an artificial steer mannequin. The motion involves angular elevation and depression of the rump and tail segment, and kicking motion of the hind legs. Each leg is modelled as a single rigid segment, and the two legs move together in unison. The devices also have a mannequin head with horns that can be used for head roping practice.

Naturally, the quality and value of training with these devices depends, at least in part, on how realistically the mannequin mimics the motion of a live steer. However, the realism of these training device motions has yet to be quantified and documented. In fact, few studies have attempted to quantify mechanical replication of animal motion [33, 47,51]. The purpose of this study is to use high-speed and high-resolution motion capture techniques to compare the motion patterns of two Heel-O-Matic training devices with that of a live steer during simulated roping trials. The two devices investigated include *The Pro* (older device), and *The Trainer* (newer device). For this study the motion patterns of two key anatomical markers, the tail and fetlock, is emphasized for their importance to the heeler. The fetlock (just above the hoof) is a measurable representative of the motion of the targeted hooves, and the tail is reported by heelers as a point of focus indicating the timing of the hoof motions.

*Methods*

The three-dimensional motion patterns of a single live steer, and two training simulators, were recorded during a series of simulated roping trials. Data recording and analyses emphasized the sagittal plane since the motion of the hopping steer and the simulators occurs primarily in this plane.

Three-dimensional motion data were recorded at 120 frames per second using an eight-camera Vicon optical motion capture system (Vicon Motion Systems, LTD, Oxford, UK) [52]. The eight cameras were oriented and distributed to capture an observation space about 10 meters (~33 feet) long in the direction of motion travel. On the steer, spherical reflective markers were placed adhesively at the rear fetlock joint, tarsal joint, stifle (knee), hip, hook (pelvis), tail setting (tail), mid-back, and shoulder joint. On each training device, spherical reflective markers were placed at the artificial points corresponding to the same anatomical features as marked on the live steer (Figure 2.2) [53,54].

a)

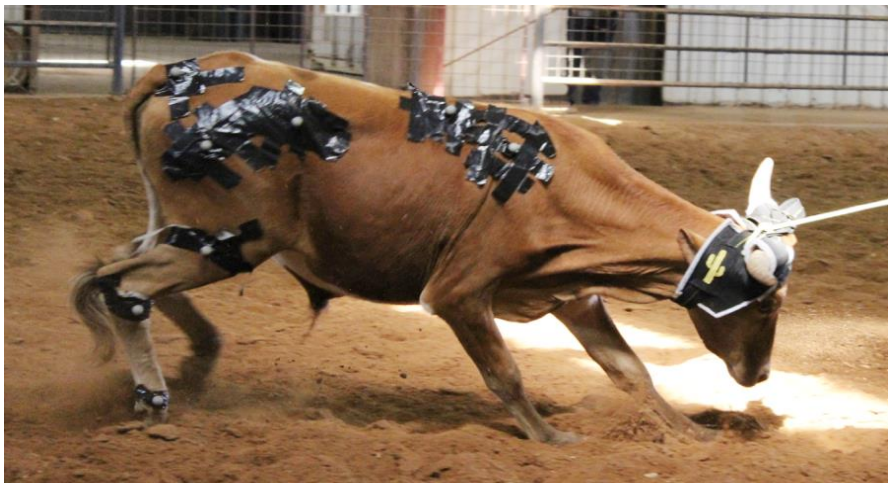

b)

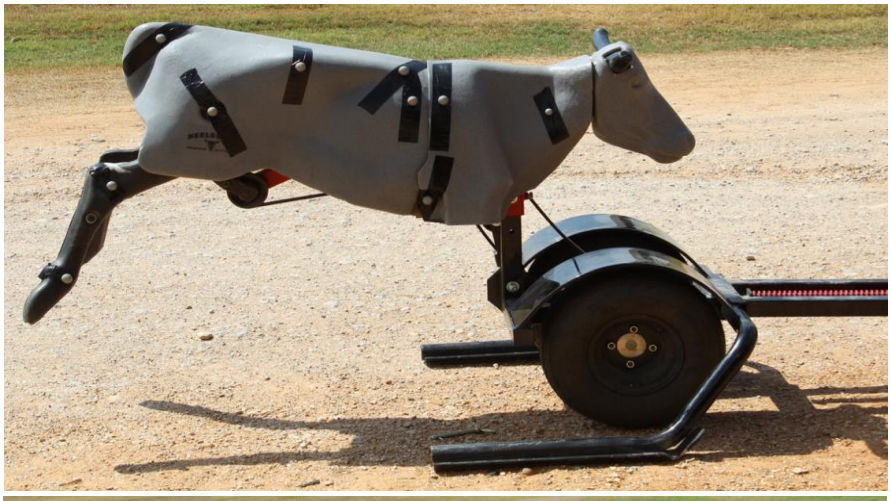

c)

Figure 2.2: Positioning of reflective markers for motion capture recording of the a) steer, b) newer device called The Trainer, and c) older device called The Pro.

*Trials*

All trials were performed by a pair of highly experienced team ropers in a covered riding arena at the Highlander Ranch in Waco, Texas. A live steer was roped at the horns and pulled through the observation space by one cowboy and horse as would be done during the team roping event. A second cowboy and horse trailed behind the steer as if for heeling, though no rope was thrown at the hind legs. The pulling action and speed induced the steer into a "hopping" gait pattern typical of that during the roping event. To avoid fatigue of the steer and the horses, only five experimental passes were performed and recorded with the live steer, with a brief rest period between each pass.

Similar trials were performed with each of the two training simulators on the same day, at the same location, and with the same camera setup as with the live steer. The trainers were pulled by a Kawasaki four-wheeler at speeds driven by the cowboys representing those typical of training exercises. Four passes were performed with the older device (*The Pro)*, and three passes were performed with the newer device (*The Trainer)*.

*Data Analysis*

The three-dimensional (*xyz*) motion data from each pass of each animal and device were processed into individual motion cycles characterizing the movement patterns [27,55]. Data was first rotated in the horizontal plane to align the overall forward direction of movement with the principal *x*-axis of the calibrated observation space. This step was accomplished by regression-fitting a line to the pass data, computing the angle of that line with respect to the *x*-axis, and then rotating all the pass data by that angle about the vertical *z*-axis through the origin. The vertical displacement

data was plotted versus time, and data from the tail marker were used to manually identify individual motion cycles in each pass. The vertical tail displacement data naturally exhibit a roughly-sinusoidal shape reflecting the tail's up-down "hopping" motion. Cycle start frames were identified as those where the vertical displacement hit key milestones, such as high points or low points. Cycle end frames were identified as the corresponding start frame of the next cycle. In most of the experimental passes there were two to three individual cycles that could be identified, and the data from each cycle was then separated.

To correct for naturally occurring inconsistencies in gait, and to ensure repeating, periodic motion data patterns for each processed gait cycle, any translational drift of each marker, and in each coordinate direction, was subtracted out linearly. That is, a constant marker velocity covering the drift displacement over the cycle period was subtracted from the marker data so that all marker locations returned at the end of the cycle to the location where they were at the start of the cycle. One additional benefit of this drift subtraction step is the elimination of overall forward motion, thereby allowing the motion to be observed as if it were performed on a treadmill. Fifth order Fourier series functions were fit to the trajectory of each coordinate axis of each marker over the cycle period, and used to smooth the trajectory mildly, repopulate the data to a consistent 100 samples per cycle, and ensure periodic and smooth data positions, velocities, and accelerations [56]. In all cases, the key features and characteristics of the trajectories were preserved.

All cycles from the various passes and conditions were synchronized in cycle time by identifying and aligning the cycle instant where the tail marker reaches its most superior and anterior peak following its prominent rise phase. Cycle alignment was

accomplished by phase shifting all cycles so that this tail peak occurs at the cycle beginning (zero percent cycle). Averages were then computed across aligned cycles of each of the various steer passes, respectively, all passes of the older device, and all passes of the newer device.

## *Results*

The motion capture experiments resulted in high quality data that provides detailed representation of the steer and both training devices during the simulated roping trials. At least seven good cycles of motion data were captured over multiple passes for each of the devices, and multiple (2-4) good cycles were captured for each of four passes with the live steer (only steer pass 3 had only two good cycles). During the second pass of the steer it was observed that the steer did not enter a typical hopping gait, but instead an irregular and erratic motion pattern, so data from that pass was not included in this analysis. Data from the other various passes of the steer are presented individually to examine consistency of motion across passes and any possible effects of fatigue.

### *Stride Characteristics*

Figure 2.3 shows the average cycle periods, average stride lengths, and average speeds over the various cycles for the steer passes, and for each training device. The speed at which the steer was pulled varied somewhat from pass to pass, ranging from 4.33 m/s in the first pass to 6.81 m/s in the third pass. The other two steer passes had very similar speeds around 5.56 m/s. All steer passes were faster than the speeds at which the training devices were pulled (4.19 m/s older, 3.63 m/s newer). Stride length was relatively similar between the four steer passes (average 3.08 m, standard deviation

0.43 m), and the older device (2.85 m). However, the stride length of the newer device (1.80 m) was substantially less, being only 63% that of the older device. Steer stride length correlated strongly and positively with forward speed (0.96 correlation coefficient). Cycle period was quite consistent across all steer passes (average 0.55 sec, standard deviation 0.03 sec) and the newer device (0.50 sec), whereas the older device took 36% longer (0.18 s) than the newer device.

(a) Speed Average (Meter/Second)

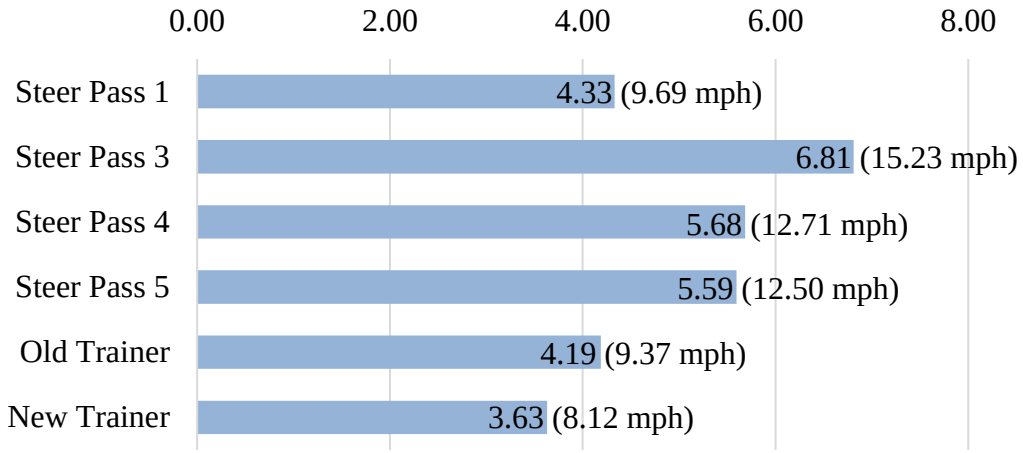


(b) Period Average (Second)

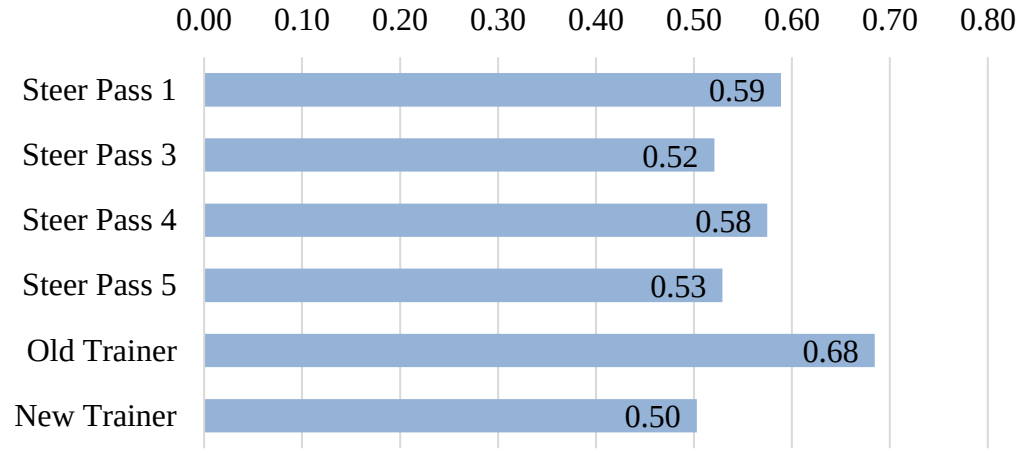

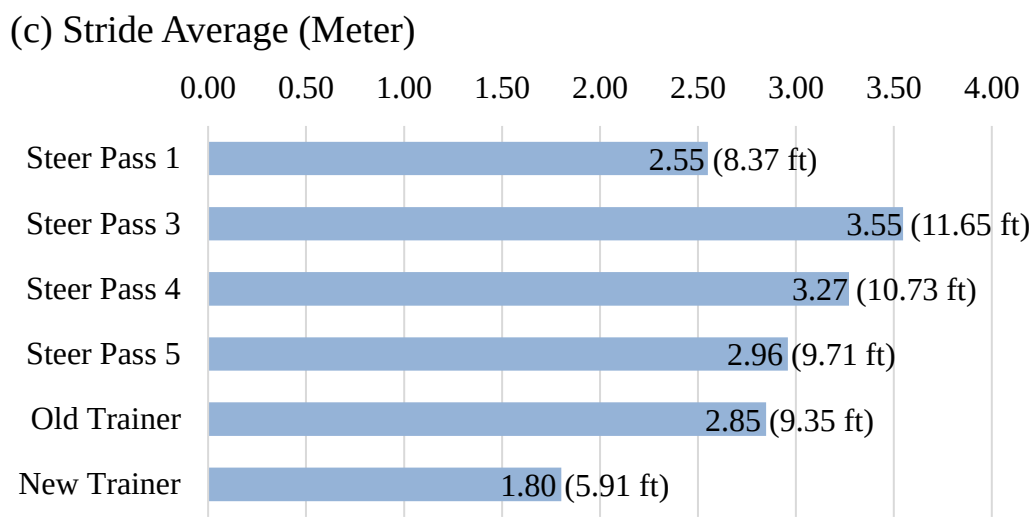


Figure 2.3: Stride characteristics for each steer pass and the two training devices based on averages over multiple cycles. Results show the steer was pulled faster by horse than were both devices by vehicle (a). At the respective pull-speeds the older device had the longest cycle period (b). Steer stride length correlated with speed (a,c). The device stride lengths are independent of speed. The newer device's stride was much shorter (c).

*Tail Displacement Trajectories*

Figure 2.4 shows the tail horizontal and vertical displacements versus percent cycle time, and the tail sagittal plane trajectories. Tail motion patterns are very similar across the steer passes and both training devices, as all exhibit a rocking motion upward and forward and then downward and backward, corresponding to the hopping motion. The horizontal displacement ranges (with forward motion subtracted out) for the steer passes are all very similar (range: 11-14cm, average: 12 ± 1cm), and are similar to the horizontal displacements of the old (13 cm) and new (15 cm) devices. The vertical displacement ranges are also similar, but a bit larger for the devices. The steer passes had a range of 14 - 24 cm (average 19 ± 4 cm), whereas the devices had vertical displacements of 24 and 29 cm, respectively.

As noted in the methods, the plotted cycle data are synchronized in phase to the superior-anterior corner of the tail trajectory, so naturally the patterns versus percent

cycle time align well. The horizontal motion patterns all have a very similar sinusoidal shape across steer passes and devices, and all exhibit similar timing with peak anterior translation at 0% cycle (as synchronized), and generally the most posterior translation around 50% cycle. The vertical motion patterns are also similar, exhibiting peaks right near 0% cycle time (as synchronized), and then falling to the lowest trajectories at around 45% cycle for the devices, and around 60% to 65% for the steer passes. The fact that steer pass 1 reaches its absolute vertical peak at 9% cycle rather than 0% is due to the tail continuing to rise slightly after it starts looping backwards once passing the peak superior-anterior point.

The steer tail looping trajectory pattern is most prominent in pass 1, but is also seen in the other steer passes, as the tail rise with hoof propulsion occurs slightly more anterior than the tail fall during the hoof return stroke. The absolute vertical position of the steer tail remains relatively high in pass 1, then is about 8 cm lower for passes 3 and 4, and then is lower again by about 5 cm for pass 5. The vertical tail displacement of both devices matches remarkably well with the latter 3 steer passes, although the device tail trajectories follow a more arced pattern consistent with their mechanical origins of motion about a fixed pivot point.

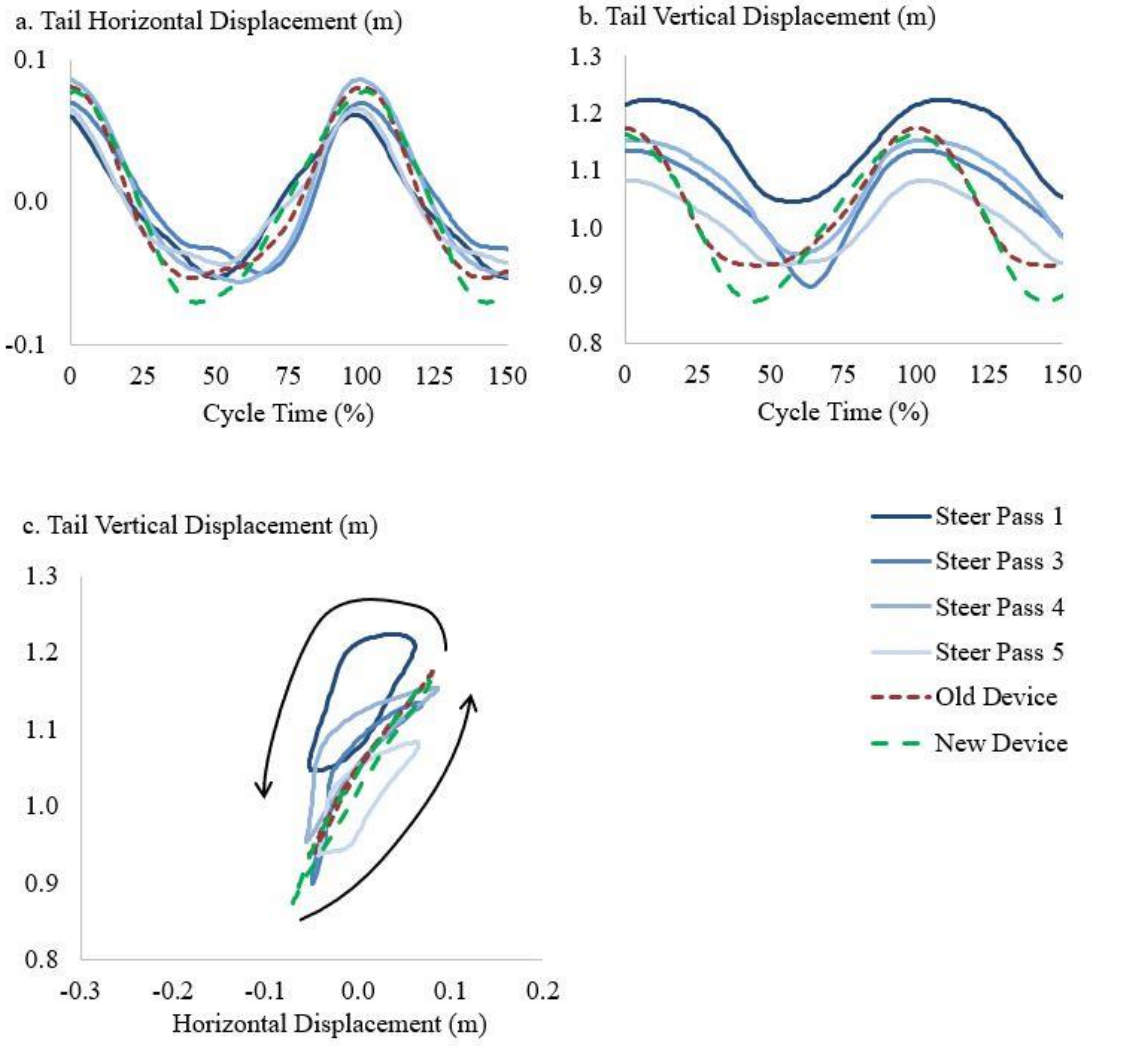


Figure 2.4: Tail displacement trajectories for each steer pass and the two training devices based on averages over multiple cycles. Cycle data are synchronized in time such that the tail marker reaches the most superior, anterior point at the cycle start. Synchronized this way, the tail horizontal motion patterns are very similar across the steer passes and both devices (a). The tail vertical displacements are also quite similar, with the device tails reaching low points a bit earlier in the cycle than the steer (b). The first steer pass vertical displacement reaches a high point slightly after the cycle start because the tail continues to rise a bit after its most anterior horizontal displacement (c), and as the hooves start moving forward. The sagittal plane trajectories (c) reveal a slightly looping tail pattern for the steer (arrows indicate direction), while the device tails arc about a mechanical center simulating the steer hopping motion. The device tail motions match the steer quite well in basic amplitude and trajectory direction.

*Fetlock Displacement Trajectories*

Figure 2.5 shows fetlock vertical and horizontal displacement versus percent cycle time, and the fetlock sagittal plane trajectories. As with Figure 4, the cycle times are synchronized according to peak superior-anterior tail displacement. The fetlock trajectories of the steer and both training devices exhibit a similar, generally-elliptical looping pattern as the hooves propel along the ground and then lift up and over for the return stroke. The steer passes are all very similar to each other, with a fairly horizontally-oriented elliptical shaped trajectory, and no apparent trends of variation over successive passes. The older device fetlock trajectory similarly has a horizontally-oriented elliptical shape, but it is smaller, and occurs higher vertically than that of the steer. The elliptical shape of the newer device is oriented with its major axis angled about forty degrees off horizontal, and it also is higher vertically than the steer.

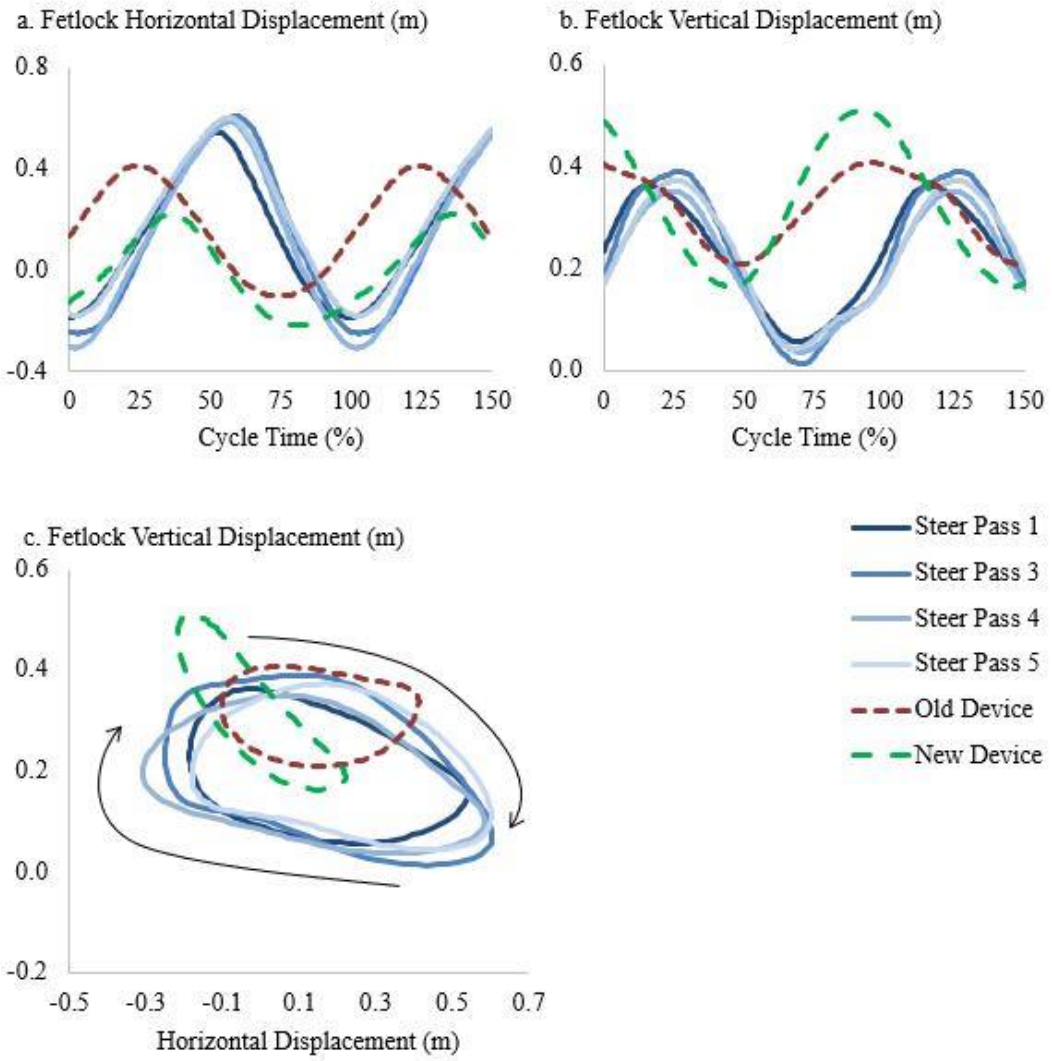


Figure 2.5: Fetlock displacement trajectories for each steer pass and the two training devices based on averages over multiple cycles. As with Figure 4, the cycle data are synchronized in time such that the tail marker reaches the most superior, anterior point at the cycle start. Good consistency is shown across the various steer passes despite somewhat varying pull speeds. The horizontal amplitude of fetlock displacement is seen to be higher for the steer than for either device, and the device initiation of forward fetlock displacement occurs earlier in the cycle than with the steer (a). The vertical fetlock displacement data shows the steer hooves coming all the way down to the ground, whereas the device hooves remain higher above the ground at the lowest point (b). The steer and device fetlock trajectories all exhibit a roughly elliptical shape (c). The steer and older device ellipse long axes are fairly horizontal, and the steer ellipses are larger overall. The new device ellipse has a long axis angled above the horizontal.

The horizontal ranges of the steer passes vary from 72.8 to 89.4 cm (average 81.5 ± 7.4 cm), whereas the older and newer devices have horizontal ranges of 51.6 and 43.8 cm respectively. The major axis of the newer device trajectory ellipse is about 52.7 cm, considering the inclination of its trajectory. The vertical ranges of the steer passes vary from 30.5 to 37.6 cm (average 33.1 ± 3.1 cm), whereas the older and newer devices are 19.8 and 34.5 cm, respectively. Again, factoring out the inclination in the newer device trajectory, its ellipse minor axis is about 13.7 cm.

With the cycle data synchronized by superior-anterior tail peak, the fetlock displacements of the various steer passes are all aligned with each other very well in time. The steer passes all have vertical peaks and valleys at around 25% and 70% of cycle time, respectively, and horizontal peaks and valleys at around 60% and 2% of cycle time, respectively. Thus, the steer tends to initiate the forward return stroke of the hooves about the same time each cycle as the tail peak occurs (near 0% cycle). The timing of the training devices is phase shifted somewhat earlier in the cycle. The older device hits the most anterior (positive) and posterior (negative) horizontal displacement at about 35% and 32% earlier in cycle time, respectively, than of the corresponding moments in the steer cycle. The newer device is closer to the steer, hitting the most anterior (positive) and posterior (negative) horizontal displacement at about 22% and 20% earlier in cycle time, respectively, than in the steer cycle.

## *Discussion*

In this study, the motion patterns of a live steer were compared to those of two popular mechanical training devices for the purpose of quantifying and assessing the motion integrity of the devices for application to team roping training. Overall, the timing of tail rise and fall is matched quite well between training devices and the live steer. Similarly, the trainers exhibit a similar basic pattern of motion for the fetlock joint, though the device hooves don't fully touch the ground, and there are some discrepancies in the stride length and trajectory pattern with the newer device, and with the phase timing for both devices.

### *Stride Characteristics*

The variation of speeds across the steer passes is not surprising given the context of the steer being pulled by a horse. However, the steer speed variations observed in these experiments are helpful in illuminating the strong correlation between forward speed and stride length. It is intuitive that a longer stride length would cover greater distance and therefore accommodate a faster speed. And, the steer seems to choose, at least when pulled, to increase speed by increasing stride length rather than by reducing gait cycle duration (period, which essentially remains unvaried with speed or stride length).

The speed of the devices is simply a matter of the driver's choice, and in these experiments the drivers were highly experienced at both team roping and at using the trainers. The fact that their chosen driving speeds were consistently slower than the steer speeds may reflect the need for more awareness and careful control of trainer driving speeds. The overall average steer speed in these experiments was about 20km/hr (12.5

mph) with standard deviation of about 3.6 km/hr (2.2mph), so a recommended training device driving speed from about 14 to 23 km/hr (9 to 14 mph) may be appropriate.

Unlike speed and period, the stride length in the mechanical trainers should not be affected by driver choice. Since the stride motion mechanics is driven by rotation of the wheels, the resulting stride length depends on the wheel circumference and the internal linkage transmission ratio (assuming minimal ground slippage), regardless of speed. Indeed, the standard deviation of stride length over all cycles for each training device was only about 5% of the respective averages, whereas for the steer it was 13%. Interestingly, both devices were pulled about the same speed, but the stride length of the newer device was substantially less than that of the older device and the steer passes, reflecting a difference in its overall transmission ratio from the older device. Assuming a linear regression trend of steer speed and steer stride length based on the strong positive correlation in those variables, a steer would need to be pulled at about 9 km/hr (5.6 mph) to reach a stride length matching the essentially fixed stride length of the newer training device.

*Tail Displacement Trajectories*

Tail displacement trajectory is a key factor in team roping given the prominence of the tail in the heeler's view of the steer from behind. The heeler can synchronize his riding and throwing motion with the steer's tail motion. In these experiments both trainers match the steer tail motion fairly well, with a sharp rise and falling pattern. The trainers also match the vertical position of the steer tail very well, but they have a slightly larger vertical range than the steer. The slight looping pattern of the steer tail trajectories, most prominent in steer pass 1, is not replicated in the training devices as the device tail

pivots about a fixed point. However, this slight deviation is very apparent when the forward motion is subtracted out as in the graphs of Figure 4, but it may not be very noticeable in the larger context of live action with the steer or trainer moving forward.

The fact that the steer tail vertical height tends to drop over the successive passes may reflect the onset of fatigue in the animal. The additional tail height does not seem to come from actually hopping higher, as the fetlock trajectories do not show a similar trend. Rather, in the earlier cycles when the steer was fresher, it may have extended its legs further during the hopping motion. Regardless, however, since the fetlock height and overall trajectory didn't change much over successive passes, the drop in tail height may not have much impact from the roper's perspective.

*Fetlock Displacement Trajectories*

Though the hooves may be the most critical anatomical point for the purposes of the team roping event, in these experiments the fetlock was tracked instead because the steer hooves tend to imbed into the arena dirt and become obscured during the ground contact phase. Nevertheless, the fetlock is very near the hooves, and should serve well as a representative of the hoof trajectory for the comparison purposes of this study. Also, for fair comparison, in this study the fetlock was tracked for the steer and both training devices.

The older device fetlock trajectory proved a good match for that of the steer in terms of its similar, horizontally-oriented, generally-elliptical shape. During the hoof return stroke, it achieved a height above the ground (~39cm) that is quite similar to that of the steer (~36 cm). However, its overall horizontal range is about 63% that of the steer, and it remains higher by about 15 cm above the ground during the propulsion

phase. In neither device do the hooves fully touch the ground during the cycle, whereas the steer hooves touch the ground for about 30% of the cycle.

The newer device fetlock trajectory did match the vertical range of the steer quite well, but that comes as a result of its 40-degree inclined elliptical shape. Its highest vertical point is 50 cm above the ground, which is well above the 36 cm for the steer. The most posterior position of the newer device fetlock is essentially equivalent to that of the steer, both being about 20 cm behind the tail, compared to about 10 cm behind the tail for the older device. The newer device matching that position of the hooves relative to the tail may be significant from the heeler's perspective. Perhaps less significant to the heeler is that the newer device fetlock doesn't travel nearly as far anteriorly relative to the tail (21 cm) as does the steer fetlock (59 cm).

Whereas the older device better matches the horizontal elliptical fetlock trajectory, the newer device better matches the tail to fetlock timing sequence. As noted, the tail motion can be a key factor in helping the heeler time a throw to catch the hind legs. The window of opportunity for roping the heels is just after the hooves leave the ground, and before they travel too far forward underneath the steer, and ideally while they are rising up underneath the tail. Both devices reach the lowest vertical fetlock displacement at around 50% cycle time, initiating vertical fetlock rise about 20% of the cycle period before the steer. And, the fetlock in both devices rises vertically essentially simultaneously, but the subsequent forward horizontal motion of the fetlock is slightly more delayed in the newer device than in the older device. Therefore, whereas the older device is more than halfway through its forward hoof return stroke when the steer initiates forward hoof motion, the newer device is only about 10 cm ahead of the steer

fetlock at that instant, and with the newer device's shorter horizontal stroke, the steer fetlock actually catches up with and passes the newer device fetlock during the horizontal return phase (at about 25% cycle time). Interestingly, at that same time the vertical displacement of the steer and newer device fetlocks are also very similar, so they essentially intersect in time and space at that point.

*Significance and Limitations*

This study represents the first to quantitatively compare motions of key anatomical features between steer and training devices for the team roping rodeo event. This event's popularity and financial support results in a very high-level of competition, and a number of products have been designed and developed to aid training of the highly-skilled athletes. This study analysed two popular training devices and found that both have qualities that match the action of a live steer, and both have room for improvement. The older device better captured the horizontally-oriented elliptical shape of the fetlock trajectory, whereas the newer device more closely matched the tail to fetlock motion phase timing. Both devices could be improved with increased range of fetlock motion, cycle time with hooves touching the ground, and with a fetlock forward return stroke that initiates more closely in synchronization with the moment of peak superior-anterior tail displacement.

The success of this study demonstrated that using an optical motion capture system in an outdoor setting is feasible. The main thesis study drew techniques learned from this study to measure and record the kinematics of horses, camels, and human subjects.

# CHAPTER THREE

## Motion Capture Methods of Camel Riding, Horse Riding, and Walking

The objective of the current study was to quantitatively measure and compare the human pelvic motion when walking and when riding a horse or camel. The testing performed included three-dimensional motion capture of human subjects riding camels and horses, and human subjects walking. A common pool of subjects was used for both the riding trials and the walking trials. The Baylor Internal Review Board (IRB) and the Institutional Animal Care and Use Committee (IRCUC) reviewed and approved the study.

### *Participants*

Three adults and two adolescents were recruited to participate in this study. Subject demographics are shown below (Table 3.1). All subjects were in good health with no neurological or musculoskeletal impairments. None of the subjects was experienced in horse or camel riding. One subject participated in all components of the study, including horse riding (H), camel riding (C), and walking (W). The rest of the subjects participated in some components of the study (Table 3.1). Two camels, one Arabian (King Arthur, Camel 1) and one Bactrian (Camel 2), were used in the study. Three horses of varying size and gait pattern were used, and each was trained for and familiar with the practice of HPOT. The horses included a 15-year old Paint mare (Callie, Horse 1), a 5-year old Thoroughbred gelding (Clyde, Horse 2), and a 23-year old Appaloosa gelding (Levi, Horse 3).

Table 3.1: Human Subject Demographics.

| Subject | Age | Gender | Height (in) | Weight (lb) | Participation |
|---|---|---|---|---|---|
| 1 | 49 | F | 65 | 118 | H, C, W |
| 2 | 23 | M | 72 | 145 | C, W |
| 3 | 17 | F | 69 | 135 | H |
| 4 | 17 | F | 62 | 115 | H, W |
| 5 | ? | F | ? | ? | H, C |

## *Camel and Horse Riding Studies*

### *Experimental Setup*

The motion capture experiments of camel and horse riding were conducted at the Heart of Texas Therapeutic Riding Center near West, Texas, USA (Figure 3.1). Riding trials were recorded in the shaded section of the riding center arena. The ground surface of the arena was covered by arena dirt. The dimension of the observation space was approximately 10 m (35 ft) in length and 3 m (10 ft) in width. The lengthwise dimension of the observation space was aligned with the forward direction of movement.

Eight Vicon Vantage Cameras (Vicon Motion Systems, LTD, Oxford, UK) and two high speed Bonita cameras (Vicon Motion Systems, LTD, Oxford, UK) were set up to record the observation space. The capture frequency of the cameras was 120 Hz. One researcher supervised the setup and calibration of all cameras. Four Vicon Vantage Cameras were placed on each side of the observation space along its length (Figure 3.1). The cameras were spaced approximately 2 m (7 feet) apart. On one side of the observation space, one Bonita camera was placed in the middle while the other was place on the end to record video footage of each trial. All cameras were calibrated at the start of each collection day using a wand with markers at known locations.

Figure 3.1: Heart of Texas Therapeutic Riding Center. The motion capture camera system was setup around the observation space of the experiment.

*Marker Placement*

*Human subjects.* All subjects completed and signed the IRB approved consent form before the placement of markers. The same researcher supervised the placement of markers for all subjects. Infrared reflective passive markers were selected for this study. Passive markers can be placed on subjects of all body types and do not require a power source or wires that may interfere with the study [57]. A total of 39 markers were placed on the subjects' bodies according to the Vicon Plug-in Gait full body marker set guidelines [57]. The detailed marker placement locations can be found in the diagram below (Figure 3.2). Markers were generally placed on the skin over bony landmarks to reduce inaccuracies caused by soft tissue artifacts. In some instances, markers were placed on spandex or other tight-fitting clothing worn by subjects only if the clothing did not move relative to the underlying skin. Key markers of interest in this study included left/right anterior superior iliac spine marker (LASI/RASI) and left/right posterior superior iliac spine marker (LPSI/RPSI).

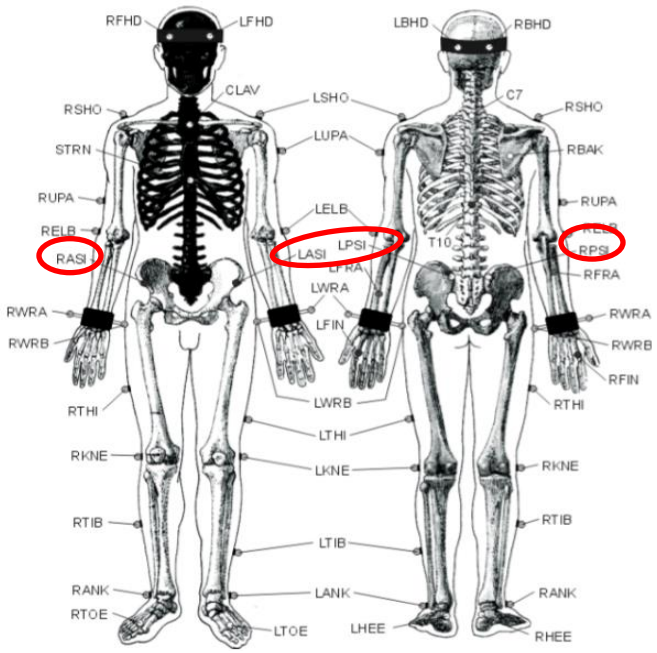


Figure 3.2: Vicon Plug-in Gait full body marker set used in this study

*Camel/Horse subjects.* The caretakers of the animals placed markers on various bony landmarks of the animals under the supervision of the same researcher. The markers were secured onto the animals using a combination of black duct tape, elastic wrap, and leather straps. On horses and camels, the markers were placed on the joints (fetlock, knee, elbow, shoulder, hock, hip), tail, pelvis, scapula, and head (Figure 3.3). Additional markers were placed on the hump(s) of the camels.

Six markers were placed on each saddle of the animals: one marker on each corner of the saddle, one marker on the handlebar (horn) of the saddle, and one marker in the rear of the saddle. In instances where no saddle was used during the riding trials, six markers were placed on the animals on similar locations where the saddle would have been placed.


Figure 3.3: Marker placement locations shown on the sagittal plane of the horse. For camels, the markers were placed on analogous anatomical locations.

*Saddles*

*Horse riding data collection*. Two saddles (Figure 3.4) were used on all three horses. The first saddle (saddle 1) was a traditional leather saddle that included a seat, stirrups, and a horn. The second "saddle" (saddle 2) was a surcingle only having a metal handlebar with no seat or stirrups, for which the riders sat directly on the back of the horses.

Figure 3.4: Horse saddles used in the study (left: saddle 1, right: saddle 2).

*Camel riding data collection*. The two saddles (Figure 3.5) used during the camel riding collection were species specific. The saddle for the Arabian camel allowed the subject to sit behind the single hump of the camel. The saddle for the Bactrian camel allowed the subject to sit between the two humps of the camel. The subjects also rode each camel with no saddle.

Figure 3.5: Arabian camel saddle (left) and Bactrian camel saddle (right) used in the study. Note that the riders sat behind the single hump of the Arabian camel.

*Experimental Protocol*

All camel riding data was collected in a single day session, and all horse riding data was collected during a single day session on the following day. Two subjects (subject 1,2) participated in the camel riding session, while three subjects (subject 1,3,4) participated in the horse-riding session. The camels were led by one experienced camel trainer. The horses were led by trained HPOT clinical staff (Figure 3.6). Prior to recording, several practice trials were performed to familiarize horses/camels, riders and lead walkers with the study environment and protocol. Each trial consisted of one subject riding a horse/camel through the observation space for a recorded pass (Figure 3.6). Each rider rode one horse/camel equipped with one saddle at varying paces for multiple passes

(4 slow passes and 2 fast passes for camels; 4 slow passes, 4 fast passes and 2 trot passes for horses). The saddle was then changed, and each rider rode the same animal at varying paces again. When all riders had ridden an animal with all saddle conditions, the next animal was equipped with markers and saddles to continue the trials. In short, all riders in the camel/horse riding session rode all the camels/horses with all saddle conditions.

Figure 3.6: The HPOT clinical staff leading the horse and rider through the observation space in a typical horse riding trial.

*Pace of the horses/camels*. The pace of the horse/camel during each trial was determined by the HPOT trained clinical staff/camel trainer leading the animals. The same camel trainer led the camels in all camel riding trials to ensure consistency of pace between trials. During camel riding trials, the camels walked at two paces: a slow walking pace and a fast walking pace. During horse riding trials, two HPOT trained clinical staff led the horses at three paces: a slow walking pace similar to that typical in the HPOT practice, a fast walking pace, and a trot pace.

## *Walking Study*

### *Experimental Setup*

The motion capture experiments of human walking were conducted at the Baylor Biomotion Lab in the Baylor Research and Innovation Collaborative in Waco, Texas, USA (Figure 3.7). The motion capture system in the lab consists of fourteen Vicon Vantage Cameras (Vicon Motion Systems, LTD, Oxford, UK) and two high speed Bonita cameras (Vicon Motion Systems, LTD, Oxford, UK). The capture frequency of the cameras was 120 Hz. All cameras were calibrated at the start of each collection day using a wand with markers at known locations.

Figure 3.7: Baylor Biomotion Lab.

### *Marker Placement*

The same researcher supervised the placement of markers for all subjects. A total of 17 markers were placed on the subjects' bodies. These markers represented the selected markers from Vicon Plug-in Gait full body marker set [57] that measures the movement of the pelvis and torso (regions of high interest for the study). Key markers of

interest included left/right anterior superior iliac spine marker (LASI/RASI), left/right posterior superior iliac spine marker (LPSI/RPSI) and left/right heel (LHEE/RHEE).

### *Experimental Protocol*

Three subjects (subject 1,2,4) participated in the walking sessions. Each subject was recorded walking through the observation space 15 times at 3 self-selected walking paces, including slow, normal, and fast paces (5 passes for each pace). Prior to recording, several practice trials were performed to help the subjects settle on comfortable paces.

## *Data Processing*

To analyze the six variables of interest, the pelvic trajectory data for each trial was first processed and exported from the Vicon Nexus software (Vicon Motion Systems, LTD, Oxford, UK) in the form of xyz coordinate values for each marker location at each capture frame over the duration of each trial pass. The trial passes were then divided into single periods of gait cycle. Finally, the gait cycles were synchronized and averaged for each of the conditions. The next sections describe details of this process.

### *Raw Data Extraction*

The first step in the data processing was to visually label the 10 key marker trajectories (Pelvic markers: LASI, RASI, LPSI, RPSI; Saddle markers: LF_Saddle, RF_Saddle, LB_Saddle, RB_Saddle, F_Saddle, B_Saddle) and fill the gaps of each trajectory for every trial. Gap filling ensures that all markers have location data at all frames of each trial pass. Because both the human pelvis and horse saddle can be modeled as rigid bodies, the rigid body trajectory fill function of the Vicon software was used. The rigid body fill requires a total of three markers to be present in order to gap fill

a fourth marker located on the same rigid body segment. If the rigid body fill could not be used (i.e. more than one out of the four pelvic marker trajectories were missing), the gaps were filled with the pattern fill. The pattern fill uses the trajectory of a nearby marker to estimate and fill the gaps. Once the marker trajectories were labeled and the gaps were filled, the data was exported from the Vicon software. Figure 3.8 below is a Vicon screen capture representation after all markers were labeled.

Because the horse and camel riding portions of this study were conducted in a riding arena (instead of a controlled lab setting), sunlight and other background lighting interfered with the marker IR signals observed by the cameras. This signal noise significantly increased the instances of trajectory gaps of the motion capture recordings. While most horse and camel riding data of motion trajectories were successfully processed and extracted from the Vicon software, the data from Camel 2 riding had too many gaps and was therefore excluded from further analysis.

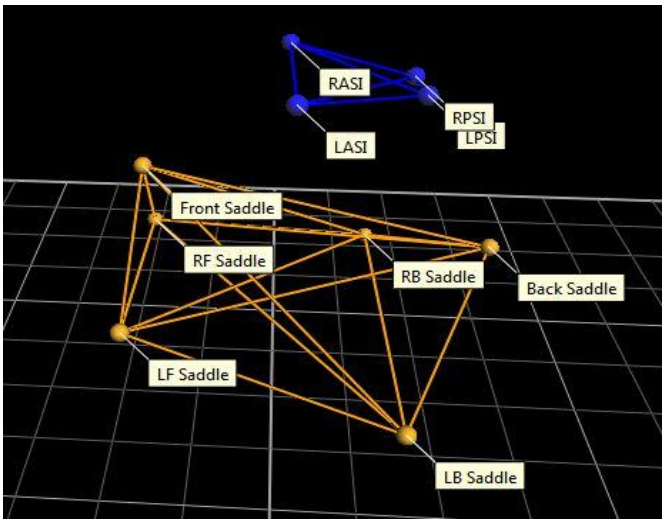


Figure 3.8: Vicon screen capture of human pelvis and horse/camel saddle with all markers labeled

*Dividing and Averaging Gait Cycles*

Because this study was built upon the previous study by Garner and Rigby [27], similar data processing algorithms and procedures were used so that the data collected from this study can be directly compared to the Garner and Rigby study.

Data processing algorithms were designed to achieve the following goals [27].

1. Correct for minor drift of the average forward motion from a straight line aligned with the X-axis.
2. Identify a single period of the gait cycle.
3. Smooth out noise using third order polynomial curve fit.
4. Coerce the data trajectories into periodic form consistent with the cyclic nature of gait.

The following steps were incorporated in the algorithms to achieve the goals [27].

1. Fit a linear regression line to the data in the transverse (x–z) plane and rotate the data until the regression line aligns with the x-axis.
2. Fit a quadratic regression line to the data in the x–z plane and rotate out any quadratic, curved component until the quadratic regression line becomes straight and aligned with the x-axis.
3. Identify consecutive valleys in the y-axis data to mark the beginning and end of a single gait cycle, as shown in Figure 3.9 below.
4. Subtract out the average forward motion.
5. Fit a $5^{th}$ order Fourier series function to the data trajectories and use the function fits to smooth and generate periodic, uniformly-populated data sets by which all trials could be compared in normalized time.

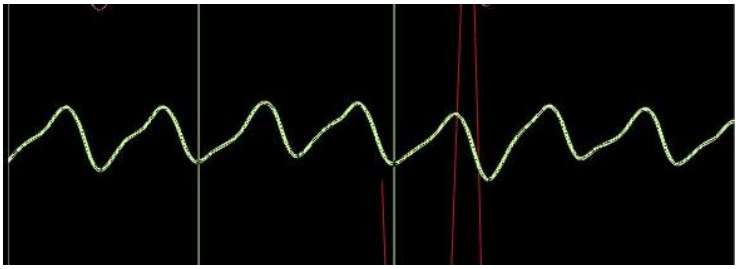

Figure 3.9: A sample graph generated by the algorithms to divide the gait cycles. The highlighted green line in the plot represented the vertical trajectory of the back-saddle (B-Saddle) marker in the X-Y plane. The gait cycle identified here was shown between the two vertical green lines.

The gait cycles were synchronized across trials based on the valley points in the vertical displacement and normalized in time based on gait cycle period [27]. Averages of the pelvic and saddle marker trajectories were computed at each corresponding instant in the normalized time over the trial groups of: (1) each subject; (2) all subjects on each horse and camel; (3) all horses; and (4) all subjects walking. The average of the LPSI and RPSI marker trajectories were computed to represent the trajectory of the center posterior pelvis.

# CHAPTER FOUR

## Results

There are six variables of interest presented in this chapter: pelvic displacements in the Forward (X), Vertical (Y), and Lateral (Z) directions, and pelvic angles including list (X-axis rotation), twist (Y-axis rotation), and tilt (Z-axis rotation). Along the x-axis, the anterior direction was defined as the positive direction; along the y-axis, the upwards direction was defined as positive; and, along the z-axis, the rightward direction was defined as positive. Data for each of the six variables are presented versus normalized cycle time. In addition, displacement data is presented in spatial form as: frontal displacement versus lateral displacement (top view), vertical displacement versus lateral displacement (back view), and vertical displacement versus frontal displacement (side view). The conditions presented include (1) the average of all subjects riding each individual horse and camel at normal speed and on a given saddle; (2) all trials averaged over all horses; (3) the average of all trials of each subject walking (Subject 1,2,4); and (4) the average over all subjects walking. This chapter will present key data results and comparisons. A collection of graphs for all various comparisons can be found in the Appendix.

*Key Results*

The results of the kinematics of human pelvis during horse riding, camel riding, and walking were analyzed in the following order.

1. For each horse/camel, compare the pelvic kinematics of each human subject.
2. Compare the averaged pelvic kinematics generated by each horse/camel
3. Compare the averaged pelvic kinematics of horse-riding, camel-riding and walking

Nine plots were generated for each of the comparisons made. For pelvic displacement and angle comparison plots, the first 50% of the normalized cycles were repeated at the end of the normalized cycles (150% normalized cycle in total) to demonstrate the repetitive nature of the cycles.

1. Frontal displacement (mm) vs. Lateral displacement (Top View)
2. Vertical displacement (mm) vs. Frontal displacement (Back View)
3. Vertical displacement (mm) vs. Lateral displacement (Side View)
4. Frontal (X) displacement (mm) vs. normalized time (0 - 150%)
5. Vertical (Y) displacement (mm) vs. normalized time (0 - 150%)
6. Lateral (Z) displacement (mm) vs. normalized time (0 - 150%)
7. List angles (degrees) vs. normalized time (0 - 150%)
8. Twist angles (degrees) vs. normalized time (0 – 150%)
9. Tilt angles (degrees) vs. normalized time (0 -150%)

*Subject Comparison on Horse 1*

*Spatial views*. Data averaged across all subjects riding on Horse 1 are shown in Figure 4.1. Pelvic displacement from the top view (Figure 4.1A) exhibit an infinity-shape motion pattern for most subjects. From the neutral position, the subjects' pelvises swept laterally with posterior displacement, and then remained lateral during anterior movement, before reciprocating in the other direction. The motion pattern seen in subject 4 is more compressed than the rest because the magnitude of lateral displacement is smaller in subject 4. From the back view (Figure 4.1B), pelvic displacements exhibit an infinity-shape motion pattern as well. The subjects' pelvises moved inferiorly with lateral displacement, remained lateral during superior displacement, before reciprocating in the other direction. From the side view (Figure 4.1C), the subjects' pelvises moved posteriorly with inferior displacement, before moving anteriorly with superior displacement. The loops of pelvic displacement are somewhat compressed along a near 45-degree line. In all three spatial views, the pelvic kinematics of each subject are reasonably aligned with each other.

*Frontal / Vertical / Lateral displacement*. Because each trial was normalized and synchronized according to the peaks and valleys in vertical displacement, the extremes in Figure 4.1E tend to align. Similarly, the peaks and valleys of forward and lateral displacements tend to align. The two peaks and valleys observed in each gait cycle of the vertical displacement likely correspond to the horse's left and right hind limb motions during the cycle. Subject 5 displays a larger range of displacement compared to the other subjects. In pelvic horizontal displacement (Figure 4.1D), there are also two peaks and

valleys that, again, likely correspond to the horse's left and right limb motions. For most subjects, there is one major peak and one minor peak in pelvic forward displacement pattern, suggesting asymmetry where the pelvis moved more anteriorly with the leftward movement of horse 1 than with the rightward movement (The lateral movement directions can be seen in Figure 4.1F). In contrast, subject 5 have two almost equally-sized peaks and valleys in forward displacement. In the lateral displacement (Figure 4.1F), there is one peak and valley that reveals a sway to the left side then the right side. Subject 4 experienced smaller magnitudes of lateral sway than the other subjects.

*Twist / List / Tilt angles.* The twist angle pattern (Figure 4.1G) reveals a single peak in each direction, exhibiting a triangular shape where the subjects' pelvises rotated to one side, followed by a reciprocal rotation to the other side. The list angle patterns (Figure 4.1H) display one rectangular peak and valley, indicating a listing to one side and then a reciprocating list to other side once per gait cycle. The tilt angle patterns (Figure 4.1I) contain two peaks and valleys for each subject, showing that the pelvis rolls backward then forward twice during each gait cycle. While most of the subjects' angle patterns are well aligned, the tilt angle of subject 5 is slightly out of phase compared to the other subjects. Subject 5's pelvis tilted backward and forward slightly earlier than the others.

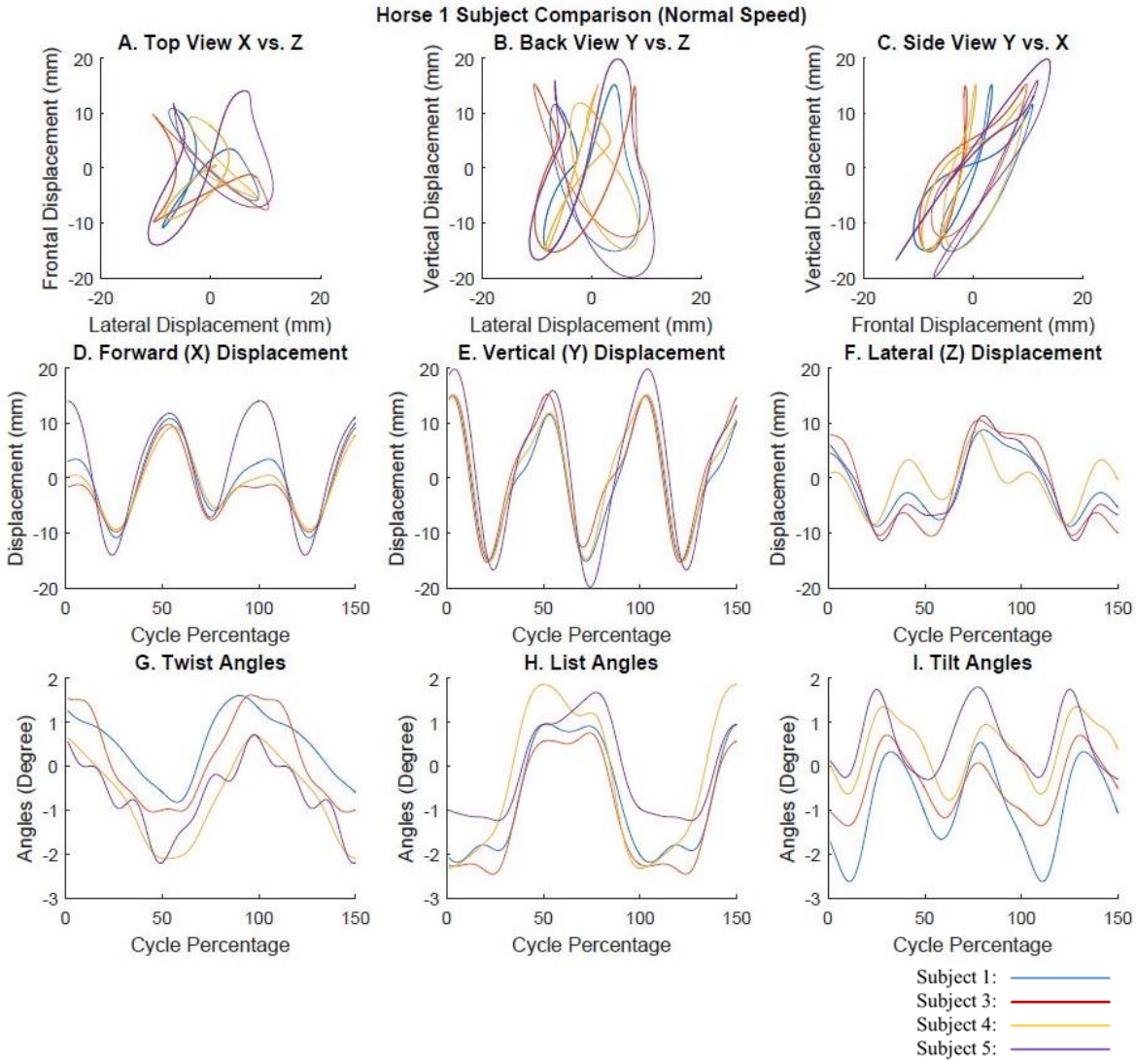


Figure 4.1: Pelvic spatial views (A,B,C), pelvic displacements versus gait-period normalized time (D,E,F), and pelvic angles versus gait-period normalized time (G,H,I) when each subject was riding horse 1. The thin, solid, colored lines correspond to riding averages for each subject.

*Subject Comparison on Horse 2*

*Spatial views*. Data averaged across all subjects riding on Horse 2 are shown in Figure 4.2. Pelvic displacement from the top view (Figure 4.2A) exhibit a horizontally elongated infinity-shape motion pattern for most subjects. The subjects' pelvises swept laterally with slight posterior displacement, and then remained lateral during anterior movement, before reciprocating in the other direction. From the back view (Figure 4.2B), the pelvic displacements exhibit a U-shape pattern. The subjects' pelvises swept laterally, moved superiorly with more lateral displacement, paused at peak vertical displacement, followed by inferior movement with reciprocating lateral displacement towards the other side. Pelvic displacement from the top and back view of all subjects tend to align well. From the side view (Figure 4.2C), the pelvic displacements exhibit a harp-shape pattern. The subjects' pelvises moved superiorly, followed by anterior movement with minimal vertical displacement, before moving inferiorly and repeating the cycle. The pelvic displacement of subject 5 in the sagittal plane exhibit a more compressed shape than the rest of the subjects.

*Frontal / Vertical / Lateral displacement*. The pelvic vertical displacement (Figure 4.2E) and lateral displacement (Figure 4.2F) of all subjects are well aligned. Similar to horse 1, there were two peaks and valleys in vertical displacement and one peak and valley in lateral displacement. However, some variance could be observed in forward displacement (Figure 4.2D). While the peaks and valleys of subjects 1, 3, and 5 are aligned, subject 5 experienced more forward motion (larger peak) around 50% and less forward motion around 100% of normalized cycle. The pelvic horizontal

displacement of subject 4 has more defined peaks, while other subjects display a plateau-shape peaking, showing a more gradual transition between forward and backward motion.

*Twist / List / Tilt angles*. As in horse 1, the twist angle pattern (Figure 4.2G) reveals a single peak in each direction, exhibiting a sinusoidal shape. The list angle pattern (Figure 4.2H) reveals differences between the subjects around 50% of normalized cycle. The pelvises of subject 3 and 4 list more to the right while the pelvises of subject 1 and 5 list more to the left. The tilt angle pattern (Figure 4.2I) reveals differences among all subjects, with subject 3 exhibiting the largest magnitude of tilt angles.

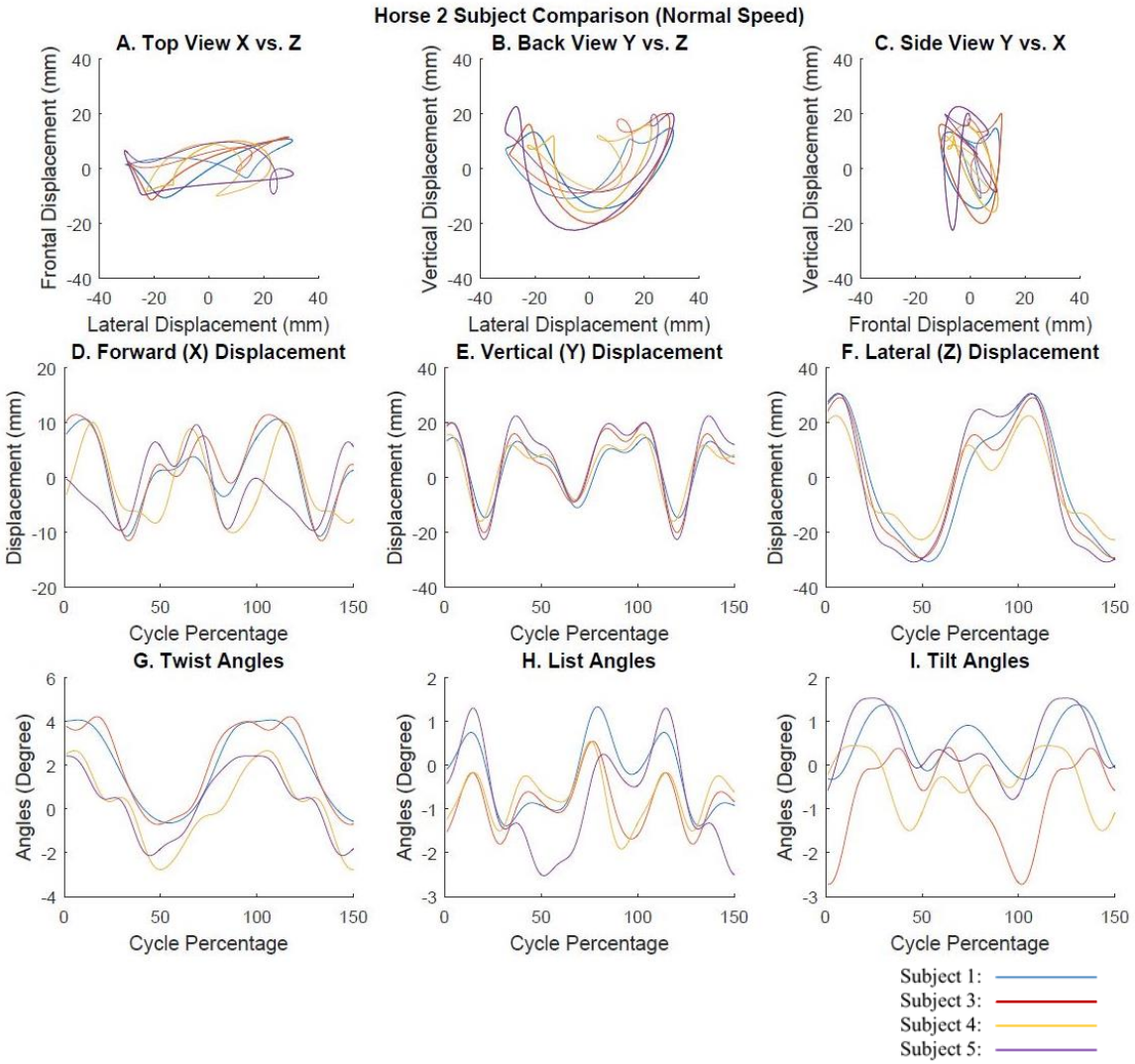


Figure 4.2: Pelvic spatial views (A,B,C), pelvic displacements versus gait-period normalized time (D,E,F), and pelvic angles versus gait-period normalized time (G,H,I) when each subject was riding horse 2. The thin, solid, colored lines correspond to riding averages for each subject.

*Subject Comparison on Horse 3*

*Spatial views*. Data averaged across all subjects riding on Horse 3 are shown in Figure 4.3. Pelvic displacements from the top view (Figure 4.3A) exhibit an 8-shape motion pattern for most subjects. The subjects' pelvises swept anteriorly with slight lateral displacement, and then remained anterior with lateral displacement toward the opposite side, before moving posteriorly with slight lateral displacement and repeating the cycle. From the back view (Figure 4.3B), the pelvic displacements exhibit a distorted circular pattern. The subjects' pelvises swept superiorly with minimal lateral displacement, followed by back and forth lateral displacements with slight vertical displacement, before moving inferiorly and repeating the pattern. Pelvic displacements from the top and back view of all subjects are reasonably aligned. From the side view (Figure 4.3C), the subjects' pelvises moved posteriorly with inferior displacement, before moving anteriorly with superior displacement. The pelvic displacement of subject 5 in the sagittal plane exhibits a more expanded shape than that of the rest of the subjects.

*Frontal / Vertical / Lateral displacement*. The pelvic frontal displacement (Figure 4.3D) and vertical displacement (Figure 4.3E) of all subjects are reasonably aligned. Similar to horse 1, there were two peaks and valleys in horizontal and vertical displacement patterns. In the lateral displacement (Figure 4.3F), some difference between subjects could be observed. Subject 3 and 4 exhibit larger peaks (more rightward sway) around 25% and 75% of normalized cycle, and shallower (less leftward sway) valleys around 50% of normalized cycle.

*Twist / List / Tilt angles*. The overall patterns of twist, list, tilt angles when subjects were riding horse 3 are similar to that of riding horse 1. One peak and valley could be observed in twist and list angle patterns, while two peaks and valleys are found in tilt angle patterns. Some variation could be observed between the subjects. In the list angle pattern (Figure 4.3H), Subject 1 and 3 experienced larger magnitudes of listing around 50% of normalized cycle. The tilt angle pattern (Figure 4.3I) of subject 3 and 5 differ from that of subject 1 and 4. The pelvis of subject 3 tilted backward more than the other subjects, while subject 5 experienced little tilt in either direction.

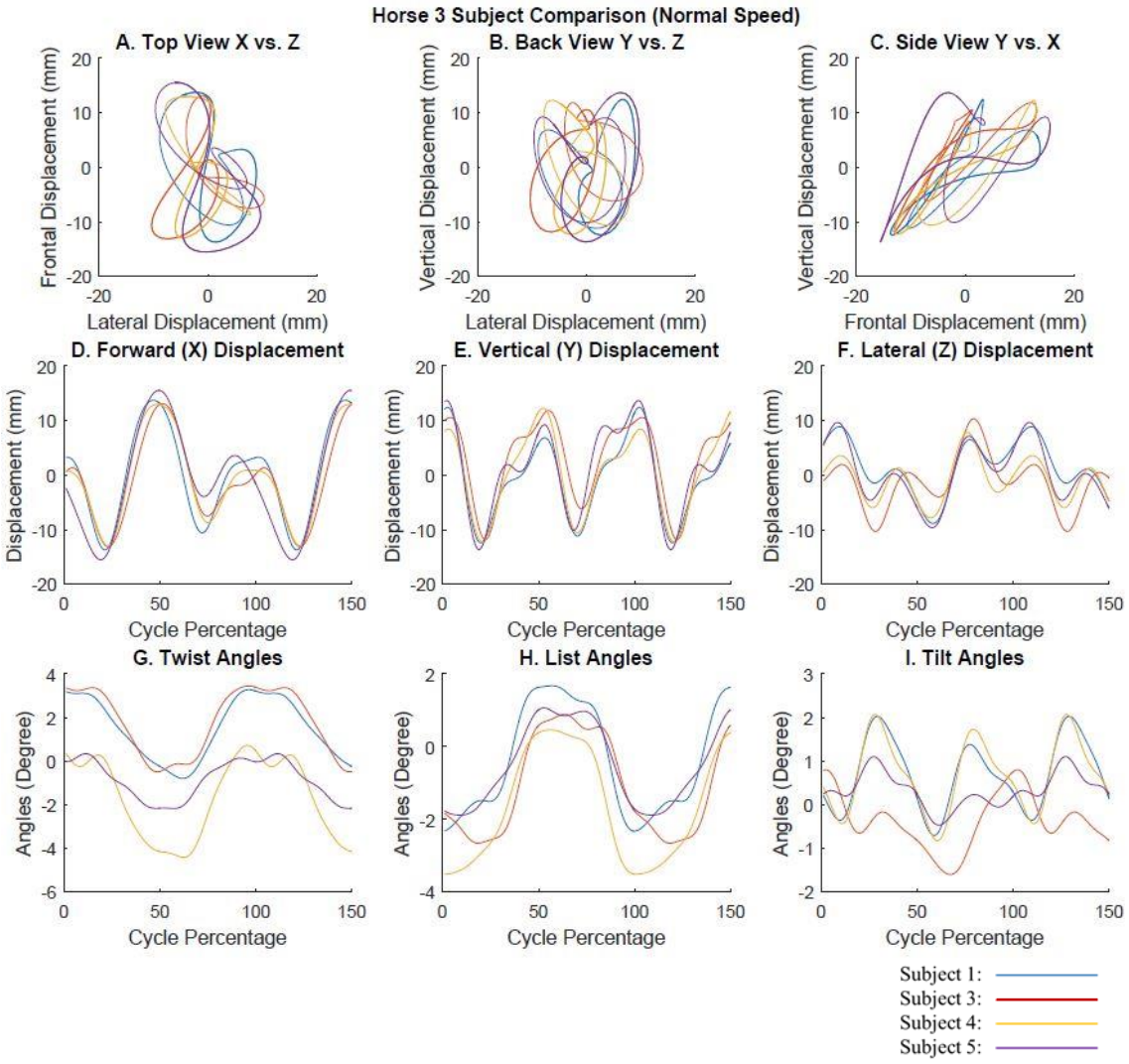


Figure 4.3: Pelvic spatial views (A,B,C), pelvic displacements versus gait-period normalized time (D,E,F), and pelvic angles versus gait-period normalized time (G,H,I) when each subject was riding horse 3. The thin, solid, colored lines correspond to riding averages for each subject.

*Comparison between Horses*

*Average ranges of motion*. Average ranges of motion riding each horse (1, 2, and 3) are compared in Figure 4.4 below. While the horizontal and vertical displacement ranges are similar across horses, the subjects' pelvises experienced significantly larger lateral displacement riding horse 2 compared to riding horse 1 or 3.

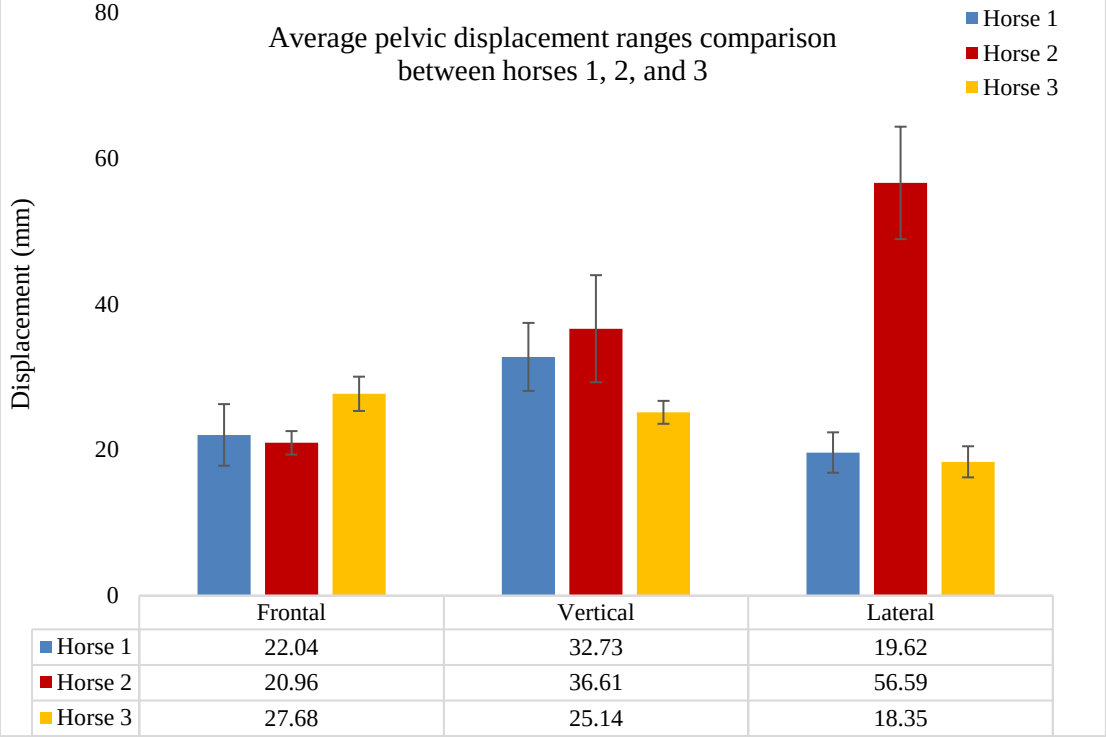


| | Frontal | Vertical | Lateral |
|---|---|---|---|
| Horse 1 | 22.04 | 32.73 | 19.62 |
| Horse 2 | 20.96 | 36.61 | 56.59 |
| Horse 3 | 27.68 | 25.14 | 18.35 |

Figure 4.4: Average pelvic displacement ranges comparison over all subjects riding horses 1, 2, and 3. The error bars correspond to SD of each average range.

*Spatial views*. Motion data averages across all subjects riding each horse are compared in Figure 4.5 below. Pelvic displacements from the top view (Figure 4.5A) exhibit an infinite-shape pattern when subjects were riding horse 1 and 3. The pelvic motion pattern on horse 2 is elongated compared to horse 1 and 3 because of the much larger magnitudes of lateral displacement. Similarly, the pelvic displacement from the

back view (Fig 4.5B) on horse 2 is also elongated to a U shape pattern. From the side view (Fig 4.5C), the loops of pelvic displacement on horse 1 and 3 are somewhat compressed along a near 45-degree line, while the loop on horse 2 is more vertically oriented.

*Frontal / Vertical / Lateral displacement.* While the pelvic frontal displacement (Figure 4.5D) on the three horses all have two peaks and valleys, the peaks and valleys on horse 2 are delayed by about 10% of normalized cycle compared to horse 1 and 3. The pelvic vertical displacement (Figure 4.5E) on all horses have two peaks and valleys as well. Pelvic vertical displacement on horse 1 displays more defined peaks, while horse 2 and 3 display plateau-shaped peaks. The pelvic lateral displacement (Figure 4.5F) on horse 2 has much larger magnitude comparing to horse 1 and 3.

*Twist / List / Tilt angles.* Some differences between the horses could be observed in pelvic angle patterns as well. In the list angle pattern (Figure 4.5H), horse 1 and 3 are well aligned. However, subjects' pelvises when riding horse 2 experienced minimal upward or downward listing with no clear pattern. In the pelvic tilt angle pattern (Fig 4.5I), the pelvic tilt motion experienced by subjects on horse 2 is slightly out of phase compared to tilt experienced on horse 1 and 3. The forward and backward pelvic tilt occurred earlier on horse 2. The twist angle patterns (Figure 4.5G) reveal a single peak in each direction, exhibiting a sinusoidal shape when riding any of the three horses.

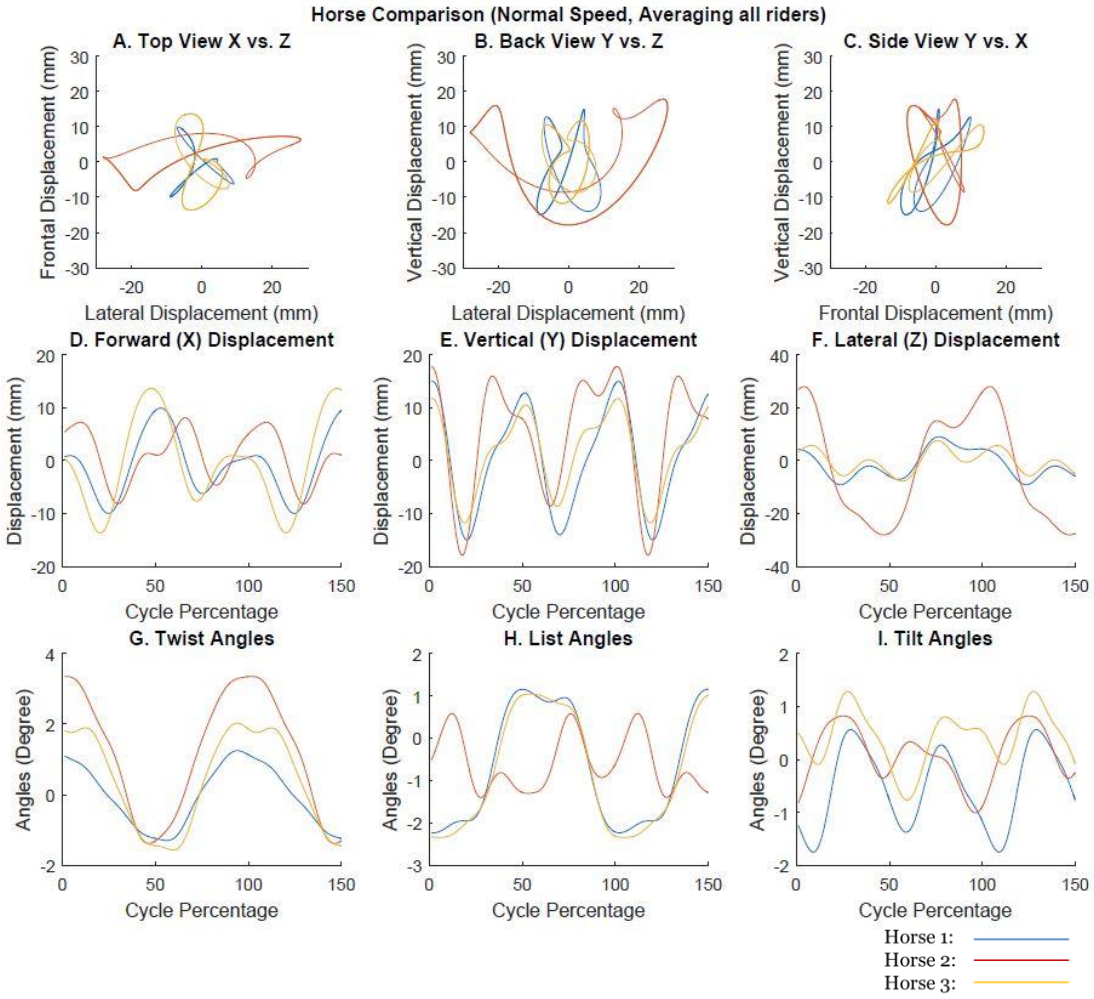


Figure 4.5: Pelvic spatial views (A,B,C), pelvic displacements versus gait-period normalized time (D,E,F), and pelvic angles versus gait-period normalized time (G,H,I) when subjects were riding each horse. The normalized cycles are the average over all subjects' riding trials on each horse (saddle 1, normal speed).

*Subject Comparison on Camel 1*

*Top / Back / Side views*. Data averaged across all subjects riding on Camel 1 are shown in Figure 4.6. Pelvic displacement from the top view (Figure 4.6A) exhibits a distorted infinity-shape motion pattern for most subjects. The subjects' pelvises swept anteriorly with lateral displacement, and then remained lateral during posterior movement, before reciprocating in the other direction. The center point of the infinite-shape pattern for subject 5 is lower than that of subject 1 and 2. Most of the lateral displacement of subject 5's pelvis occurred at the most posterior position, while the lateral displacement of subject 1 and 2's pelvises occurred at the forwardmost position. Pelvic displacement of all subjects from the back view (Figure 4.6B) and the side view (Figure 4.6C) are reasonably aligned. The back views exhibit an infinity-shape pattern. The subjects' pelvises moved superiorly with lateral displacement, remained lateral during inferior displacement, before reciprocating in the other direction. From the side view (Figure 4.6C), the subjects' pelvises moved posteriorly with inferior displacement, before moving anteriorly with superior displacement. The loops of pelvic displacement are somewhat compressed along a near 30-degree diagonal.

*Frontal / Vertical / Lateral displacement*. The frontal (Figure 4.6D) and vertical pelvic displacement patterns (Figure 4.6E) for all subjects have two peaks and valleys, and the pelvic lateral displacement patterns (Figure 4.6F) have one peak and valley, similar to that of horse riding. The forward displacements for all subjects are well aligned, while the vertical displacement extremes of subject 1 occurred earlier than that

of subjects 2 and 5. Similarly, the lateral displacement (Figure 4.6F) extremes of subject 5 occurred earlier than that of subject 1 and 2.

*Twist / List / Tilt angles*. The twist angle patterns (Figure 4.6G) varies between subjects with no clear pattern. One peak and valley could be observed in list angle patterns, while two peaks and valleys could be observed in tilt angle patterns, similar to that of horse riding. The list angle patterns (Figure 4.6H) reveal a listing to one side and then the other once per gait cycle. The tilt angle patterns (Figure 4.6I) reveal that the subjects' pelvises rolled backward then forward twice during each gait cycle. While most of the subjects' angle patterns are well aligned, the tilt angle of subject 1 is slightly out of phase compared to other subjects, tilting backward and forward slightly earlier than the others.

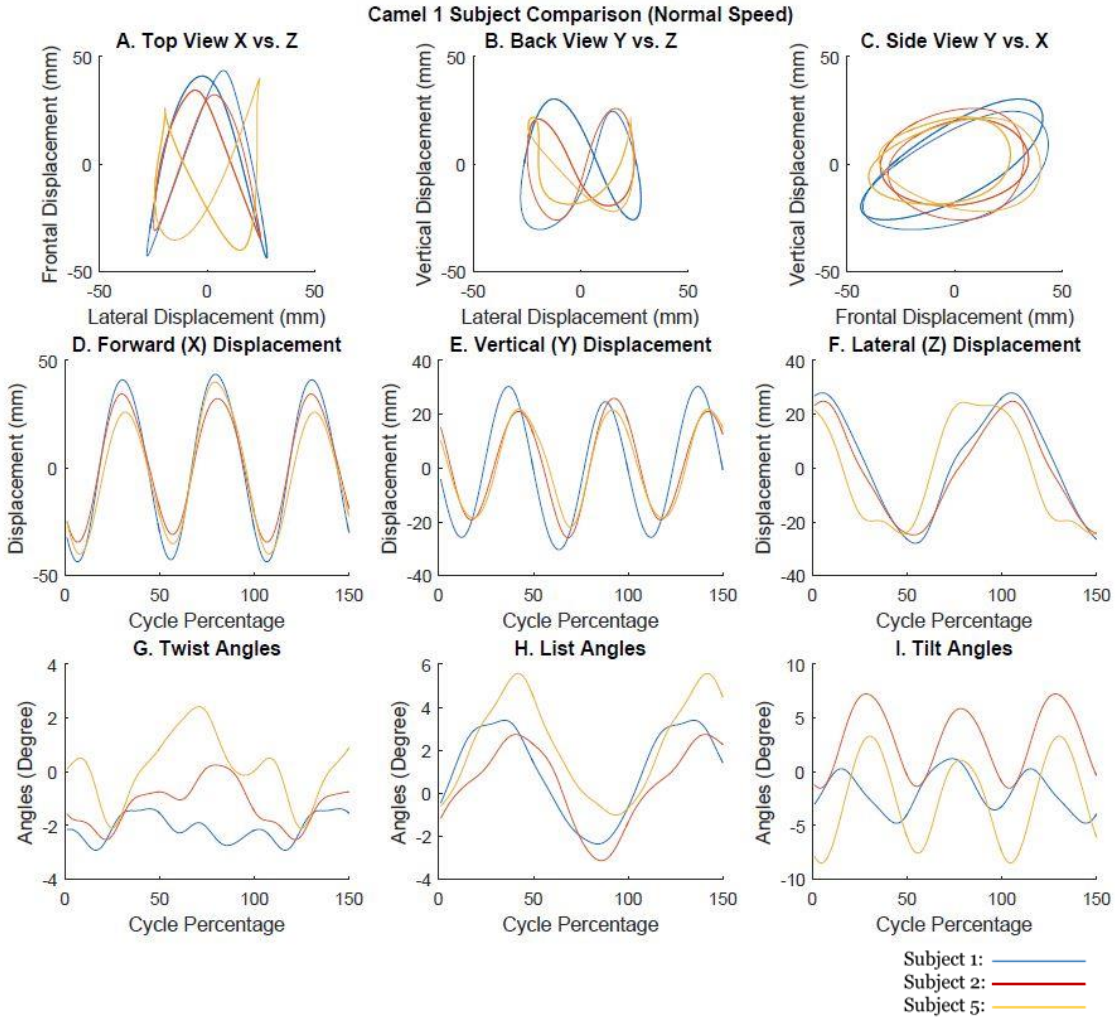


Figure 4.6: Pelvic spatial views (A,B,C), pelvic displacements versus gait-period normalized time (D,E,F), and pelvic angles versus gait-period normalized time (G,H,I) when each subject was riding camel 1. The thin, solid, colored lines correspond to riding averages for each subject.

*Walking Comparison*

*Top / Back / Side views*. Data averaged across all subjects walking are shown in Figure 4.7. Pelvic displacement from the top view (Figure 4.7A) exhibit an infinity-shape motion pattern for all subjects. The subjects' pelvises traveled anteriorly with lateral displacement, and then remained lateral during posterior movement, before reciprocating in the other direction. The center point of the infinite-shape pattern for subject 2 is higher than that of subject 1 and 4. Most of the lateral displacement of subject 1 and 4's pelvises occurred at the most posterior position, while the lateral displacement of subject 2's pelvis occurred gradually as it traveled forward. Like the top view, the back views (Figure 4.7B) exhibit an infinity-shape pattern. The subjects' pelvises moved superiorly with lateral displacement, followed by inferior movement with reciprocate lateral displacement, before repeating the pattern. Circular patterns of pelvic displacement could be observed from the side view (Figure 4.7C). The subjects' pelvises travel inferiorly, followed by anterior movement, before sweeping posteriorly and superiorly. The pelvic motion patterns in the sagittal plane are well aligned for all subjects.

*Frontal / Vertical / Lateral displacement*. The pelvic frontal (Figure 4.7D) and vertical displacement patterns (Figure 4.7E) for all subjects have two peaks and valleys, and the pelvic lateral displacement patterns (Figure 4.7F) have one peak and valley, similar to that of horse riding. The forward, vertical, and lateral pelvic displacements for all subjects are well aligned with similar magnitudes.

*Twist / List / Tilt angles*. One peak and valley could be observed in pelvic twist angle (Figure 4.7G) and list angle (Figure 4.7H) patterns. The twist angle patterns (Figure 4.7G) show the subjects' pelvises rotating back and forth once per gait cycle. The list angle patterns (Figure 4.7H) reveal a listing to one side and then the other once per gait cycle. The tilt angle patterns (Figure 4.7I) reveal that the subjects' pelvises rolled backward then forward twice during each gait cycle. The twist, list, and tilt angle patterns for all subjects are well aligned. Subject 2 experienced larger magnitudes in twist and tilt angles and smaller magnitudes in list angle compared to subject 1 and 4.

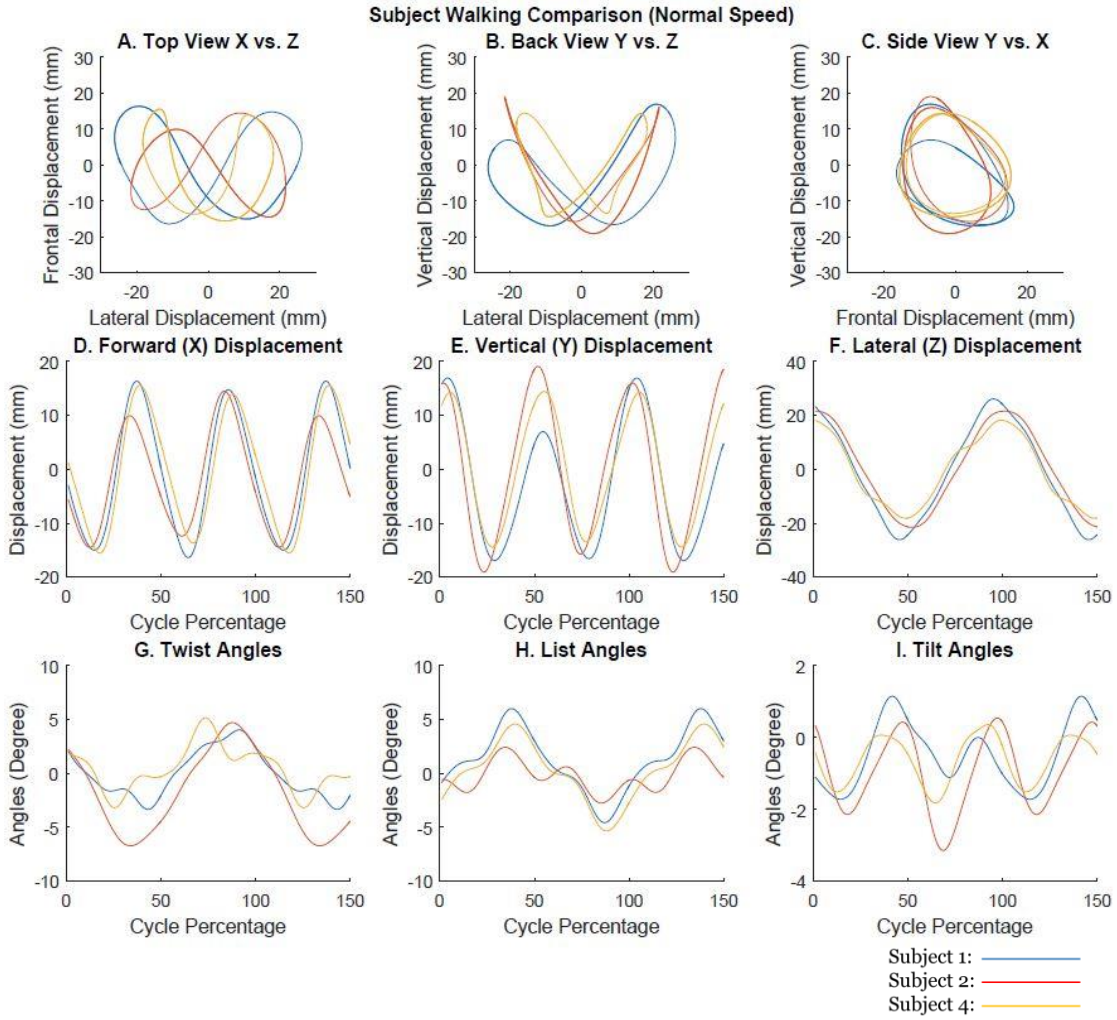


Figure 4.7: Pelvic spatial views (A,B,C), pelvic displacements versus gait-period normalized time (D,E,F), and pelvic angles versus gait-period normalized time (G,H,I) when each subject was walking. The thin, solid, colored lines correspond to walking averages for each subject.

# CHAPTER FIVE

## Discussion

The purpose of this study was to measure and compare human pelvic kinematics during natural walking, horse riding, and camel riding. Motion capture of human pelvis kinematics from three human subjects walking, riding on three horses, and riding on one camel was recorded and reported. The motion data was smoothed, segmented into individual cycles, and averaged to quantify pelvic displacement patterns (horizontal/vertical/lateral) and orientation patterns (tilt/list/twist) for the different riders, different horses, the camel, and for human walking. In this chapter will be discussed the major contributions of the study, key take-aways from the results, lessons learned from outdoor data collection, study limitations, and proposals for future work.

### *Contribution*

To the author's knowledge, this study is the first to compare human pelvic motion during camel riding, horse riding, and natural walking. The cyclical pelvic motion patterns observed during riding and walking provided more evidences to support the prevailing rationale of HPOT, that the horse induces in the rider's body a repetitive and cyclic pattern of motion that is similar to that of natural human walking [26-29]. This study built on previous work of Garner and Rigby but is novel in several key aspects [27]. Whereas Garner and Rigby collected pelvis motion using only posterior pelvic markers and did not report pelvis tilt angle, this study analyzed all three degrees of freedom, including tilt, list, and twist of the human pelvis. This study included five

adolescent and adult subjects instead of child subjects recruited in the study by Garner and Rigby [27]. This study also included a camel, and different horses than in the Garner and Rigby study, which is significant given the variability in motion patterns across different horses. This study utilized more modern and capable motion capture equipment, which allowed for capture of more data than in the previous studies, such as a greater number of markers on the rider's body, and animals body, though such data is not the focus of this thesis. Finally, the outdoor motion capture techniques were refined during this study to overcome the challenges presented by a non-ideal environment. Experiences gained in the process will improve the efficiency and results of similar outdoor studies in the future.

## *Comparison with Previous Studies*

### *Walking Motion Compared to Previous Studies*

Comparing the walking data of this study to similar data from previous studies demonstrates that the gait motion patterns exhibit by the subjects in this study are fair representations of natural human gait. Lewis et al. collected pelvic motion data on 44 healthy individuals (22 males and 22 females) while walking on an instrumented force treadmill [7]. Figure 5.1 is a side-by-side comparison of the pelvic angle plots produced by Lewis et al. with the results from this study. The general patterns of pelvic tilt, list, twist during a normalized gait cycle are similar. Both studies show a sinusoidal double-peak pattern in pelvic tilt, similar triangular pattern in pelvis list (obliquity), and one rotation to each side in pelvic twist (rotation).

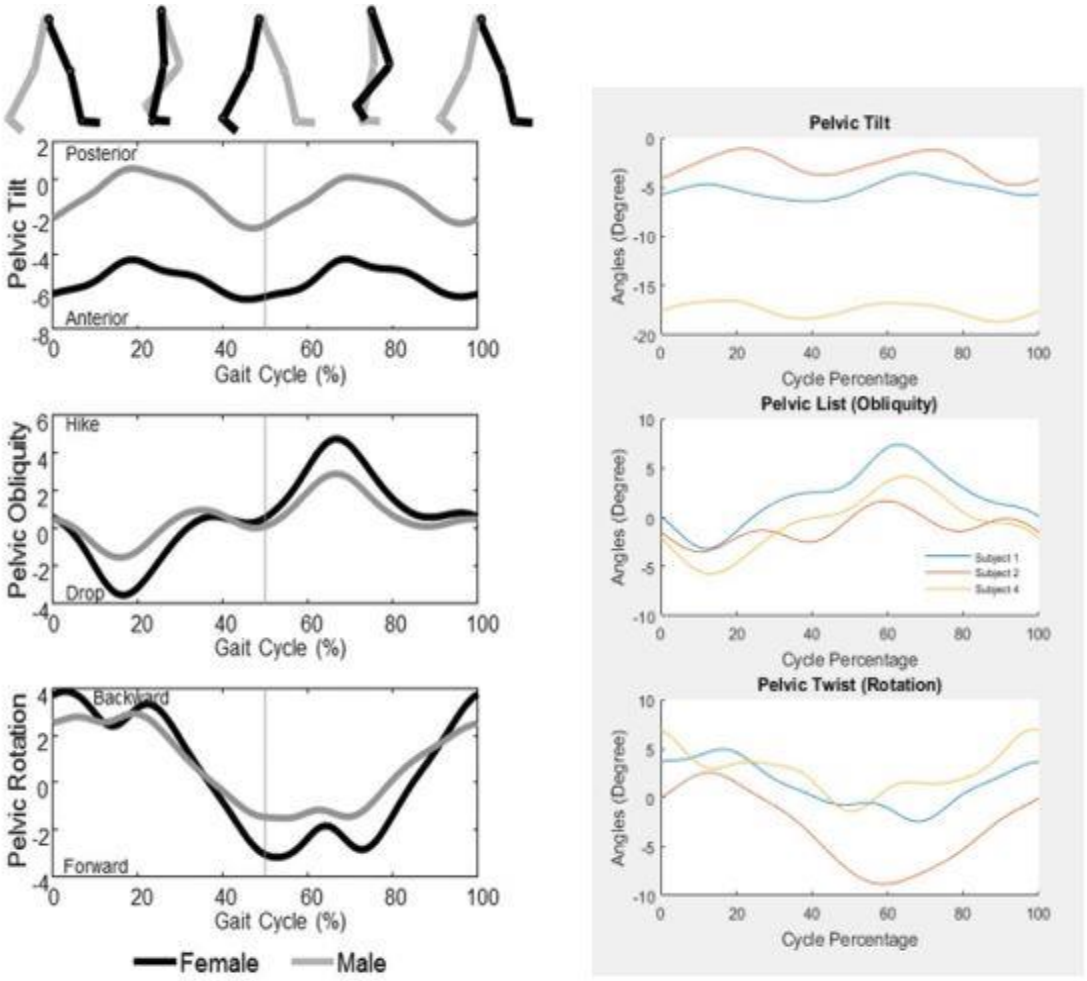


Figure 5.1: Pelvic angles (in degrees) comparison during walking: results from Lewis et al. (left) [7]; results from this study (right)

The pelvic angle ranges from this study also compared well with the Lewis et al. study (Figure 5.2). They reported the average of pelvis tilt angle ranges as 4.3 degrees with an SD of 1.1 degrees [7], which was slightly above 2.9 degrees with an SD of 0.8 degrees observed in this study. The average of pelvic list angle ranges was 7.4 degrees and SD of 2.5 degrees in the Lewis et al. study [7], which was similar to the average of 8.6 degrees and SD of 3.0 degrees observed in this study. The average of pelvic twist angle ranges was 9.5 degrees and SD of 2.9 degrees, which was close to the average of 9.1 degrees and SD of 2.1 degrees observed in this study. Both studies measured

subjects' pelvic motion at subjects' self-selected paces, which could explain the variation of results between the two studies.

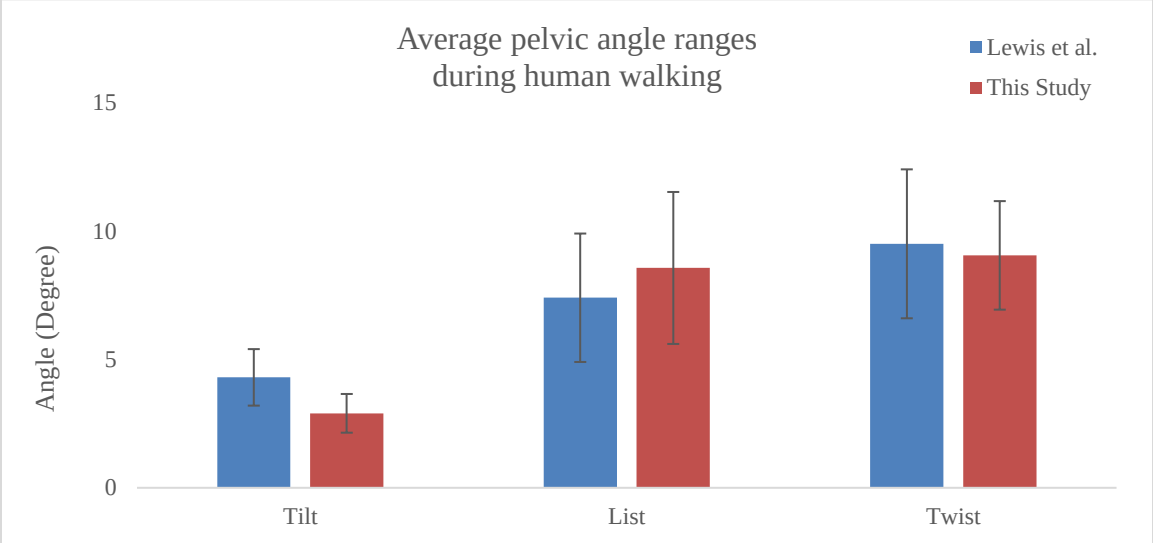


Figure 5.2: A comparison between average pelvic angle ranges (in degrees) during human walking observed in previous study by Lewis et al. and this study. The error bars correspond to SD of each average range.

*Riding Motion Compared to Previous Studies*

This study utilized similar protocols to those of the study by Garner and Rigby [27]. Therefore, the riding motion can be compared directly. Figure 5.3 is a set of pelvis displacement plots generated by Garner and Rigby. Figure 5.4 is the same set of pelvis displacement plots presenting the results from this study.

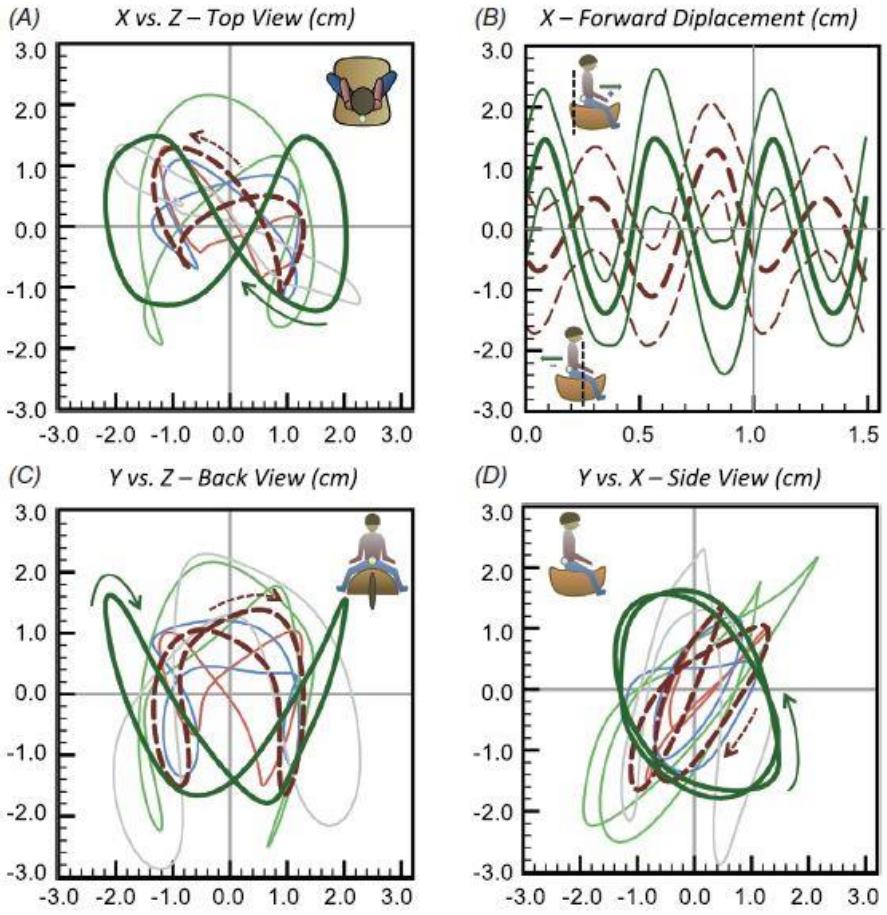


Figure 5.3: From the study of Garner and Rigby, average pelvis displacements shown spatially (A,C,D) and versus gait-period normalized time (B) for human gait (solid green lines) and when riding (dash red lines). The thin, solid, colored lines are riding averages for the individual horses [27].

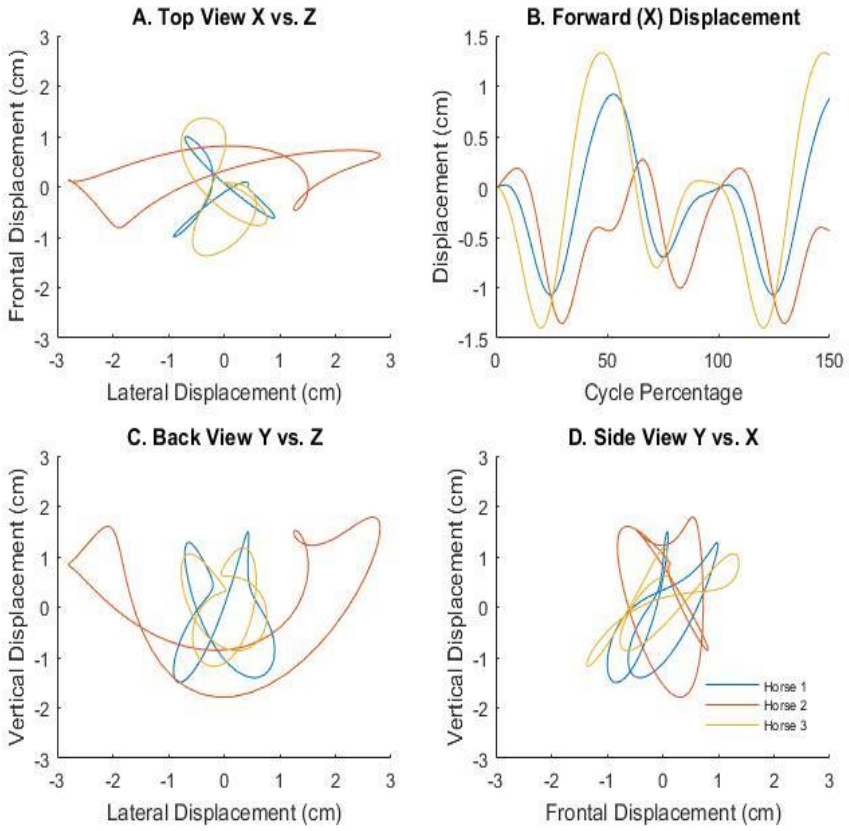


Figure 5.4: Average pelvis displacements from this study shown spatially (A,C,D) and versus gait-period normalized time (B) when riding horses. The thin, solid, colored lines are riding averages for the individual horses.

Pelvic displacements from the top and back view (Figure 5.4 A,C) of this study exhibit more variance between horses. While the motion patterns of horses from the top and back views of the Garner and Rigby study reasonably overlap with each other, each horse from this study exhibits a different motion pattern. From the side view, the loop from this study is somewhat compressed along a 45-degree line. This feature is also observed in the side views reported by Garner and Rigby [27].

The average pelvic motion ranges observed when riding a horse in this study are smaller compared to those of previous studies (Figure 5.5). The average vertical displacement range of 29.8 mm with SD of 6.1 mm observed in this study is less than the

40 mm average reported by Garner and Rigby [OO]. The 29.9 mm average lateral displacement range with SD of 22.7 mm observed in this study is also less than the 40 mm average reported by Garner and Rigby and 56 mm average reported by Fleck [27, 35].

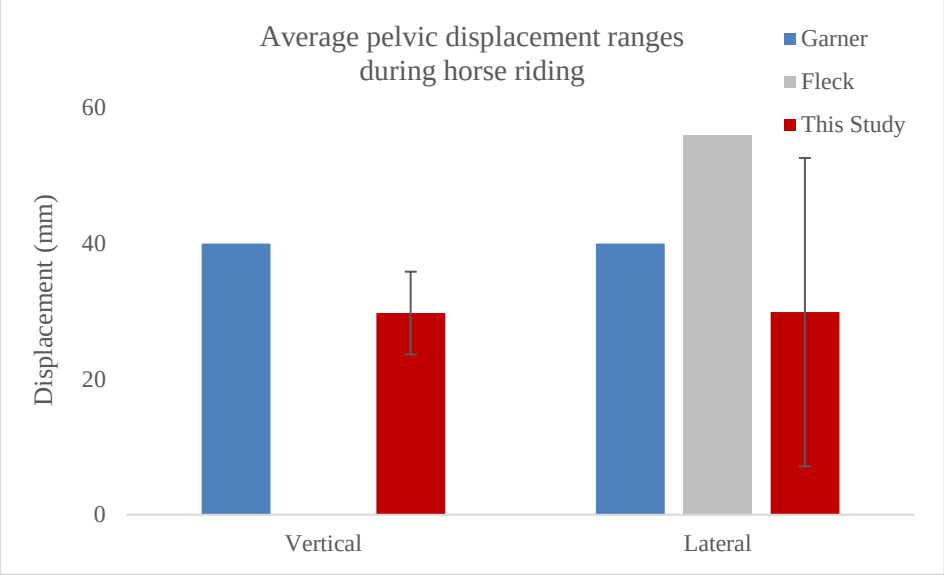


Figure 5.5: A comparison between average pelvic displacement ranges during horse riding observed in previous studies and this study. The error bars correspond to SD of each average range.

Several other studies reported pelvic angles of human subjects during horse riding (Figure 5.6). Bystrom et al., as well as Garner and Rigby, reported the average pelvic twist angle ranges to be 6.2 degrees and 5.7 degrees, respectively, which are larger than the 3.6 degrees with SD of 1.1 degrees observed in this study [27,58]. Garner and Rigby, Bystrom et al., and Fleck also reported the average ranges of pelvic list angle to be 7.9 degrees, 5.6 degrees, and 10 degrees, respectively [27,35,58]. All these results are larger than the 2.9 degrees average with SD of 0.8 degrees observed in this study.

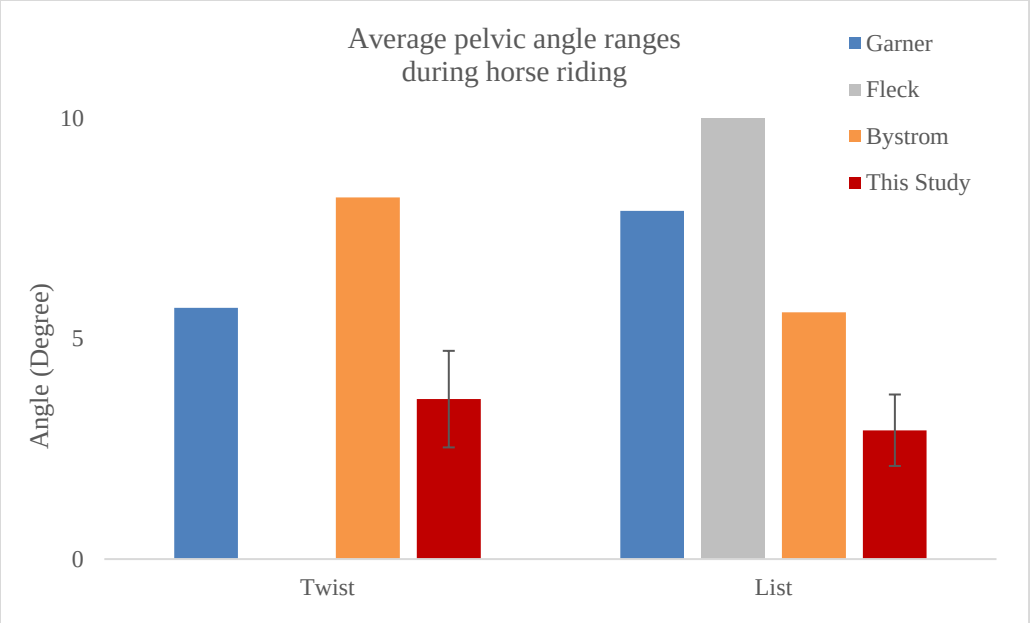


Figure 5.6: A comparison between average pelvic angle ranges during horse riding observed in previous studies and this study. The error bars corresponded to SD of each average range.

A possible explanation for the difference of results between this study and previous studies is variation within riders and horses. From Figure 4.4 it is obvious that pelvic motions on horse 2 have significantly larger ranges than any other horses. The variance between the horses could be caused by differences in girth, height, and species [32]. In addition, it is likely that there is more variance between subjects of this study compared to the Garner and Rigby study. All subjects of the Garner and Rigby study were children of similar age, weight, and height. The subjects of this study are more varied in age, weight, and height compared to the Garner and Rigby study [27]. Finally, the gait speed of the horses was not carefully controlled in this study. It is possible that the average gait speed of horses in this study was slower than that of previous studies, which could lead to smaller ranges of motion experienced by the human subjects of this study.

## *Variations between the Horses and Subjects*

### *Variations between Horses*

There were substantial differences in pelvic motions between the three different horses ridden in this study. While the horizontal and vertical displacement ranges are similar across horses, the subjects' pelvises experienced significantly larger lateral displacement riding horse 2 (56.59 mm) compared to riding horse 1 (19.62 mm) or 3 (18.35mm). Pelvic displacements from the top view (Figure 4.5A) exhibit an infinite-shape pattern when subjects were riding horse 1 and 3. The pelvic motion pattern on horse 2 is elongated compared to horse 1 and 3 because of the much larger magnitudes of lateral displacement. Similarly, the pelvic displacement from the back view (Fig 4.5B) on horse 2 is also elongated to a U shape pattern. From the side view (Fig 4.5C), the loops of pelvic displacement on horse 1 and 3 are somewhat compressed along a near 45-degree line, while the loop on horse 2 is more vertically oriented.

The variation between the averaged subjects' pelvic motion patterns on each horse could be attributed to the difference of horses' girth, stride length, and breed [32]. While the girth or stride length of the horses was not measured in this study, it is known that horse 1, 2, and 3 all belong to different breeds. Horse 1 was a Paint mare, horse 2 was a Thoroughbred, and horse 3 was an Appaloosa gelding. Differences in gait patterns, such as stance times, swing times, and stride frequencies of horses were observed between difference species in previous studies [59-61]. The potential difference in horses' gait patterns during this study could induce differences among subjects' pelvic motions.

*Variations between Subjects*

Some minor variation could be observed between the subjects. On horse 1, subject 5 displays a slightly larger range of vertical displacement compared to the other subjects (Figure 4.1E). On horse 3, subject 3 experienced more backward tilt (Figure 4.3I) than the other subjects. The difference between the subjects' weight and height (Table 3.1) could potentially lead to variations in pelvic motion patterns.

However, when comparing the motion patterns of the subjects on each horse (Figure 4.1 A,B,C; Figure 4.2 A,B,C; Figure 4.3 A,B,C), the predominant trend is that the motion patterns of the subjects mostly overlap on every horse. Furthermore, the pelvic displacements and angles show similar patterns as well (Figure 4.1, 4.2, 4.3). The similarity between the subjects is in sharp contrast with the significant difference between horse 2 and horse 1&3. Therefore, it is likely that the horses and the camel dictated the motion patterns experienced by the subjects during the course of this study.

## *Similarities and Differences between Walking, Camel Riding, and Horse Riding*

*Similarities*

The results of this study indicated that there are remarkable similarities between the human pelvic motions when walking, riding on a horse, and riding on a camel. Subjects experienced similar patterns of motion when riding the camel and walking. Figures 5.7 and 5.8 below compare the average ranges of motion for each condition and reveal that the ranges for horse riding and walking are similar.

The three measurements with strong similarity between horse riding and walking are: frontal displacement, vertical displacement, and tilt angle. Between camel riding and walking, the ranges of lateral displacement and list angle share strong similarities. Finally, the ranges of pelvic tilt angle between horse riding and camel riding are similar.

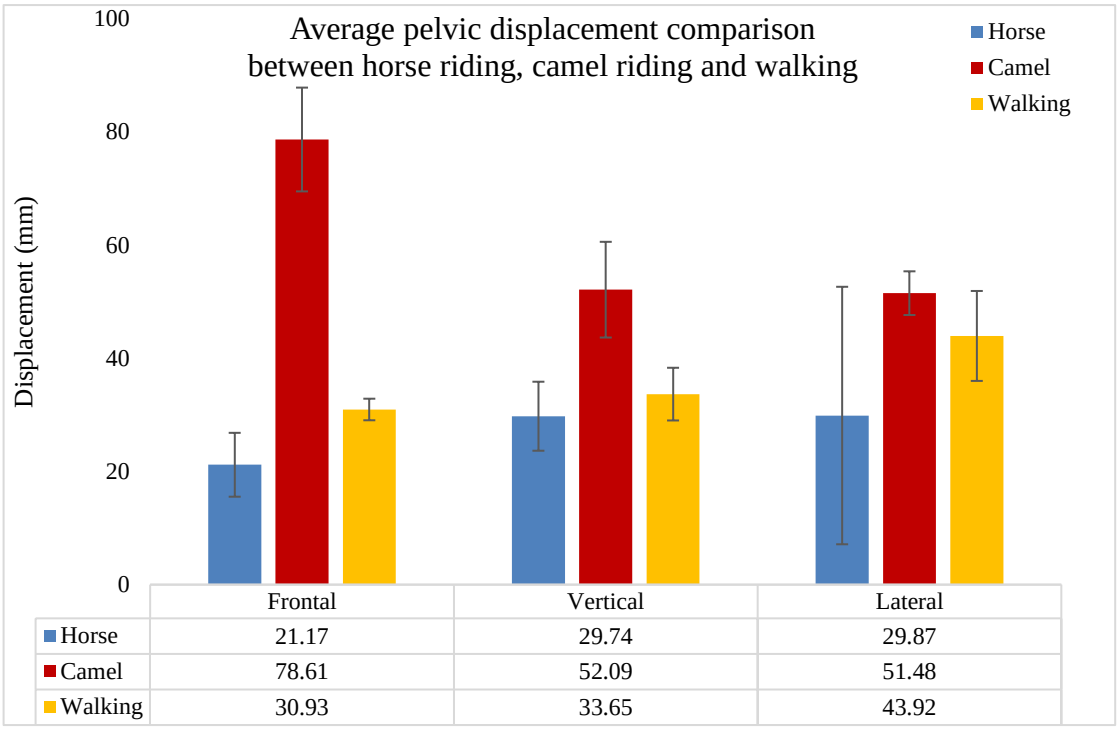


| | Frontal | Vertical | Lateral |
|---|---|---|---|
| Horse | 21.17 | 29.74 | 29.87 |
| Camel | 78.61 | 52.09 | 51.48 |
| Walking | 30.93 | 33.65 | 43.92 |

Figure 5.7: Average pelvic displacement ranges comparison between horse riding, camel riding, and walking. The error bars correspond to SD of each average range.

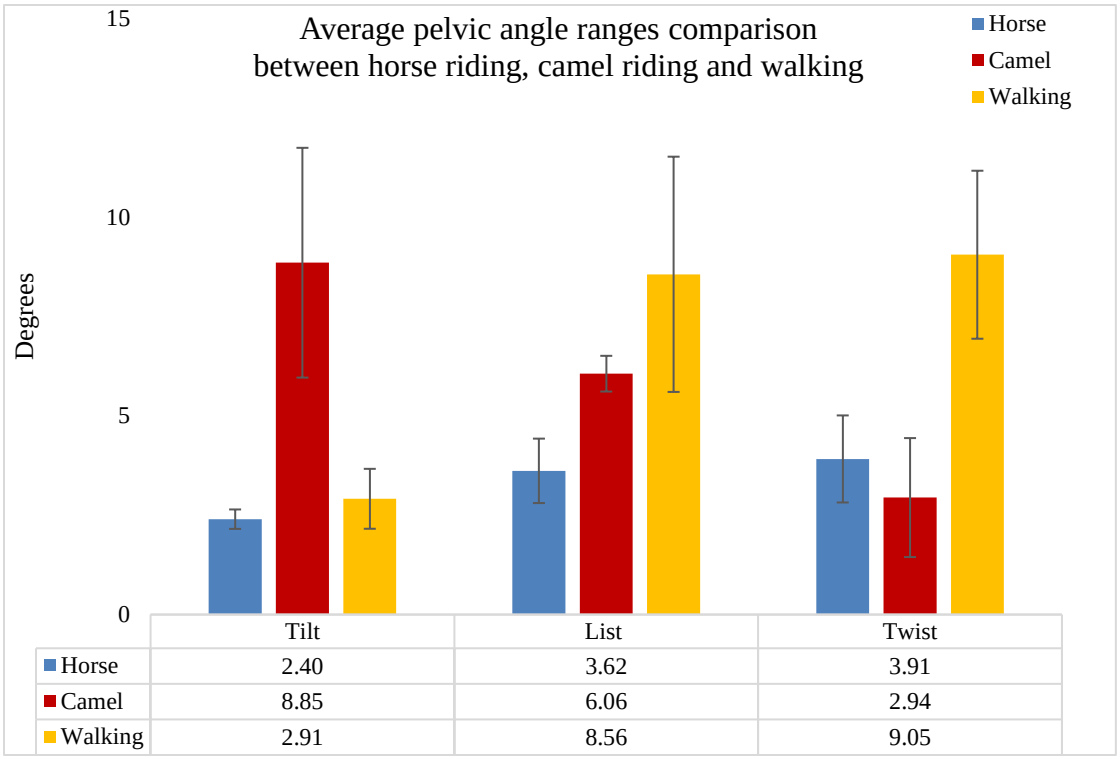


| | Tilt | List | Twist |
|---|---|---|---|
| Horse | 2.40 | 3.62 | 3.91 |
| Camel | 8.85 | 6.06 | 2.94 |
| Walking | 2.91 | 8.56 | 9.05 |

Figure 5.8: Average pelvic angle ranges comparison between horse riding, camel riding, and walking. The error bars correspond to SD of each average range.

In addition to ranges of motion, the general patterns of motion for horse and camel riding also exhibit many similarities with those of walking. Motion data average across all subjects riding all horses, riding the one camel, and walking are compared in Figure 5.9 below. The top view (Fig 5.9A) of the pelvic motion show that for all three activities the overall patterns exhibit an infinity shape. The subjects' pelvises move in similar directions when riding the camel and walking. In both scenarios, the pelvises swept anteriorly with lateral displacement, and then remained lateral during posterior movement, before reciprocating in the other direction. Similar to the top view, the back views (Figure 5.9B) of pelvic motion display a distorted infinity-shape pattern. When riding the camel and walking, the subjects' pelvises moved superiorly with lateral displacement, remained lateral during inferior displacement, before reciprocating in the

other direction. The side views (Fig 5.9C) reveal pelvic trajectories that made two loops each gait and riding cycle. The loops are oval for both walking and camel riding, and the pelvises traveled in a counterclockwise direction in both cases.

For horse riding, camel riding, and walking, the forward and vertical displacement (Fig 5.9D and E) as well as tilt angle patterns (Fig 5.9I) exhibit fairly sinusoidal shapes with double peaks and double valleys each cycle. The lateral displacement patterns (Fig 5.9C) exhibit a sinusoidal shape with one peak and valley for camel riding and walking. Likewise, the list and twist angle patterns (Fig 5.9G and H) exhibit patterns of single major peaks and single major valleys each cycle for all three activities. The peaks and valleys of twist and tilt angle patterns for camel riding and walking are well aligned.

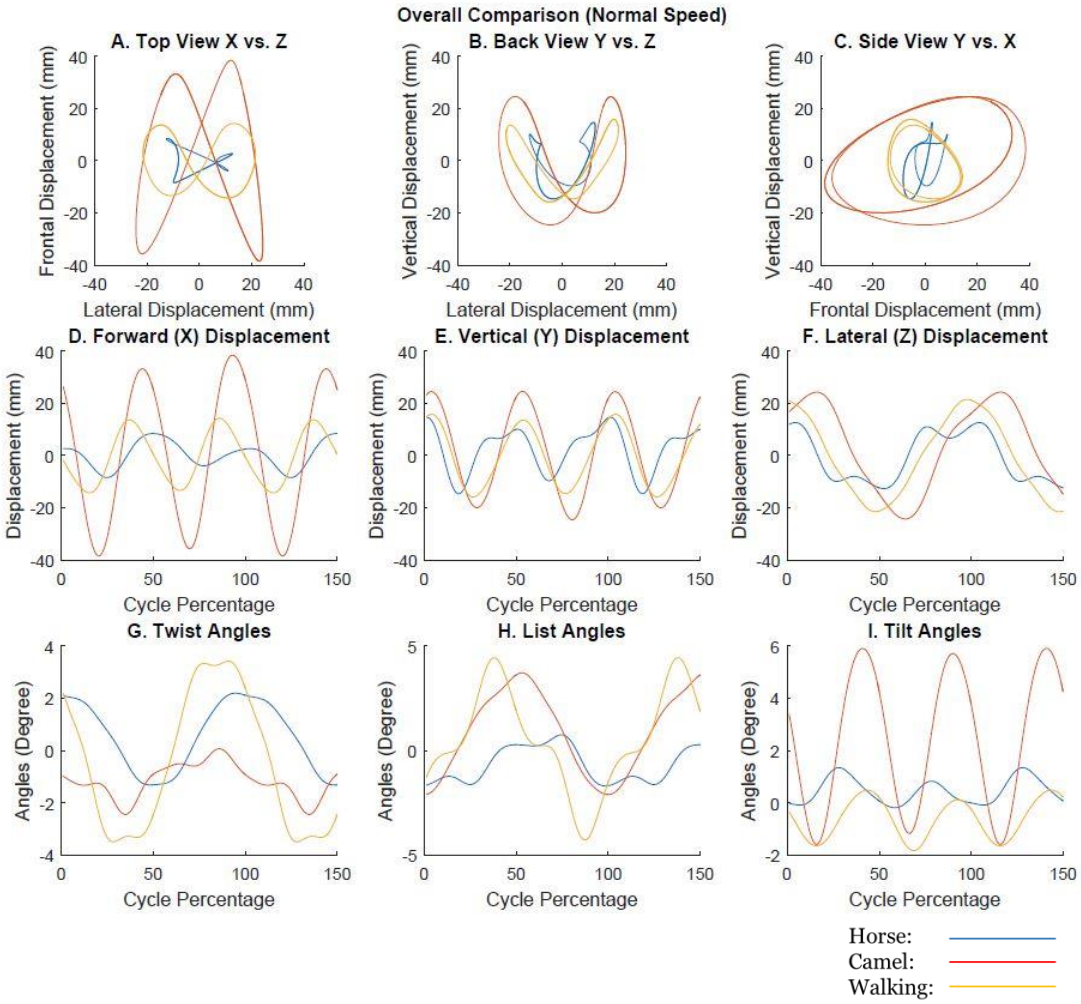


Figure 5.9: Pelvic spatial views (A,B,C), pelvic displacements versus gait-period normalized time (D,E,F), and pelvic angles versus gait-period normalized time (G,H,I) when subjects were riding horses, camel and walking. The normalized cycle for horse riding is the average over all subjects' riding trials on all horses (saddle 1, normal speed). The normalized cycle for camel riding is the average over all subjects' riding trials on camel 1 (normal speed). The normalized cycle for walking is the average over all subjects' walking trials (normal speed). The thin, solid, colored lines correspond to averaged horse riding cycle, camel riding cycle, or walking cycle.

*Differences*

Some distinct differences can be observed between the motion patterns of the human pelvis during walking, horse riding, and camel riding. The forward displacement and vertical displacement ranges of pelvic motion for camel riding are significantly larger than that of horse riding and walking (Figure 5.7). This is likely due to the much longer leg length and stride length of camels compared to horses or human. Likewise, the amplitudes of tilt angle for camel riding are larger than that of horse riding and walking (Figure 5.8). The subjects' pelvises when riding the camel experienced much more anterior and posterior tilt compared to riding horses or walking. When the subjects were walking, their pelvises listed and twisted to a larger degree compared to riding horses or camel. This observation likely means that more muscle activation would be required to keep the pelvis level and maintain the direction of travel was required when the subjects were walking.

Some qualitative differences in motion patterns between walking, horse riding, and camel riding could also be observed in Figure 5.9. The top view, back, and side views (Fig 5.9 A,B,C) of pelvic motion show that the areas of the camel riding motion pattern are the largest, followed by walking and horse riding. This observation further affirms that camel riding generated the most dynamic motion in subjects' pelvises. The pelvises' direction of travel is a key difference between the riding conditions. From the top view (Figure 5.9A), the pelvises moved anteriorly with lateral displacement, and then remained lateral during posterior movement during camel riding and walking. On the contrary, the pelvises moved anteriorly with little lateral displacement, and then traveled laterally with posterior movement during horse riding. The side views (Figure 5.9C) also

reveal similar directional differences between walking/camel riding and horse riding. During walking and camel riding, the pelvises dropped inferiorly along the posterior edge of the loop, and rises along the anterior edge, moving anteriorly along the inferior edge, resulting in a counterclockwise looping motion as viewed from the right side. During horse riding, the loop was moving superiorly, followed by anterior displacement with little vertical movement, and then moving posteriorly and inferiorly, resulting in a clockwise looping motion.

The lateral displacements and list angles (Figure 5.9F and H) for horse riding reveal flattened plateaus at each major peak instead of shape transition seen in walking and camel riding. The flatten plateaus at major peaks of horse riding suggest the pelvis remains listed at the maximum/minimum angles longer when compared to walking and camel riding. This feature is likely caused by the quadruped movement of the horses. From the video recordings of the trials, the heel strike of the front and rear limbs (on either side) of the horses did not occur at the same time. This delay between front and rear limbs' heel strikes prolonged the maximum pelvic listing and lateral displacement. While camels are also quadrupeds, their front and rear limbs' heel strikes (on either side) were more synchronized, and a sharp peak and valley was observed as that of human walking.

While there are differences between the subjects' pelvic motion patterns when riding the three horses and the camel, it is possible that the motions generated by each type/breed of animals are beneficial for specific groups of patients. For example, it is possible that Arabian camels might be better suited for patients with autism, while

thoroughbred horses might be more effective in helping patients regain mobility after cerebral vascular accidents.

## *Practical Lessons Learned*

Use of an optical motion capture camera system to record animal and human kinematics in an outdoor setting is rarely documented in the literature [47,51]. During the process of this study, many experimental procedures and setups were adjusted and refined to address the challenges of using motion capture in an outdoor environment. In the following sections are described some of the major lessons learned through this process.

### *Lighting Conditions*

One of the main challenges of using passive optical motion capture outdoors is the background lighting. Infrared radiation from many sources, including sunlight, will interfere with the motion capture cameras. If the background lighting is varying during the trials, the recordings will contain too much noise (Figure 5.10) and the kinematic results will not be accurate.

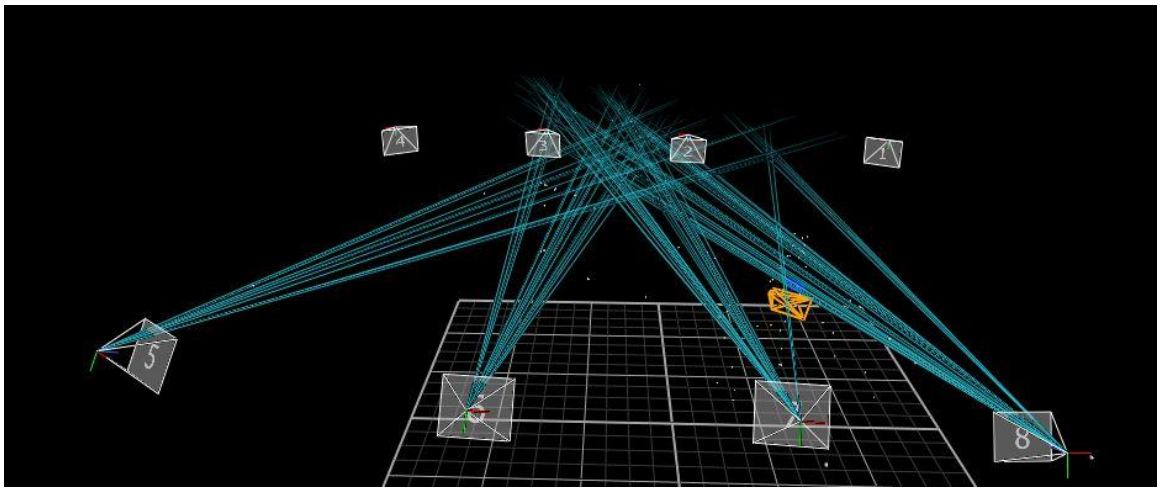


Figure 5.10: An illustration of a motion capture recording with significant background noise. Each blue array indicates a "ghost" marker (a false marker reconstruction that appears as an additional marker) capture by the cameras.

The camel and horse riding sessions from this study were conducted in a covered riding arena from around 9:00 a.m. till 3:00 p.m. on two sunny days. A significant amount of lightening came through the opening between the fences of the area and the roof. During the camel riding sessions, attempts were made to block the sunlight with tarps, as shown in Figure 5.11 below. This measure was effective until increasing winds kept tending to blow the tarps out of their clamps. During the horse riding session, the study was conducted in a shaded area of the arena. However, the shade varied during the day, and the quality of recordings was not consistent. Some motion capture system adjustments, including changing the position of the cameras to be up high pointing downwards, reducing the aperture of the cameras, adjusting the sensitivity and circularity internally for what constitutes a reflective marker in the software, masking the cameras, and recalibrating the system, helped to improve the overall quality of the recordings.

Figure 5.11: Tarp used in this study to block the sunlight

*Marker Placement on Animals*

Placing motion capture markers on animals is challenging. It is difficult to secure the markers on the animals, especially on the extremities. The fur from the animals may also reduce the visibility of the markers to the cameras. While the larger size markers may increase the visibility of the markers, these markers are more likely to interfere with the movement of the animals. In this study, the markers used were first attached to leather straps with screws. The leather straps were then attached to the anatomical landmarks of the animals using duct tape and elastic athletic tape, as shown in Figure 5.12. (The silver duct tape initially used in this study was reflective and interfered with the motion capture system. It was replaced with black duct tape to minimize the interference.) A preferred tape for future studies would be of a black, non-glossy variety.

Figure 5.12: The markers attached to the camel leg using duct tape.

*Recommendations for Future Studies*

Using the motion capture system (intended for use in a controlled lab setting) outdoor will present many unique and unexpected challenges. A thorough preparation before the study is warranted to overcome these challenges. The location of the study should be scouted well in advance to gather information about lighting conditions, power sources, camera placements, etc. If at all possible, the motion capture study should be conducted with minimal sunlight interference. One may consider recording the trials during the dawn or dusk times of the day, perhaps a study during the night if the condition allows. (In theory a cloudy day could also be ideal for an outdoor motion capture study. However, chances of precipitation may increase the risk of damaging the delicate motion capture equipment.) Camera placement should also be carefully considered before the study. The motion capture cameras need to be as close to the

recorded activity as possible to accurately capture the kinematics of the humans and animals, but not too close to interfere with the movements, and far enough away to give sufficient field of view. Finally, if animals are involved in the study, an experienced animal handler should be present to calm the animals and assist with marker placements.

More automated data extraction procedures should also be considered to reduce the data processing time. The marker trajectory data from the outdoor motion capture study was extracted by visually inspecting and labeling each marker in the recordings. This process took 10 to 20 minutes per trial depending on the quality of data. On the other hand, a walking trial collected indoor using existing marker labeling models took a few minutes or less to process. The Vicon system software Nexus 2 used in this study provides tools to create customized marker models (also called labeling skeletons). Designing and implementing a marker model should significantly improve data processing efficiency given the overall quality of data is adequate.

## *Limitations*

### *Issues Related to Analysis*

Data processing in this study included steps of synchronization, normalization, and averaging. For horse and camel riding, the synchronization step aligned the cyclic data in time based on the timing of valleys in the vertical displacement of a saddle marker. This approach placed the emphasis on comparison of motion features exerted on horse and camel saddles, rather than on relating motion features to specific gait cycle events such as heel strike and toe off. The human gait cycles were synchronized base on heal strikes, which in turn correlate pelvic motion with gait cycle event.

The averaging step blended multiple trials into a composite representation of the motion patter. This is the same approach taken by Garner and Rigby. and many others in similar human/animal kinematic studies [27,35,58]. The averaging can result in artifacts and distortions in results. If the timing of peaks and valleys in the data is out of phase, the nonalignment of these extremes may attenuate the amplitude in the computed average motion pattern.

*Gait Speed*

Previous studies suggested that gait speeds affect motion patterns in humans and horses [7,32]. However, the gait speed in the current study was not carefully controlled for either the human walking trials or the horse/camel riding trials. The human subjects were asked to choose a preferred normal walking speed, and the horses/camels were led by trainers at a speed typical in the HPOT practice. Future studies that control gait speed more tightly may produce results with less variability.

*Sample Size*

This study included five able-bodied adolescents and adults, two camels, and three horses. Future studies could expand on this subject set with additional able-bodied adults, children, and individuals with disabilities. Additional horses and camels may be beneficial as well.

## *Future Works*

### *Available Data*

The results of the current study provide an interesting first look at the pelvic kinematics during horse riding, camel riding, and walking. However, there is much more data collected during this current study that is available for analysis, according to the following suggestions.

*Gait speed and saddle.* The current study compared human pelvic motion during horse riding, camel riding, and walking with one saddle (saddle 1) and one speed condition (normal). The subjects' pelvic motion when riding on one additional saddle (saddle 2) and additional speeds (fast, trot for horse riding; fast for camel riding) was also recorded during the study. The effect of saddles and horse/camel gait speeds to human pelvises could be investigated using existing data from the current study. More studies varying saddles and gait speeds during horse riding could also help to determine which combinations of saddles and gait speeds are more beneficial for therapeutic purposes.

*Benefits to other body regions.* This study focused on the effects of horse/camel riding on the human pelvis. Available data for human torso, shoulder, thigh, and other body regions should also be analyzed to determine if horse/camel riding can produce cyclical motions in these body regions similar to that of walking.

*Horse/Camel motion.* Future studies could investigate how the movement of camels/horses induce the motion experienced by the riders. The current study recorded motion trajectory data of joints and key bony landmarks on horses and camels. The

kinematics of the animals' joints could be studied to determine how the motion of the animal's pelvis and back initiates its saddle motion, and how the saddle motion triggers the rider's movement. A better understanding of horse kinematics during riding may provide insight into the underlying mechanism of HPOT.

### *Additional Benefits of HPOT and CAI*

This study focused on simple biomechanical benefits of HPOT and CAI. It remains for future work to further investigate and quantify specific benefits of motion therapies. Future studies are also needed to investigate other therapeutic benefits of animal therapies, including benefits from interaction with live animals, stretching due to sitting on an animal, and many additional factors.

# CHAPTER SIX

## Conclusion

This study was the first to compare human pelvic movement during horse riding, camel riding, and walking. Aimed to better understand the underlying mechanisms and physical benefits of hippotherapy and camel assisted therapy, this study quantified human pelvic kinematics when riding horses, camels, and walking using motion capture techniques. The results of this study indicated that there are remarkable similarities between the human pelvic motions when walking, riding on a horse, and riding on a camel, which include overlapping distorted infinity-shape pelvic motion patterns in the transverse and frontal planes during all three activities, comparable ranges of motion in the horizontal and vertical displacements during walking and horse riding, and similar directions of motion patterns during camel riding and walking. While some variance was observed between the human pelvic kinematics on different horses, the consistency of motion patterns among subjects suggests that the horses and the camel dictated the motion patterns experienced by the subjects during the course of this study. Furthermore, many experimental procedures and setups were adjusted and refined to address the challenges of using motion capture in an outdoor environment. The success of this study provides additional evidence for similarities in horse/camel riding motions with human walking motions, which may help explain therapeutic benefits of riding.

# APPENDIX

# APPENDIX

## Additional Results

The key results from this study were presented in Chapter 4. Some additional comparisons were made between horses and subjects at different speed conditions (fast, trot). These additional results include:

- Comparing the subjects (1,3,4,5) on each horse (1,2,3) at fast and trot speeds (Figure A.1-6)
- Comparing the horses (1,2,3) for each rider (1,3,4,5) at normal, fast, and trot speeds (Figure A.7-17)
- Comparing the subjects (1,2,5) of the camel at fast speed (Figure A.18)
- Comparing the subjects (1,2,4) walking at fast speed (Figure A.19)
- Comparing the horses (1,2,3) with averaged subjects' cycles for each horse at fast and trot speeds (Figure A.20-21)
- Comparing the subjects (1,3,4,5) with averaged horses' cycles for each subject at normal, fast, and trot speeds (Figure A. 22-24)
- Comparing Subject 1 riding horses vs. riding camel vs. walking at normal and fast speed (Figure A. 25-26)
- Comparing all subjects riding horses vs. riding camel vs. walking at fast speed (Figure A. 27)

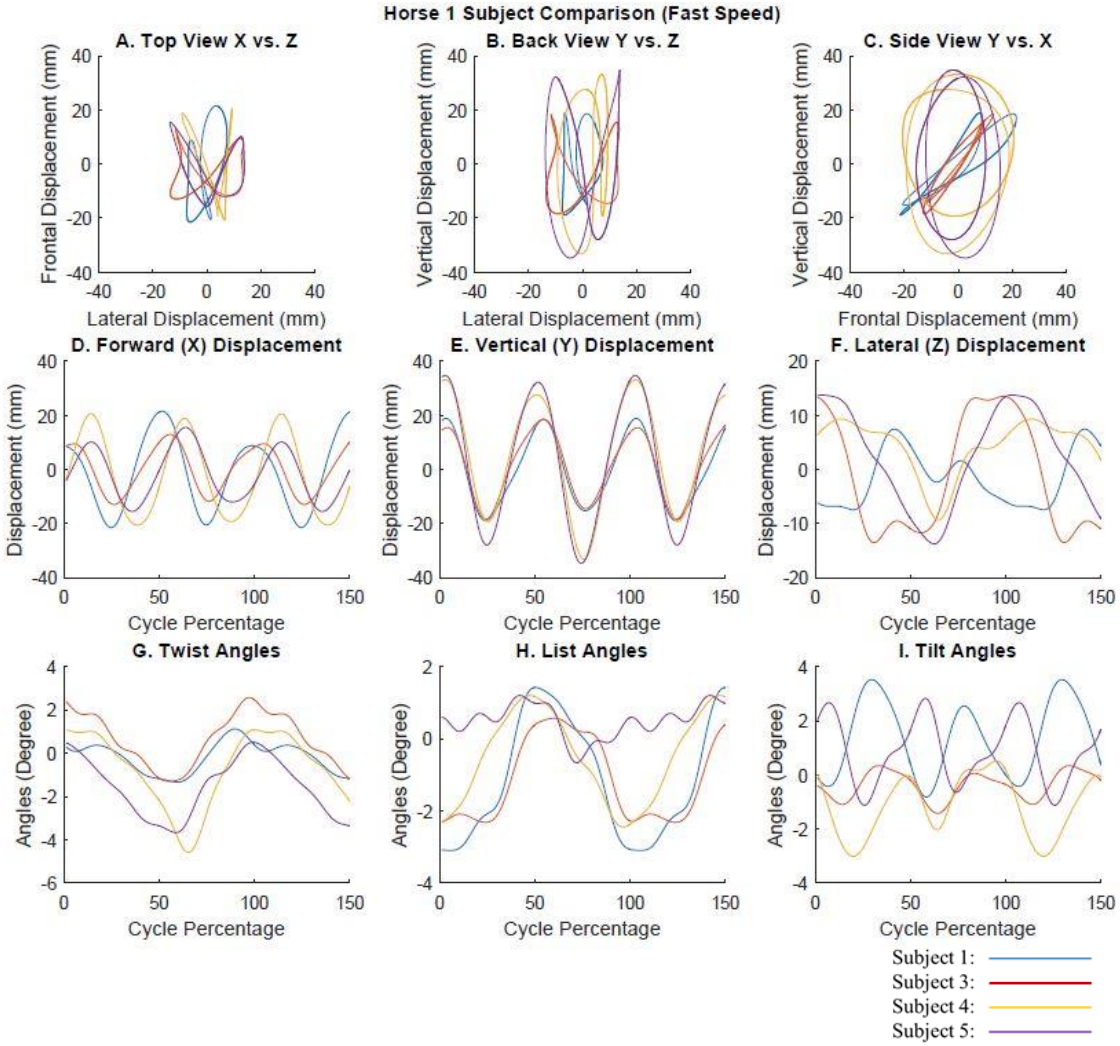


Figure A.1: Pelvic spatial views (A,B,C), pelvic displacements versus gait-period normalized time (D,E,F), and pelvic angles versus gait-period normalized time (G,H,I) when each subject was riding horse 1 at fast speed.

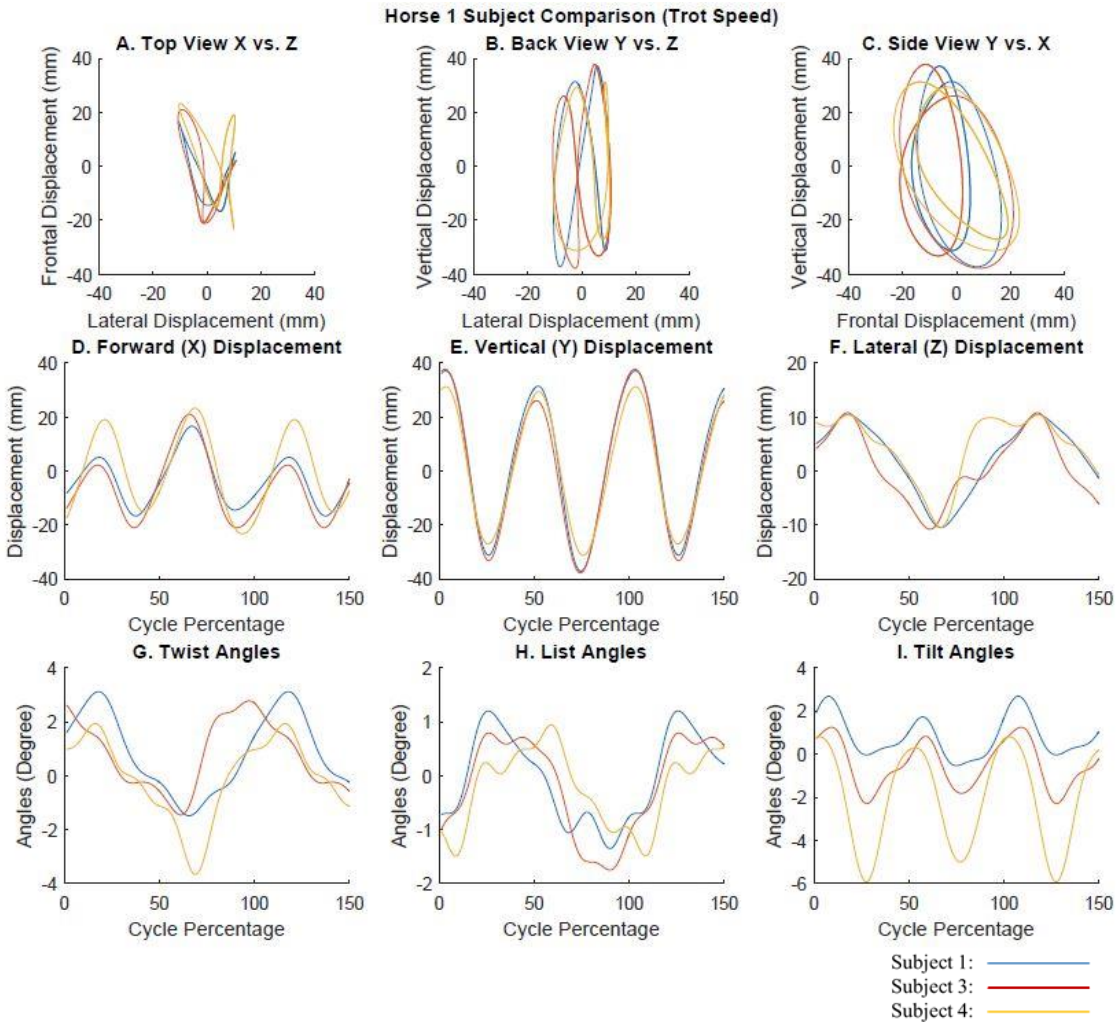


Figure A.2: Pelvic spatial views (A,B,C), pelvic displacements versus gait-period normalized time (D,E,F), and pelvic angles versus gait-period normalized time (G,H,I) when each subject was riding horse 1 at trot speed.

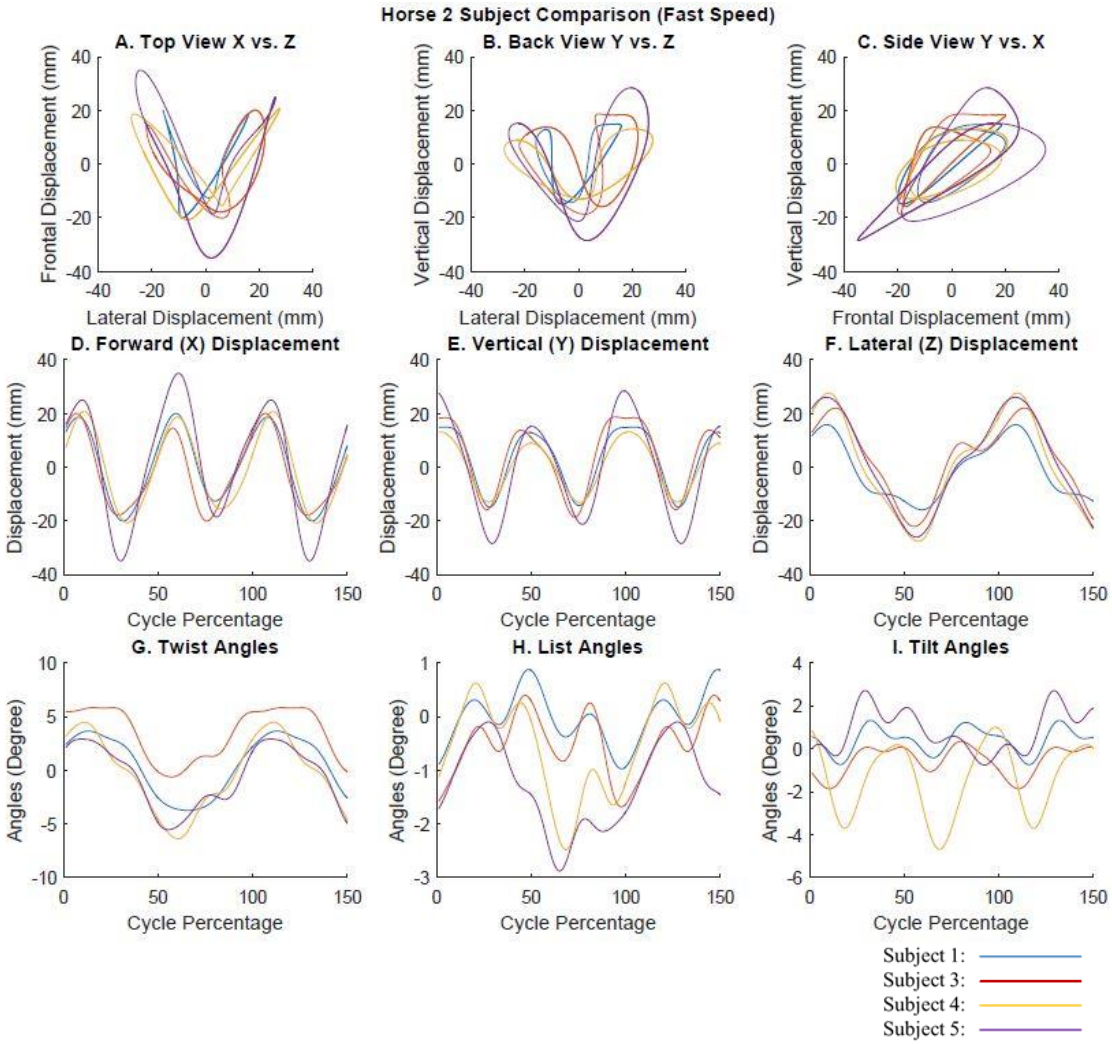


Figure A.3: Pelvic spatial views (A,B,C), pelvic displacements versus gait-period normalized time (D,E,F), and pelvic angles versus gait-period normalized time (G,H,I) when each subject was riding horse 2 at fast speed.

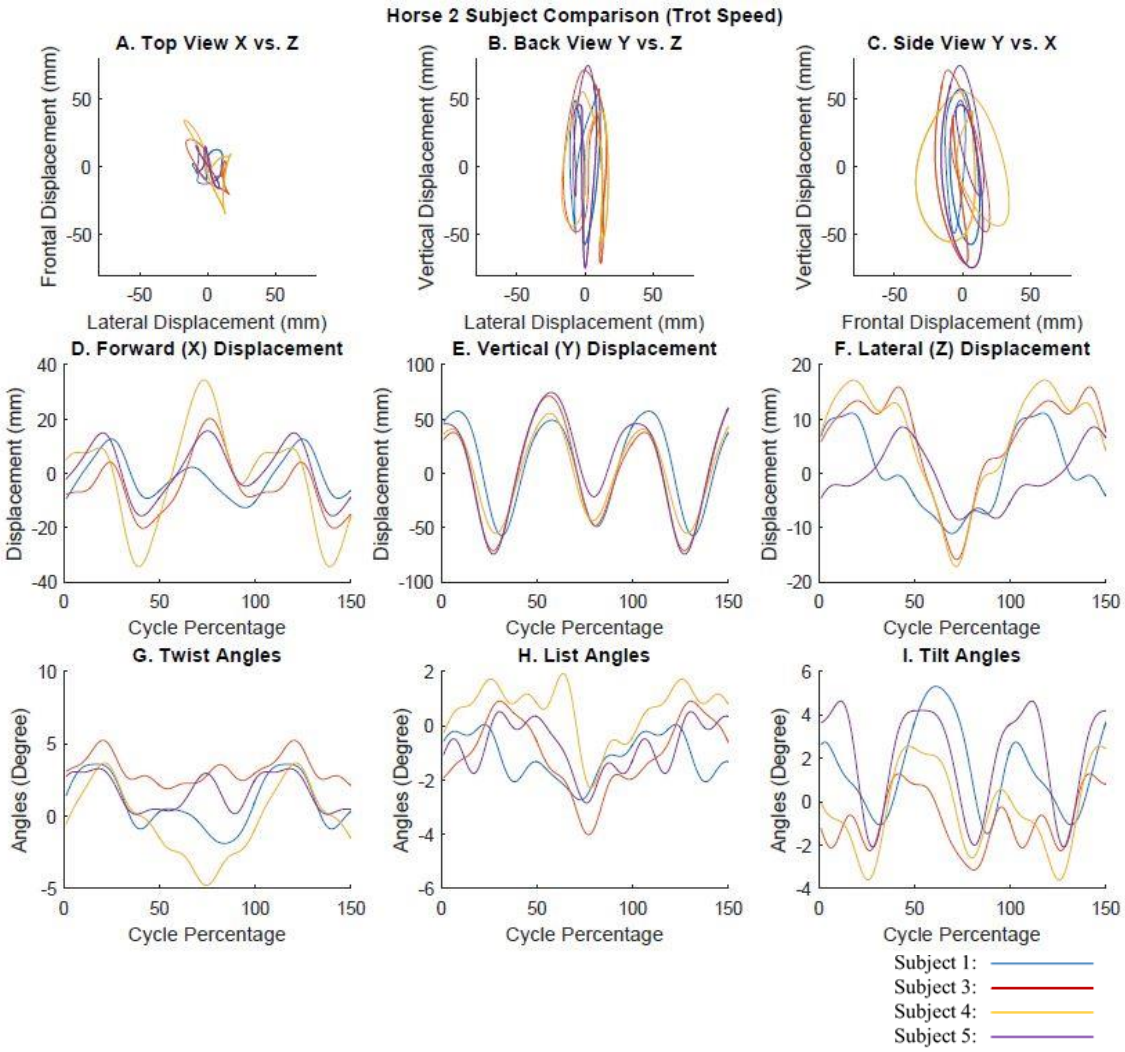


Figure A.4: Pelvic spatial views (A,B,C), pelvic displacements versus gait-period normalized time (D,E,F), and pelvic angles versus gait-period normalized time (G,H,I) when each subject was riding horse 2 at trot speed.

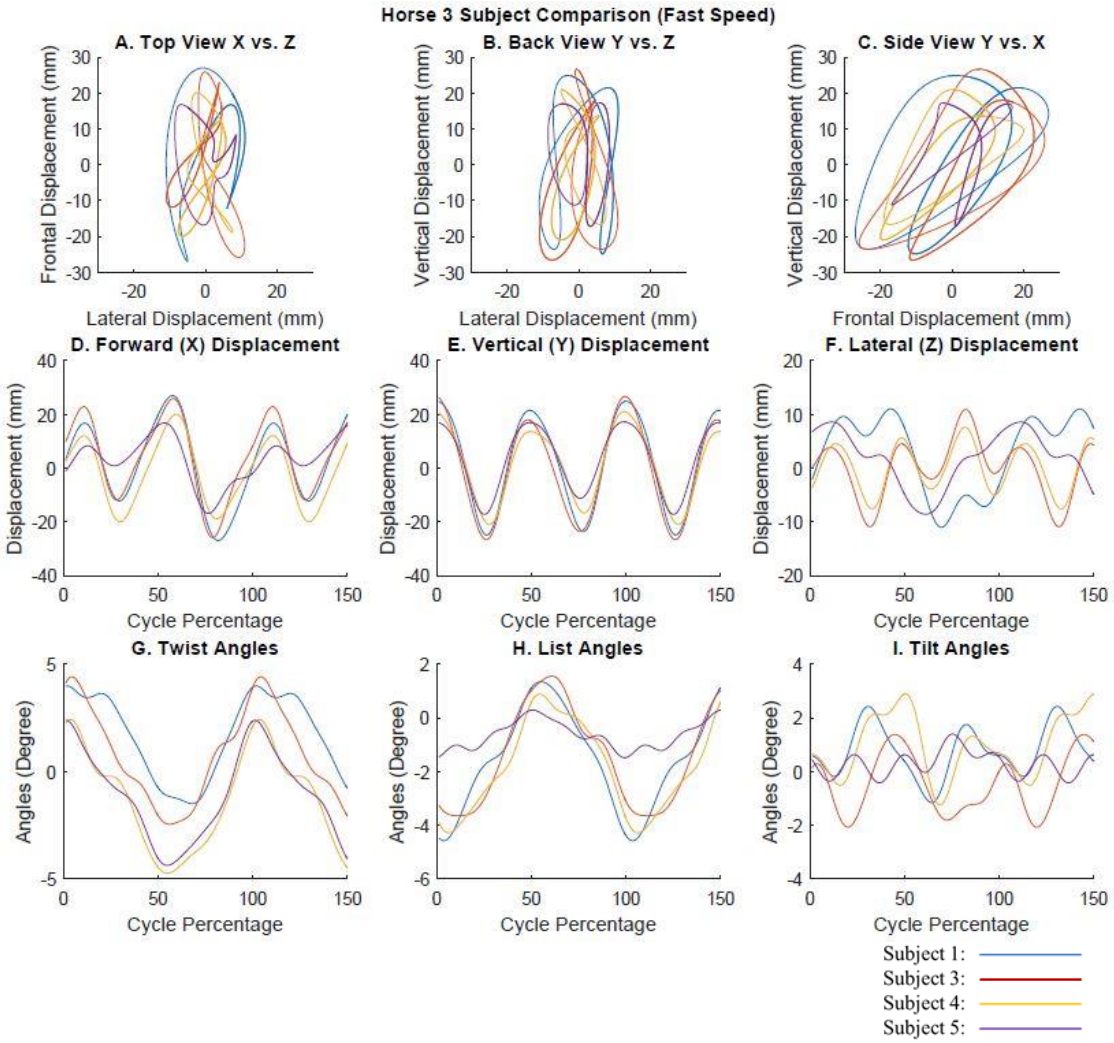


Figure A.5: Pelvic spatial views (A,B,C), pelvic displacements versus gait-period normalized time (D,E,F), and pelvic angles versus gait-period normalized time (G,H,I) when each subject was riding horse 3 at fast speed.

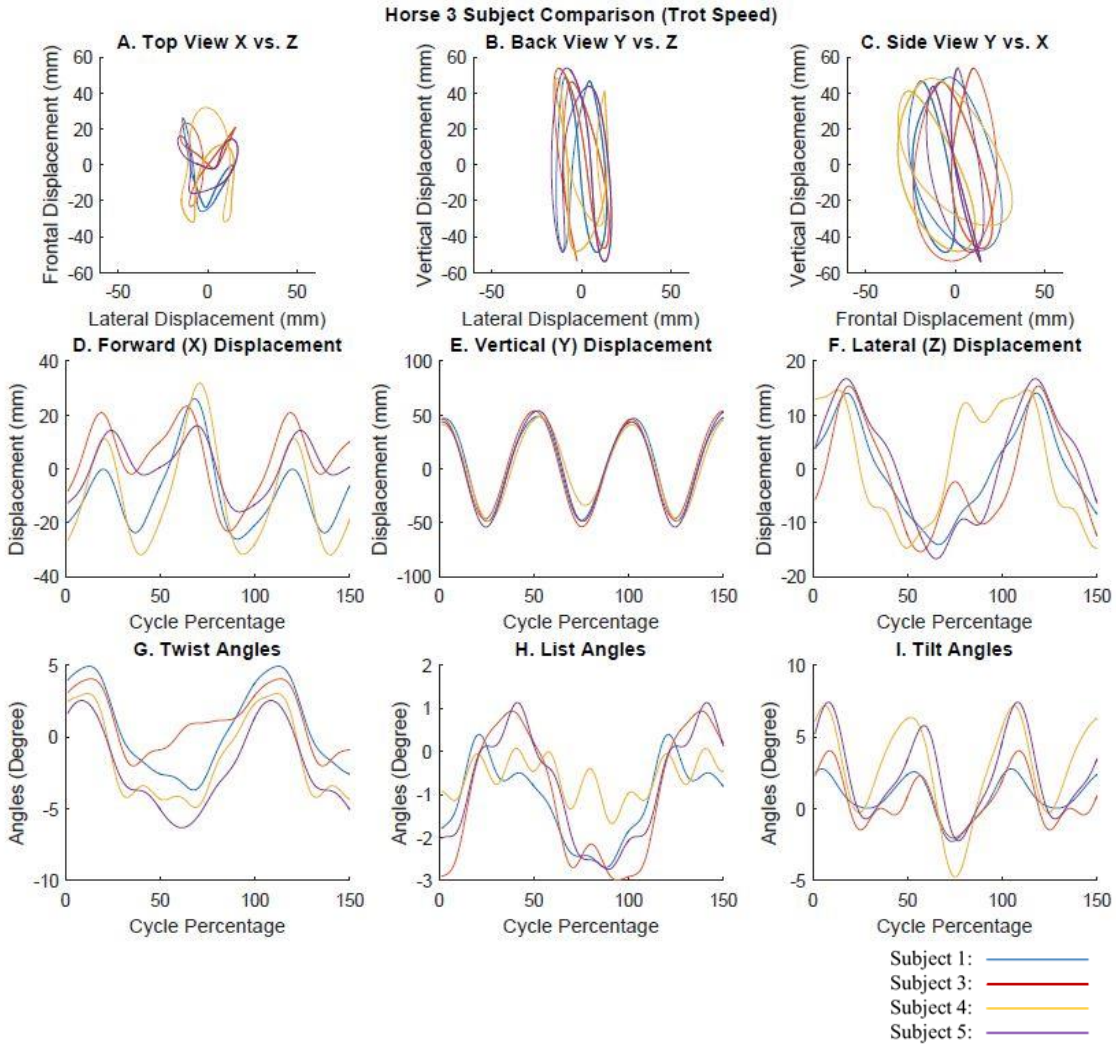


Figure A.6: Pelvic spatial views (A,B,C), pelvic displacements versus gait-period normalized time (D,E,F), and pelvic angles versus gait-period normalized time (G,H,I) when each subject was riding horse 3 at trot speed.

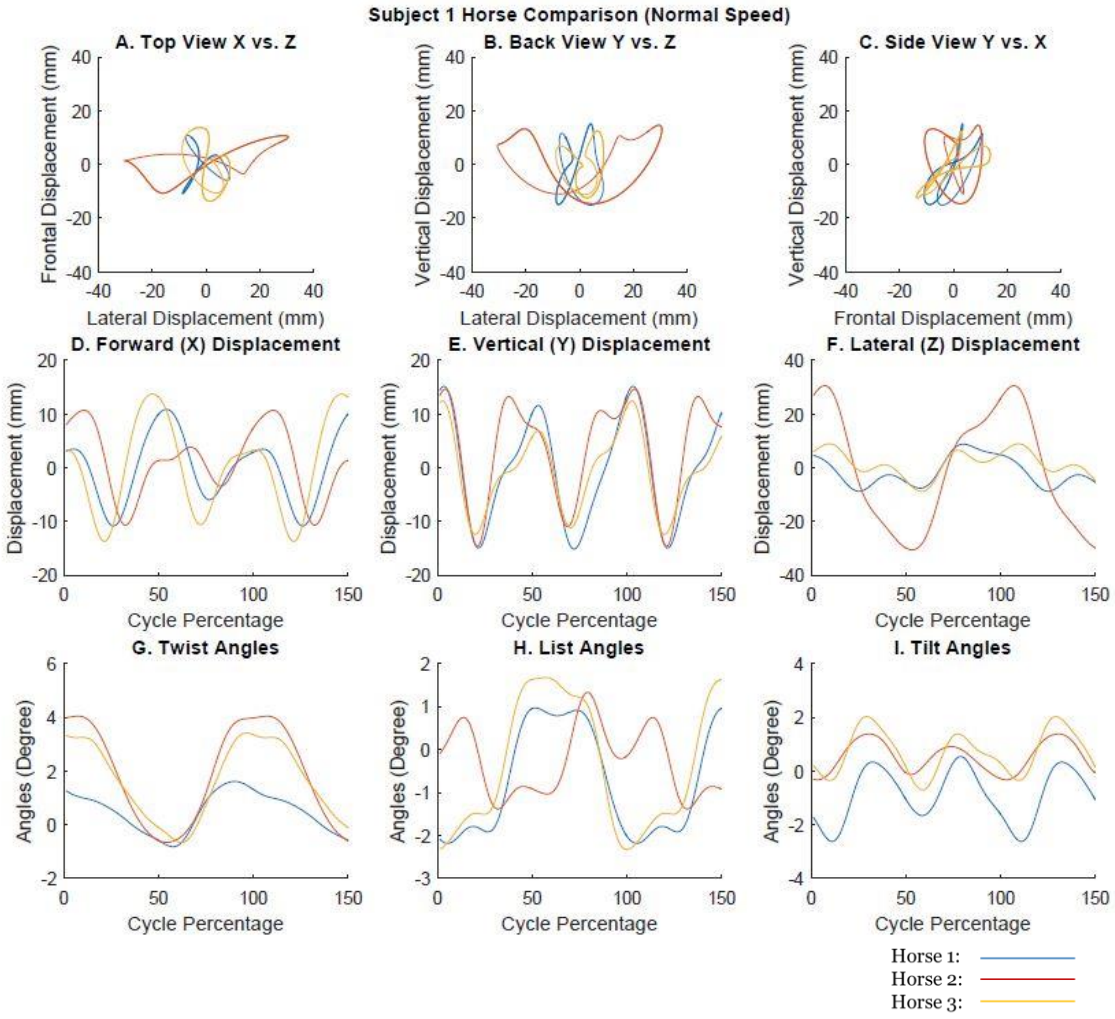


Figure A.7: Pelvic spatial views (A,B,C), pelvic displacements versus gait-period normalized time (D,E,F), and pelvic angles versus gait-period normalized time (G,H,I) when subject 1 was riding each horse at normal speed.

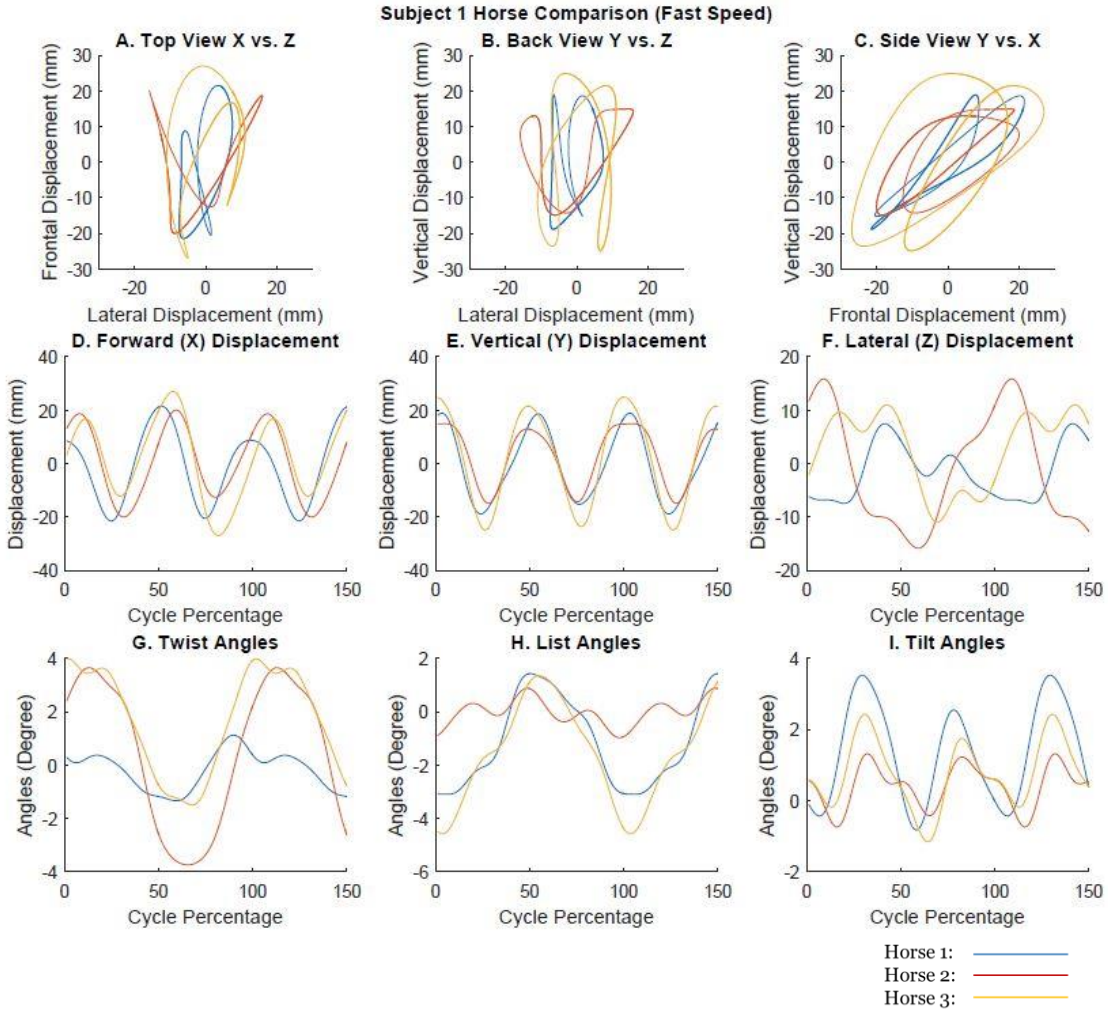


Figure A.8: Pelvic spatial views (A,B,C), pelvic displacements versus gait-period normalized time (D,E,F), and pelvic angles versus gait-period normalized time (G,H,I) when subject 1 was riding each horse at fast speed.

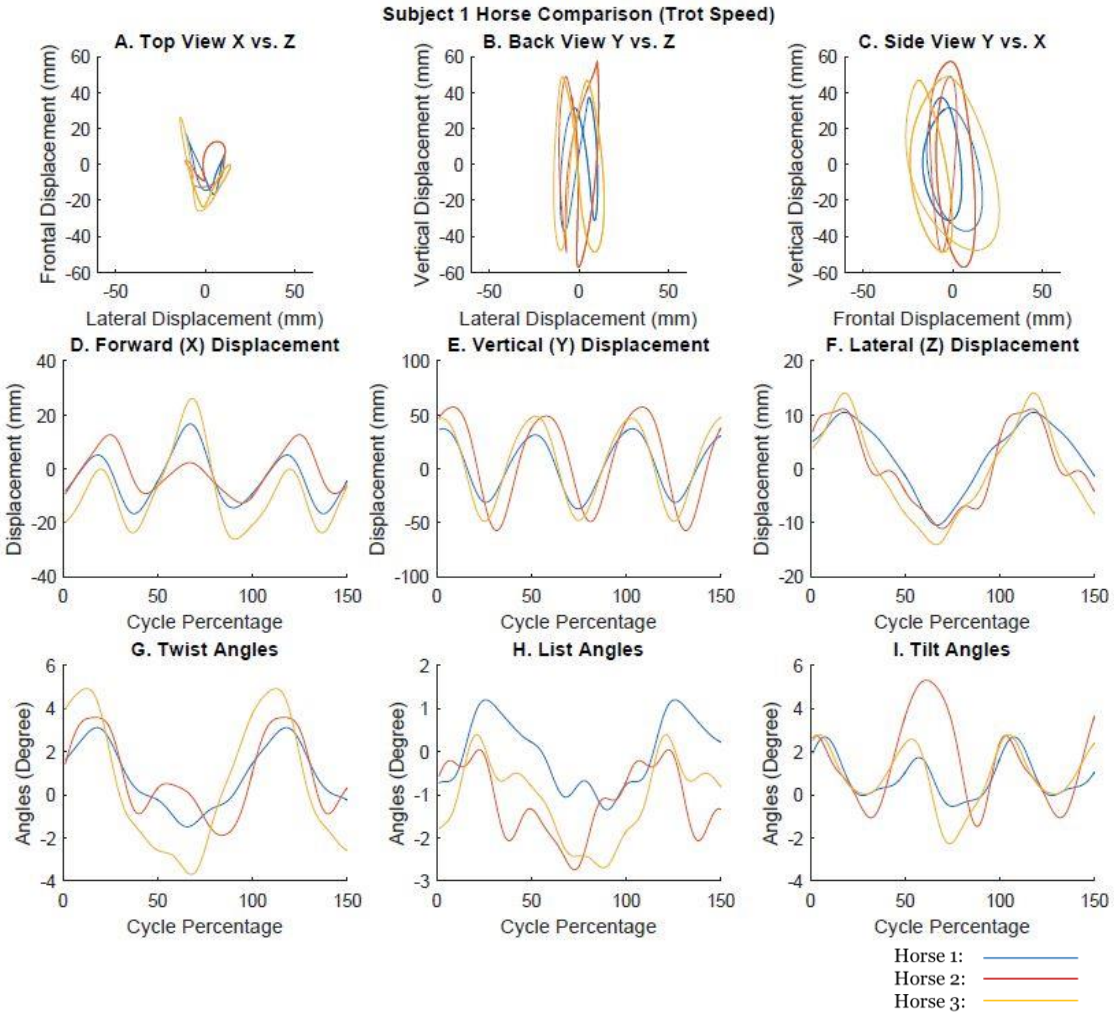


Figure A.9: Pelvic spatial views (A,B,C), pelvic displacements versus gait-period normalized time (D,E,F), and pelvic angles versus gait-period normalized time (G,H,I) when subject 1 was riding each horse at trot speed.

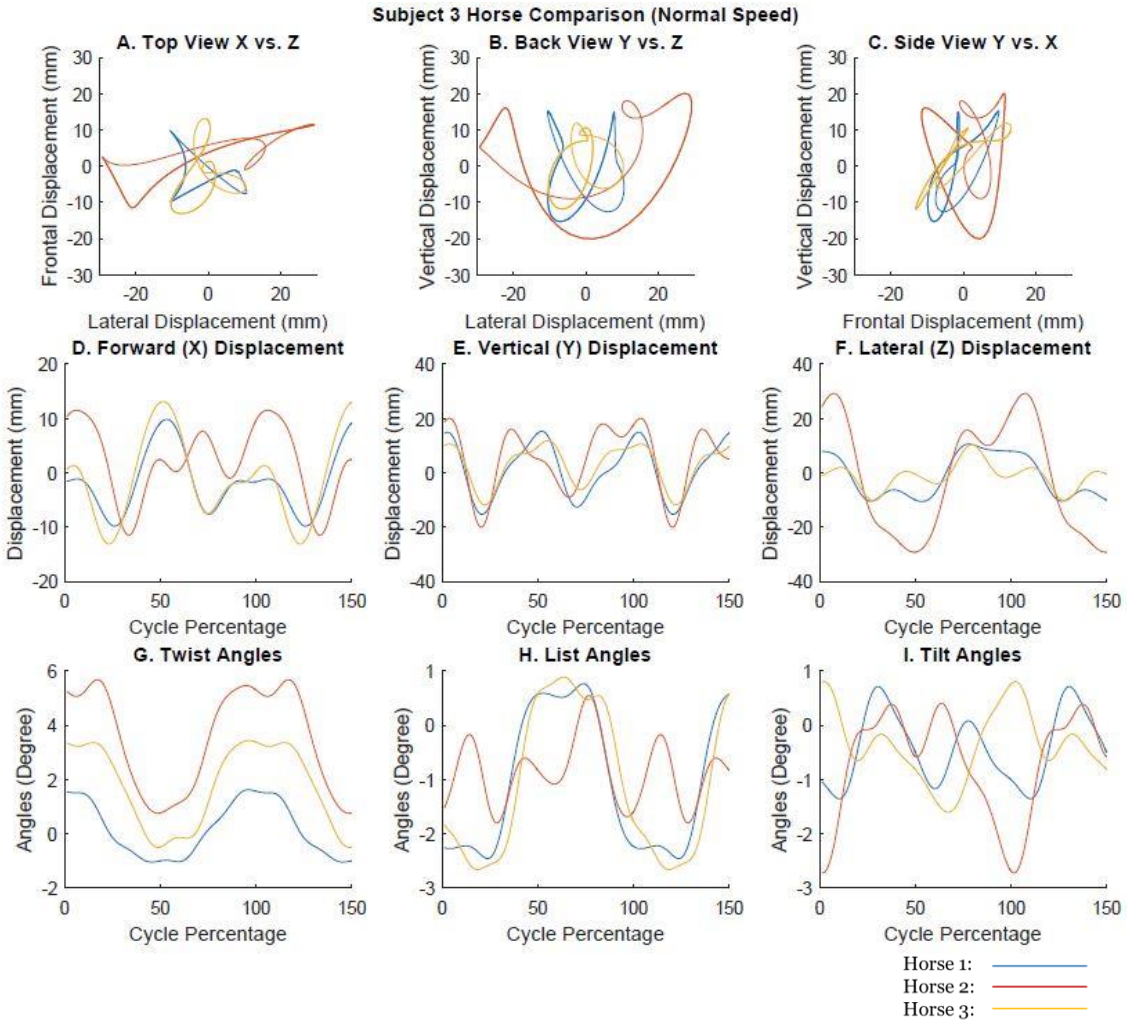


Figure A.10: Pelvic spatial views (A,B,C), pelvic displacements versus gait-period normalized time (D,E,F), and pelvic angles versus gait-period normalized time (G,H,I) when subject 3 was riding each horse at normal speed.

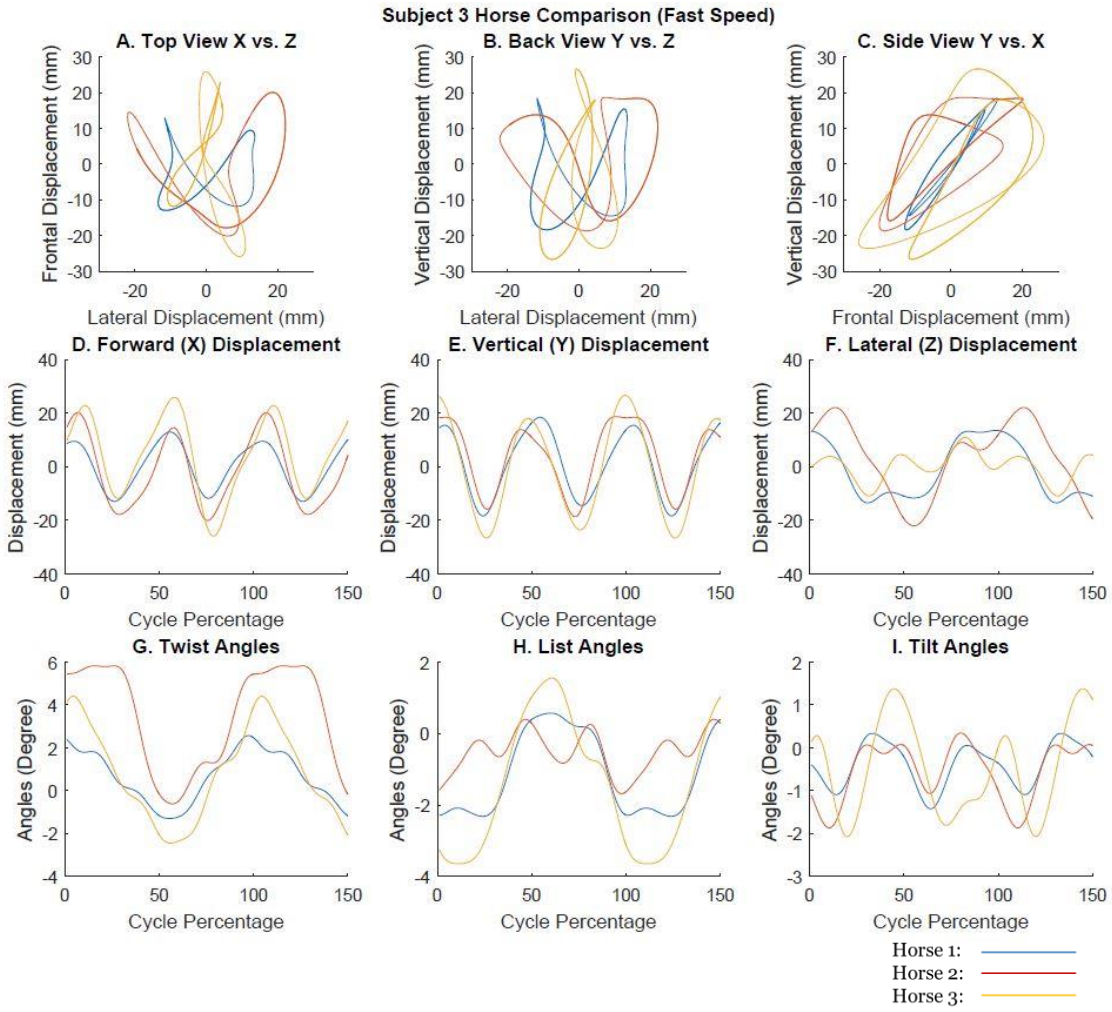


Figure A.11: Pelvic spatial views (A,B,C), pelvic displacements versus gait-period normalized time (D,E,F), and pelvic angles versus gait-period normalized time (G,H,I) when subject 3 was riding each horse at fast speed.

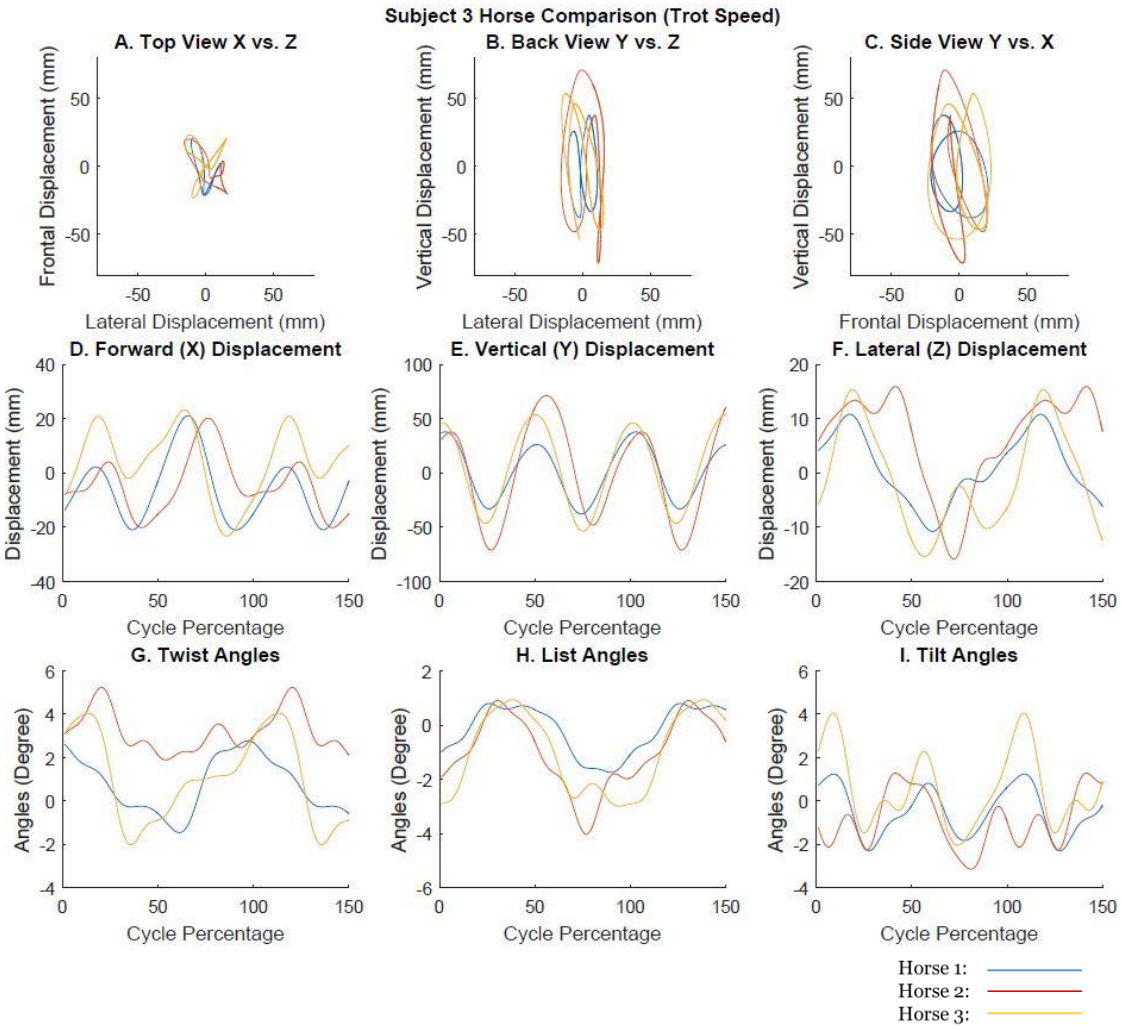


Figure A.12: Pelvic spatial views (A,B,C), pelvic displacements versus gait-period normalized time (D,E,F), and pelvic angles versus gait-period normalized time (G,H,I) when subject 3 was riding each horse at trot speed.

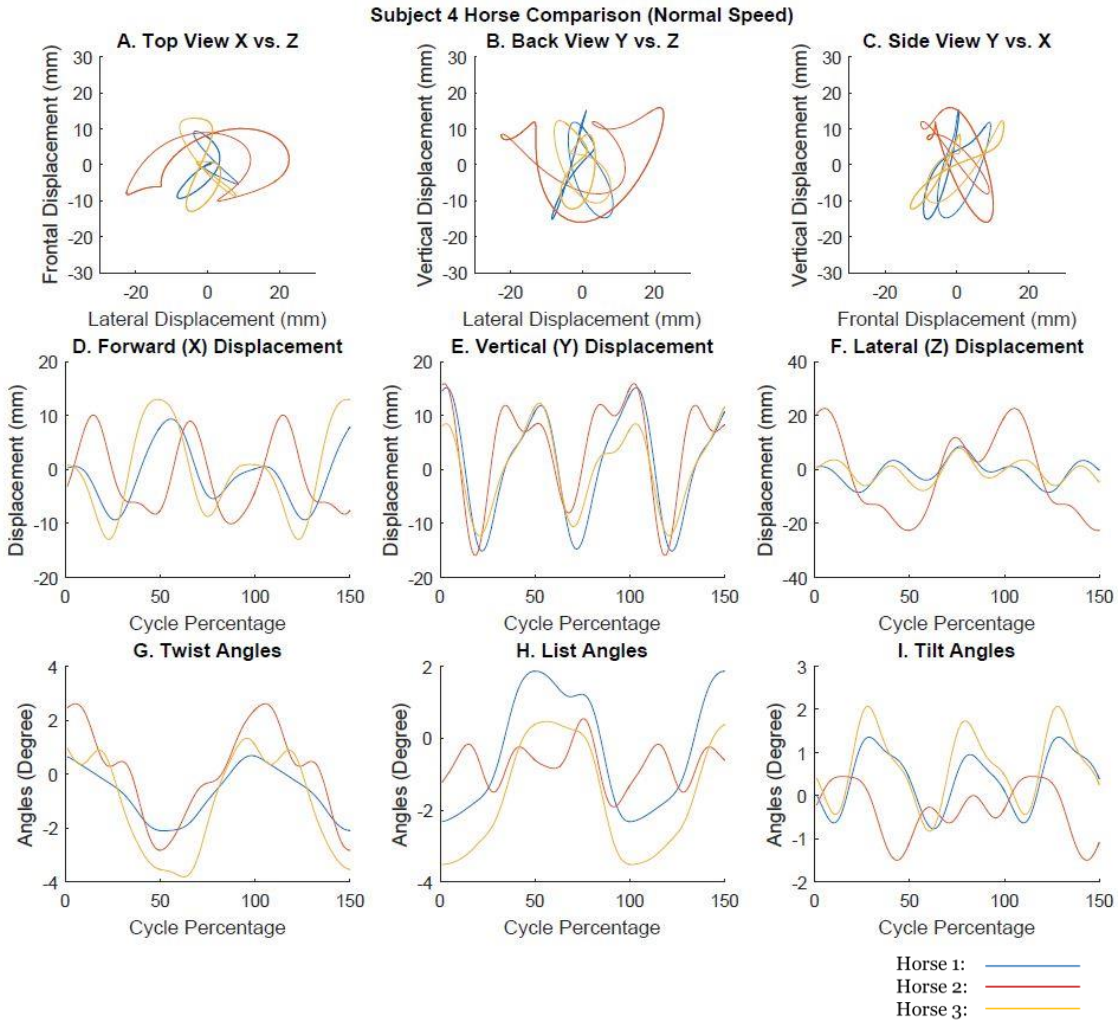


Figure A.13: Pelvic spatial views (A,B,C), pelvic displacements versus gait-period normalized time (D,E,F), and pelvic angles versus gait-period normalized time (G,H,I) when subject 4 was riding each horse at normal speed.

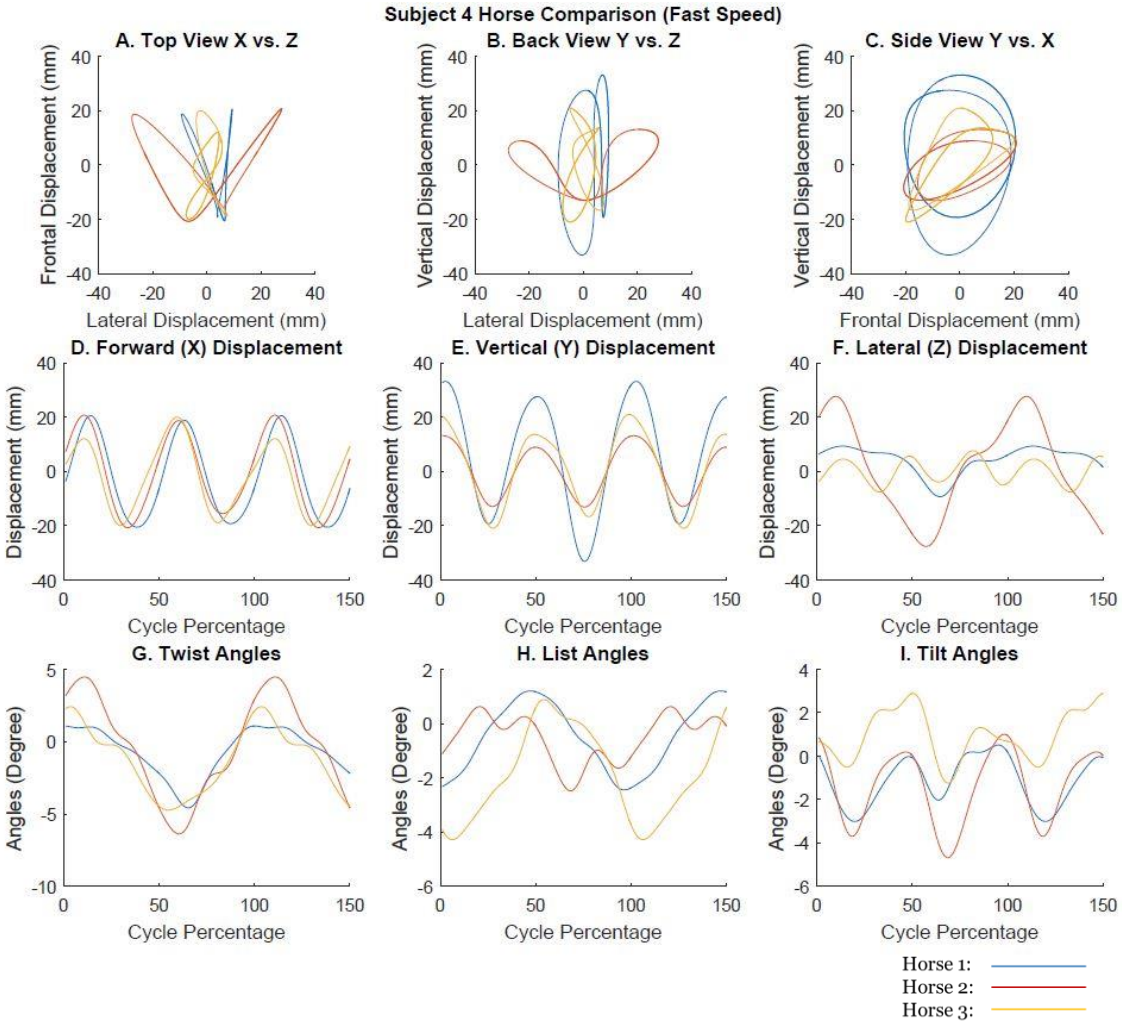


Figure A.14: Pelvic spatial views (A,B,C), pelvic displacements versus gait-period normalized time (D,E,F), and pelvic angles versus gait-period normalized time (G,H,I) when subject 4 was riding each horse at fast speed.

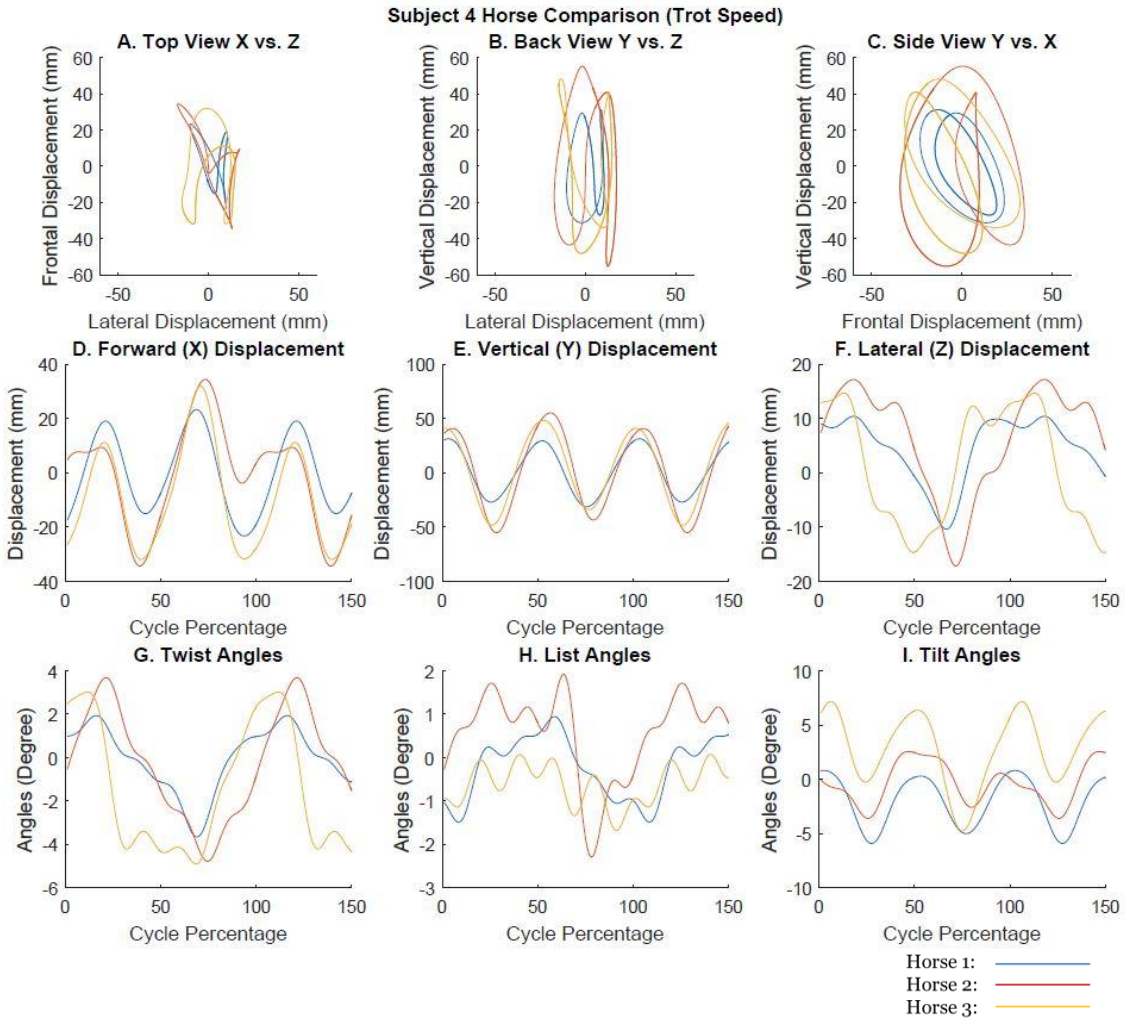


Figure A.15: Pelvic spatial views (A,B,C), pelvic displacements versus gait-period normalized time (D,E,F), and pelvic angles versus gait-period normalized time (G,H,I) when subject 4 was riding each horse at trot speed.

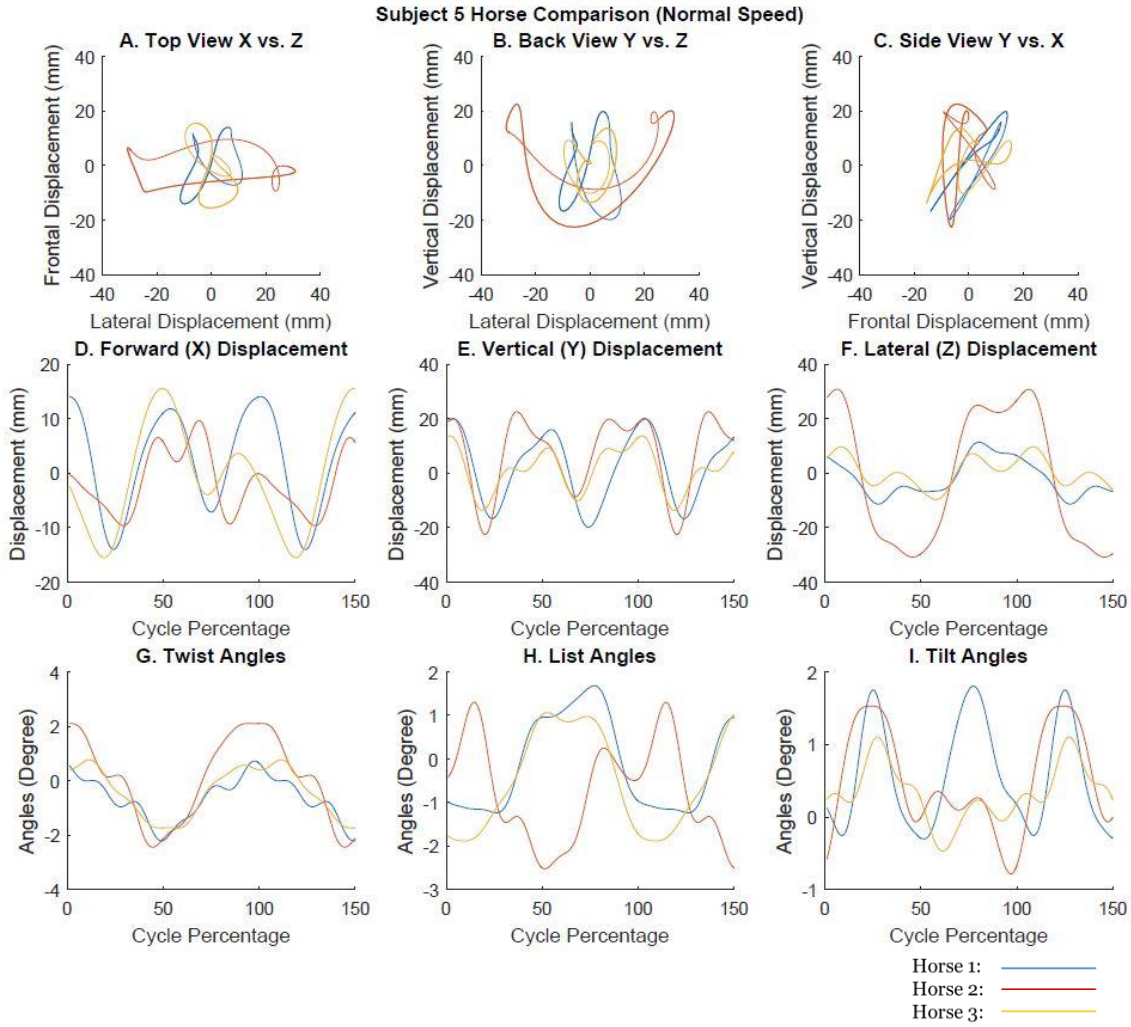


Figure A.16: Pelvic spatial views (A,B,C), pelvic displacements versus gait-period normalized time (D,E,F), and pelvic angles versus gait-period normalized time (G,H,I) when subject 5 was riding each horse at normal speed.

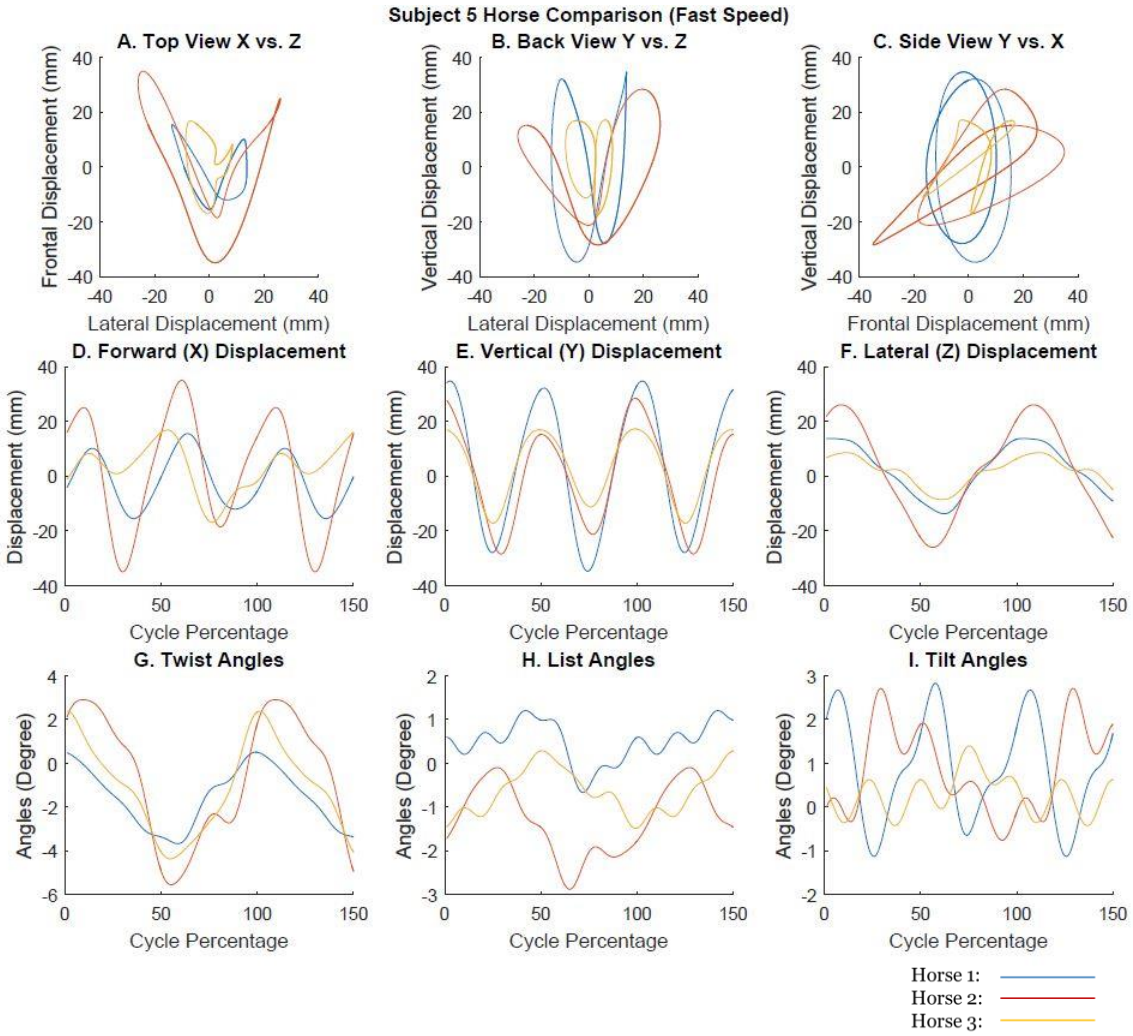


Figure A.17: Pelvic spatial views (A,B,C), pelvic displacements versus gait-period normalized time (D,E,F), and pelvic angles versus gait-period normalized time (G,H,I) when subject 5 was riding each horse at fast speed.

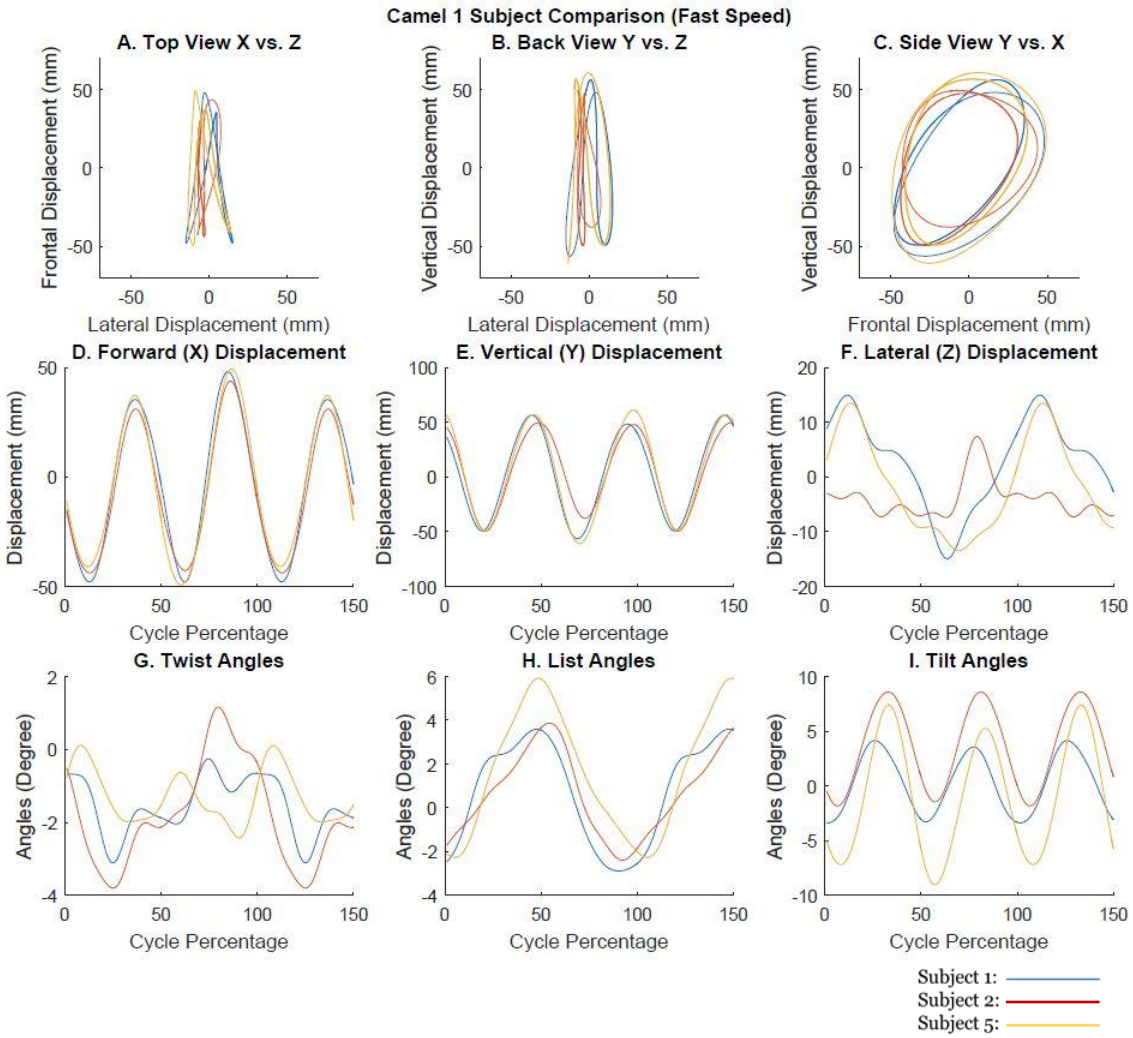


Figure A.18: Pelvic spatial views (A,B,C), pelvic displacements versus gait-period normalized time (D,E,F), and pelvic angles versus gait-period normalized time (G,H,I) when subjects were riding the camel at fast speed.

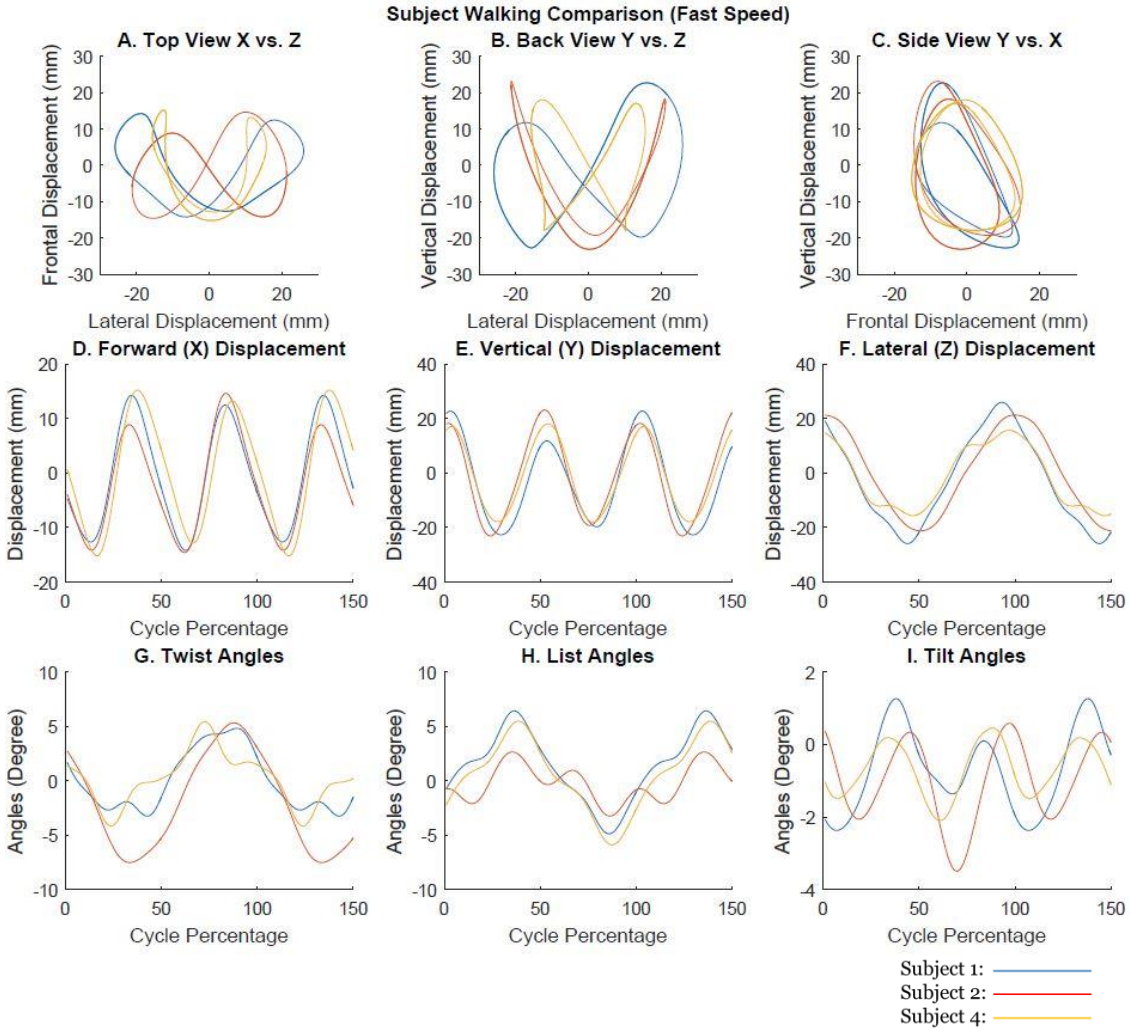


Figure A.19: Pelvic spatial views (A,B,C), pelvic displacements versus gait-period normalized time (D,E,F), and pelvic angles versus gait-period normalized time (G,H,I) when subjects were walking at fast speed.

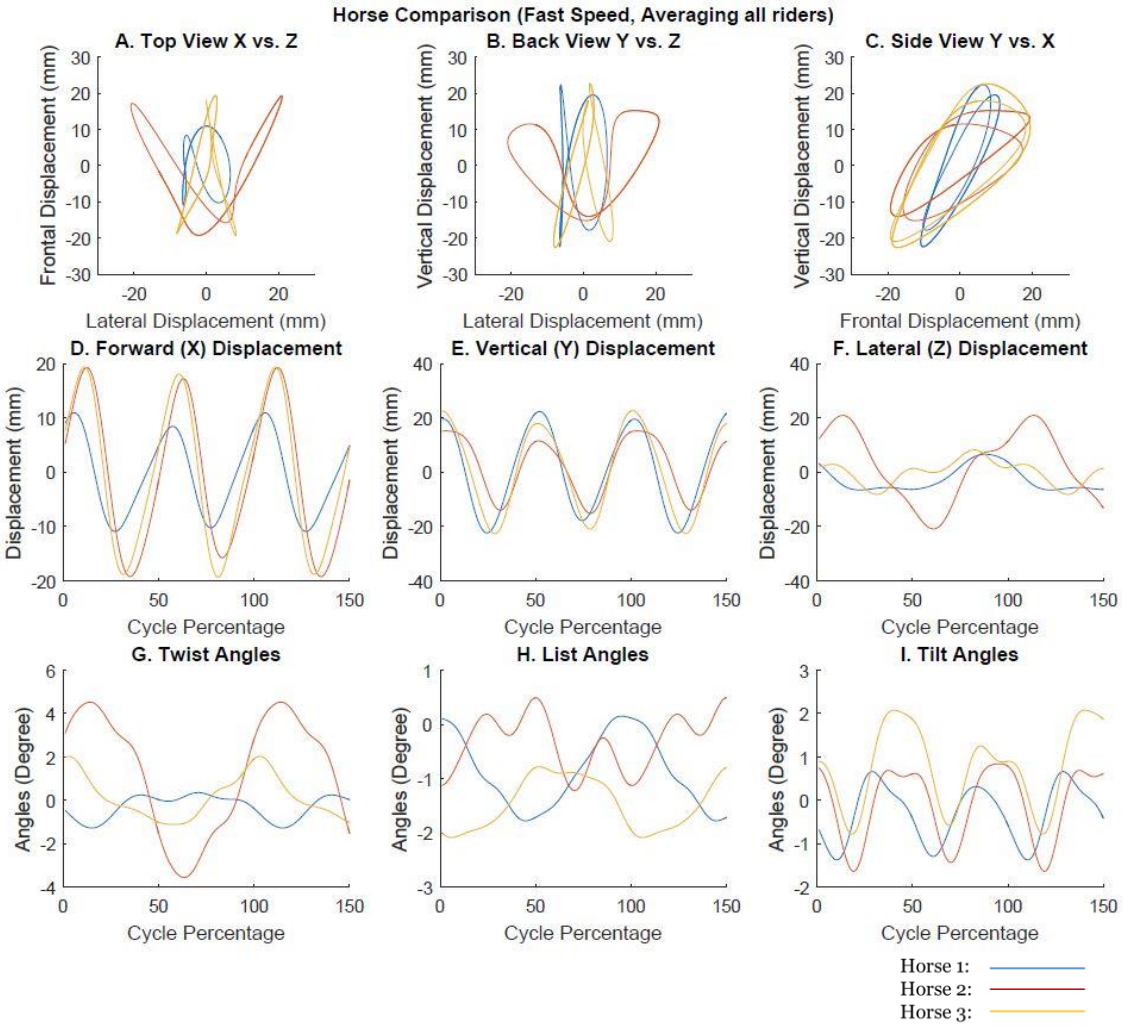


Figure A.20: Pelvic spatial views (A,B,C), pelvic displacements versus gait-period normalized time (D,E,F), and pelvic angles versus gait-period normalized time (G,H,I) when subjects were riding each horse. The normalized cycles were the average over all subjects' riding trials on each horse (saddle 1, fast speed).

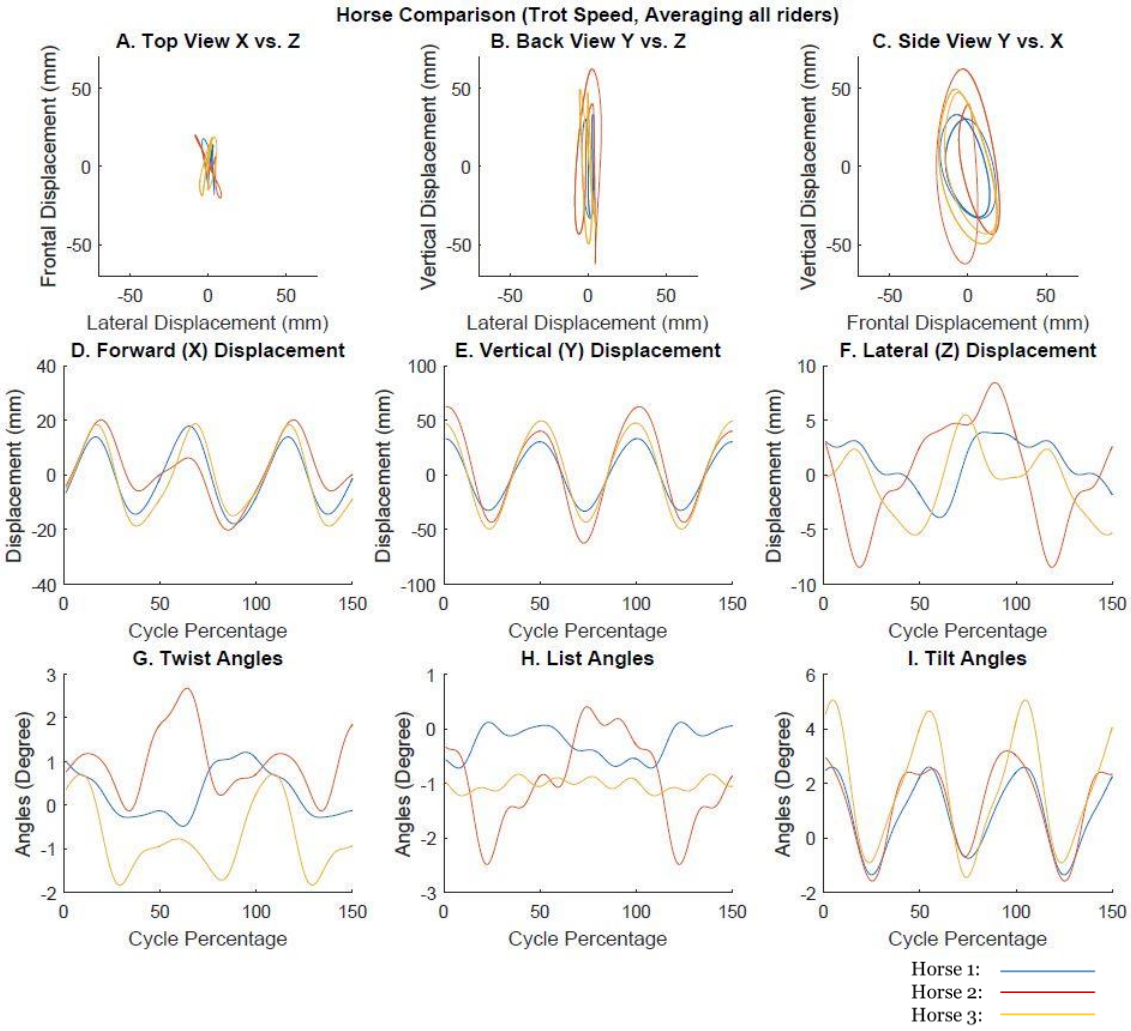


Figure A.21: Pelvic spatial views (A,B,C), pelvic displacements versus gait-period normalized time (D,E,F), and pelvic angles versus gait-period normalized time (G,H,I) when subjects were riding each horse. The normalized cycles were the average over all subjects' riding trials on each horse (saddle 1, trot speed).

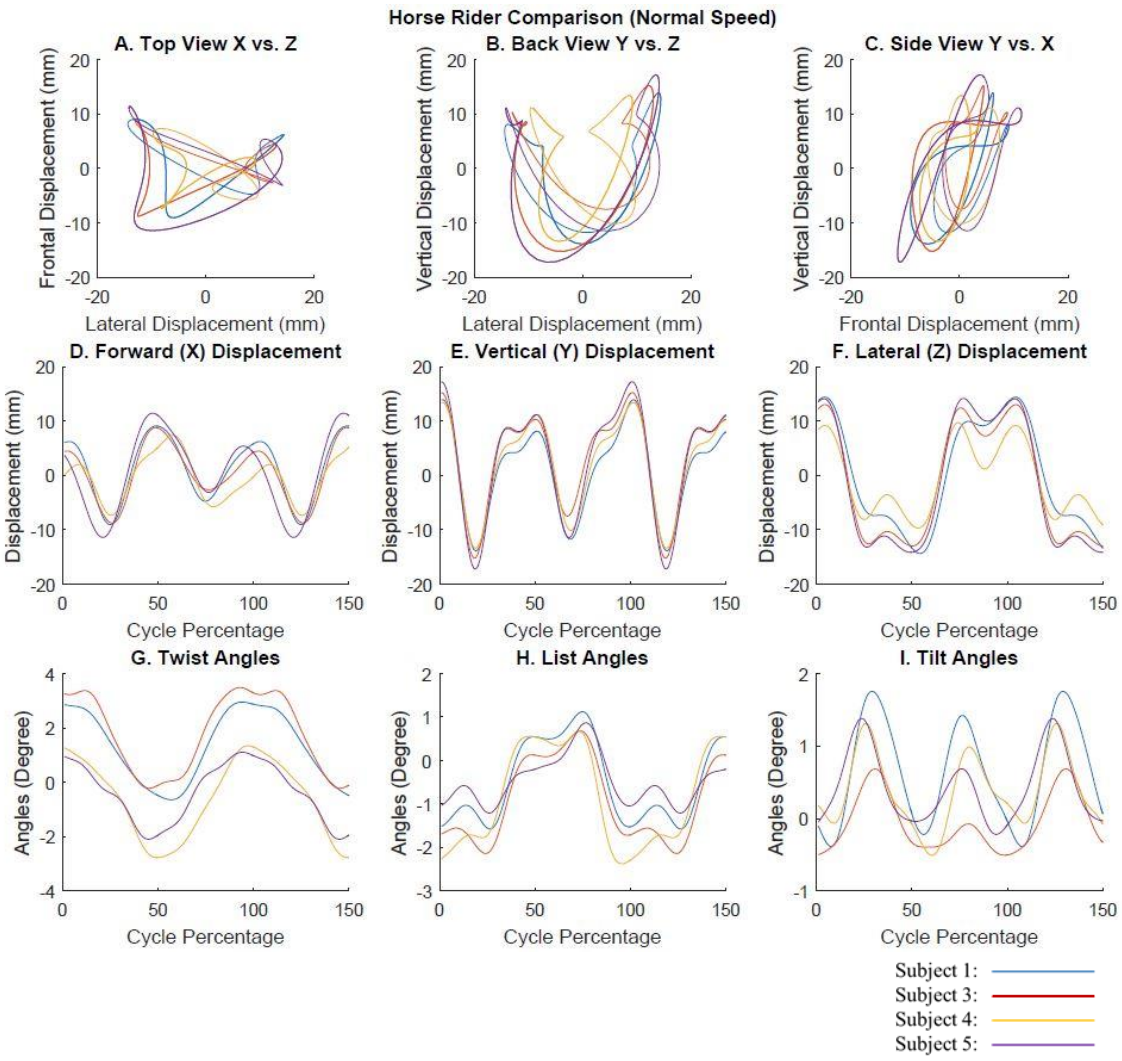


Figure A.22: Pelvic spatial views (A,B,C), pelvic displacements versus gait-period normalized time (D,E,F), and pelvic angles versus gait-period normalized time (G,H,I) when each subject was riding the horses at normal speed. The normalized cycles were the average of each subject's riding trials on all horses (saddle 1, normal speed).

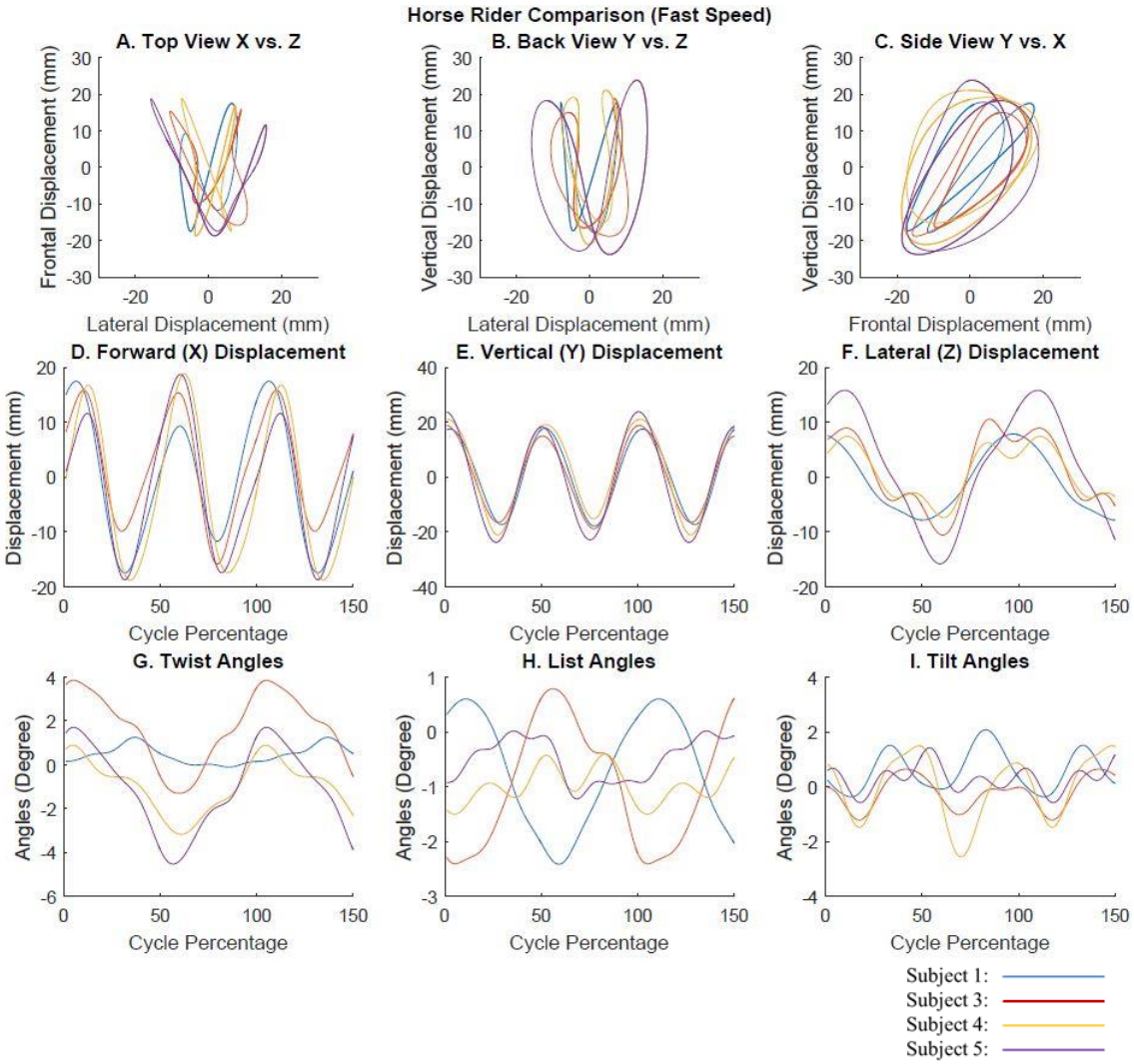


Figure A.23: Pelvic spatial views (A,B,C), pelvic displacements versus gait-period normalized time (D,E,F), and pelvic angles versus gait-period normalized time (G,H,I) when each subject was riding the horses at normal speed. The normalized cycles were the average of each subject's riding trials on all horses (saddle 1, fast speed).

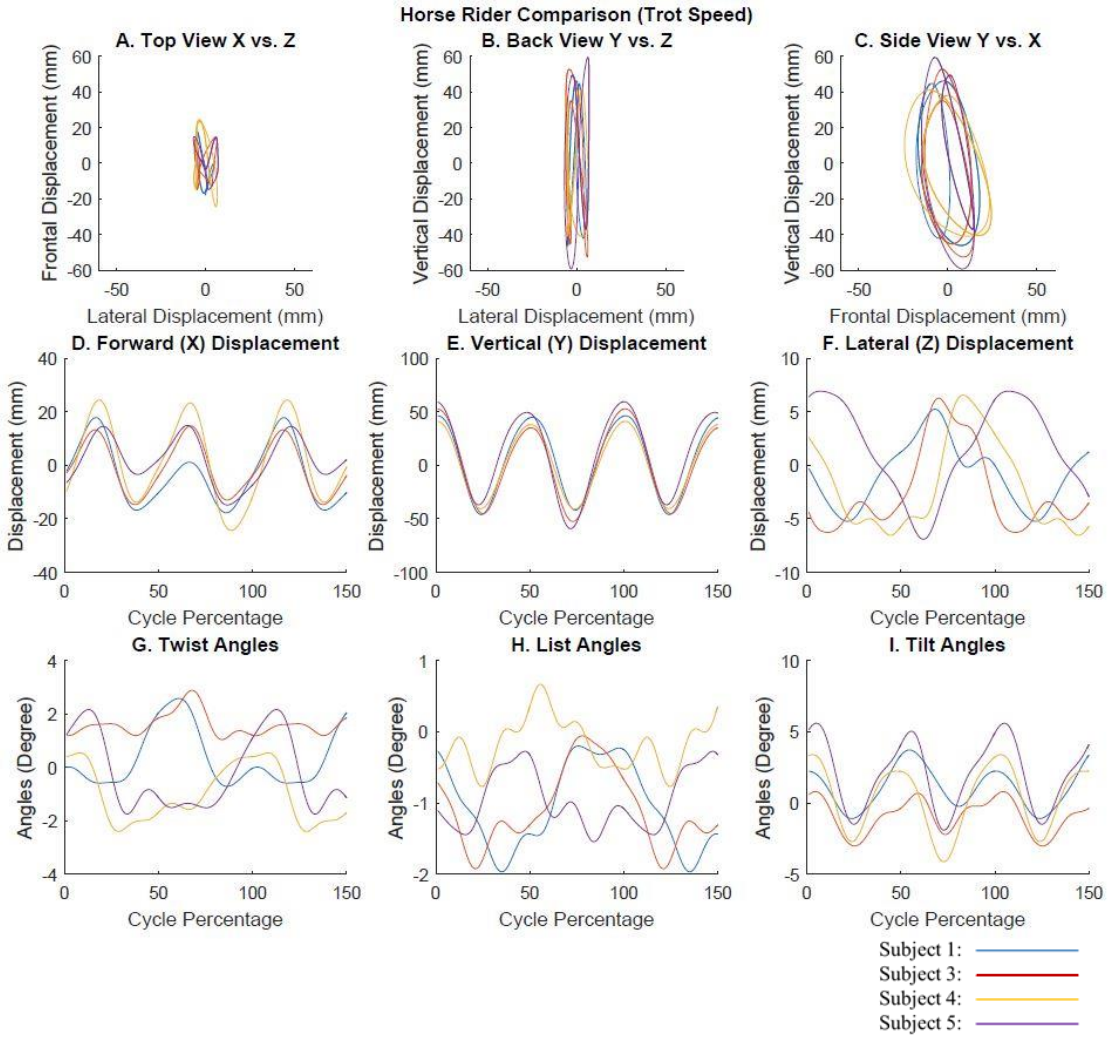


Figure A.24: Pelvic spatial views (A,B,C), pelvic displacements versus gait-period normalized time (D,E,F), and pelvic angles versus gait-period normalized time (G,H,I) when each subject was riding the horses at normal speed. The normalized cycles were the average of each subject's riding trials on all horses (saddle 1, trot speed).

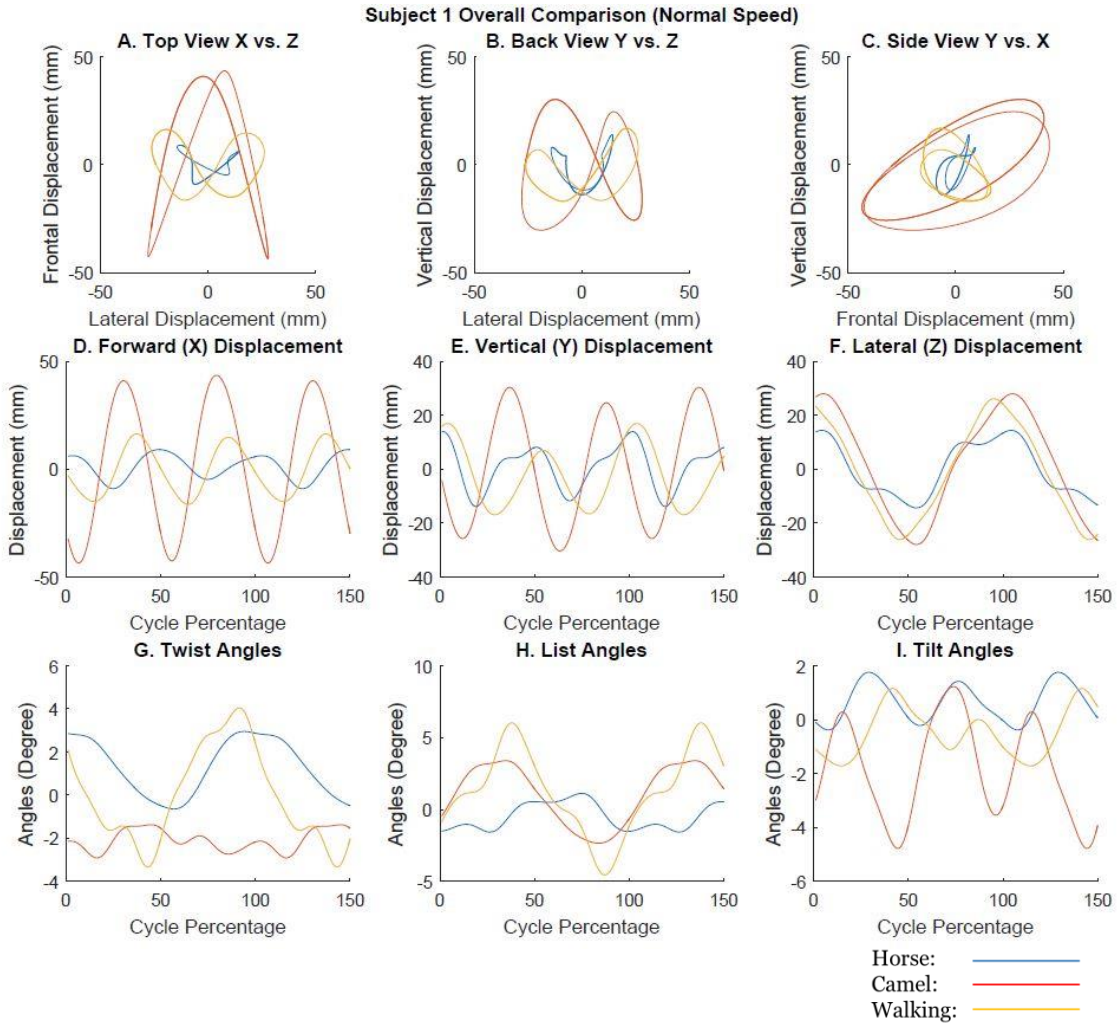


Figure A.25: Pelvic spatial views (A,B,C), pelvic displacements versus gait-period normalized time (D,E,F), and pelvic angles versus gait-period normalized time (G,H,I) when subject 1 was riding horses, camel and walking. The normalized cycle for horse riding was the average over subject 1's riding trials on all horses (saddle 1, normal speed). The normalized cycle for camel riding was the average over subject 1's riding trials on camel 1 (normal speed). The normalized cycle for walking was the average over subject 1's walking trials (normal speed).

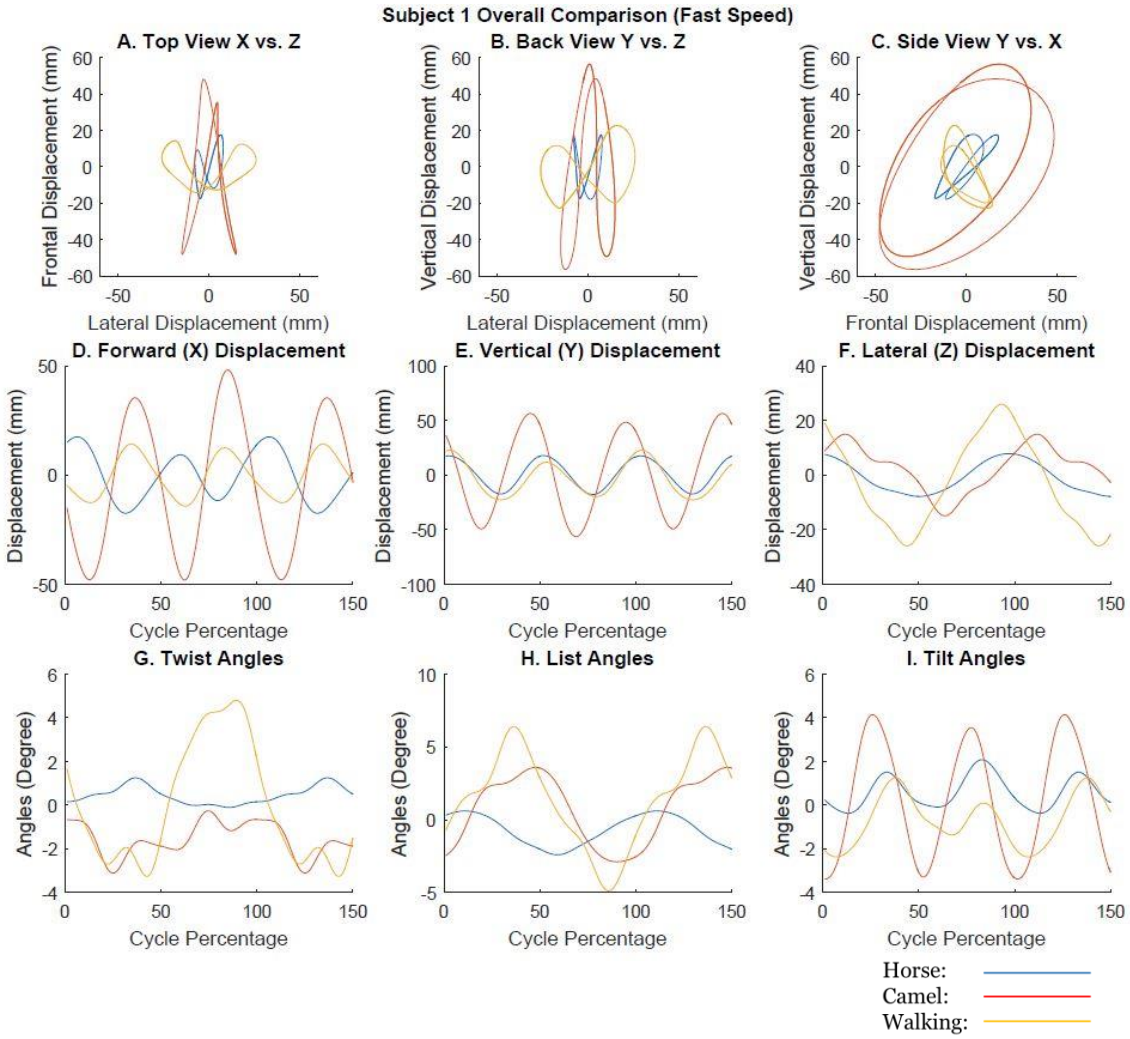


Figure A.26: Pelvic spatial views (A,B,C), pelvic displacements versus gait-period normalized time (D,E,F), and pelvic angles versus gait-period normalized time (G,H,I) when subject 1 was riding horses, camel and walking. The normalized cycle for horse riding was the average over subject 1's riding trials on all horses (saddle 1, fast speed). The normalized cycle for camel riding was the average over subject 1's riding trials on camel 1 (fast speed). The normalized cycle for walking was the average over subject 1's walking trials (fast speed).

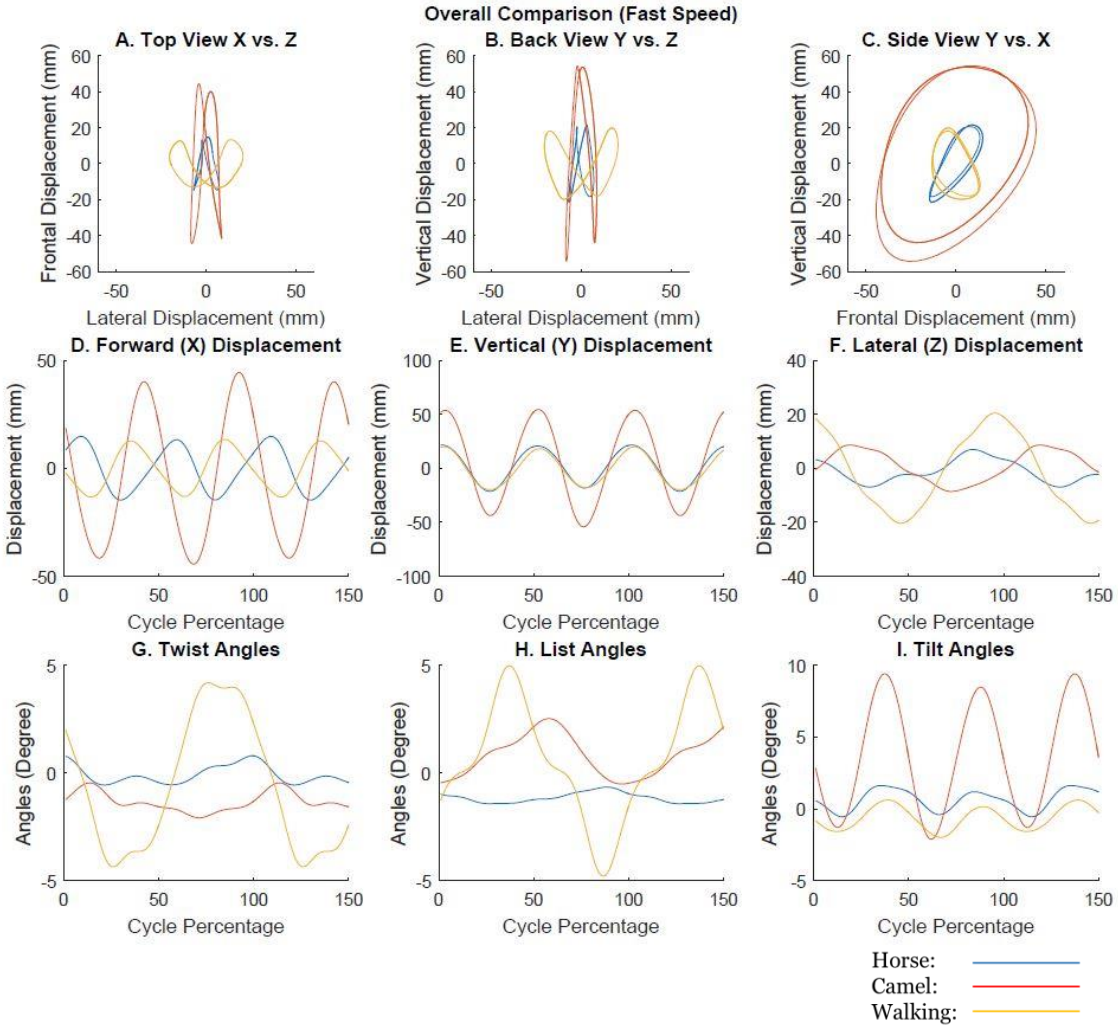


Figure A.27: Pelvic spatial views (A,B,C), pelvic displacements versus gait-period normalized time (D,E,F), and pelvic angles versus gait-period normalized time (G,H,I) when subjects were riding horses, camel and walking. The normalized cycle for horse riding was the average over all subjects' riding trials on all horses (saddle 1, fast speed). The normalized cycle for camel riding was the average over all subjects' riding trials on camel 1 (fast speed). The normalized cycle for walking was the average over all subjects' walking trials (fast speed).

# BIBLIOGRAPHY


[1] Gruss, L., and Schmitt, D., 2015, "The evolution of the human pelvis: changing adaptations to bipedalism, obstetrics and thermoregulation," Philosophical Transactions of the Royal Society B: Biological Sciences, 370(1663), p. 20140063.

[2] White, T., Black, M., and Folkens, P., 2012, Human osteology, Academic Press, San Diego, Calif.

[3] "Pelvic Fractures - OrthoInfo," American Academy of Orthopaedic Surgeons, last modified February, 2016, accessed March 20, 2020, https://orthoinfo.aaos.org/en/diseases--conditions/pelvic-fractures.

[4] Seeley, R., 2011, Seeley's anatomy & physiology, McGraw-Hill, New York, NY, pp. 230-231.

[5] Hamacher, D., Bertram, D., Fölsch, C., and Schega, L., 2012, "Evaluation of a visual feedback system in gait retraining: A pilot study," Gait & Posture, 36(2), pp. 182-186.

[6] "Gluteal Muscles : Attachment, Nerve Supply & Action," Anatomy Info, accessed March 20, 2020, https://anatomyinfo.com/gluteal-muscles.

[7] Lewis, C., Laudicina, N., Khuu, A., and Loverro, K., 2017, "The Human Pelvis: Variation in Structure and Function During Gait," The Anatomical Record, 300(4), pp. 633-642.

[8] Lovejoy, C., 2005, "The natural history of human gait and posture," Gait & Posture, 21(1), pp. 95-112.

[9] Bruening, D., Frimenko, R., Goodyear, C., Bowden, D., and Fullenkamp, A., 2015, "Sex differences in whole body gait kinematics at preferred speeds," Gait & Posture, 41(2), pp. 540-545.

[10] Bejek, Z., Paróczai, R., Illyés, Á., and Kiss, R., 2005, "The influence of walking speed on gait parameters in healthy people and in patients with osteoarthritis," Knee Surgery, Sports Traumatology, Arthroscopy, 14(7), pp. 612-622.

[11] Levangie, P., Norkin, C., and Lewek, M., 2011, Joint structure and function: A comprehensive analysis., F.A. Davis Company, Philadelphia, PA.

[12] Uyar, E., Baser, O., Baci, R. and Özçivici, E., 2009, “Investigation of bipedal human gait dynamics and knee motion control,” Izmir, Turkey: Dokuz Eylül University-Faculty of Engineering Department of Mechanical Engineering.

[13] Perry, J., k, S., and Davids, J., 1992, "Gait Analysis," Journal of Pediatric Orthopaedics, 12(6), p. 815.

[14] “Understanding Phases of the Gait Cycle”, Protokinetics Team, last modified November 28, 2018, accessed March 20, 2020, https://www.protokinetics.com/2018/11/28/understanding-phases-of-the-gait-cycle.

[15] Winiarski, S., Pietraszewska, J., and Pietraszewski, B., 2019, "Three-Dimensional Human Gait Pattern: Reference Data for Young, Active Women Walking with Low, Preferred, and High Speeds," BioMed Research International, 2019, pp. 1-7.

[16] Wilken, J., Rodriguez, K., Brawner, M., and Darter, B., 2012, "Reliability and minimal detectible change values for gait kinematics and kinetics in healthy adults," Gait & Posture, 35(2), pp. 301-307.

[17] Verghese, J., Ambrose, A., Lipton, R., and Wang, C., 2009, "Neurological gait abnormalities and risk of falls in older adults," Journal of Neurology, 257(3), pp. 392-398.

[18] Kindregan, D., Gallagher, L., and Gormley, J., 2015, "Gait Deviations in Children with Autism Spectrum Disorders: A Review," Autism Research and Treatment, 2015, pp. 1-8.

[19] Vilensky, J., 1981, "Gait Disturbances in Patients With Autistic Behavior," Archives of Neurology, 38(10), p. 646.

[20] Calhoun, M., Longworth, M., and Chester, V., 2011, "Gait patterns in children with autism," Clinical Biomechanics, 26(2), pp. 200-206.

[21] Mauritz, K., 2002, "Gait training in hemiplegia," European Journal of Neurology, 9(s1), pp. 23-29.

[22] Pennycott, A., Wyss, D., Vallery, H., Klamroth-Marganska, V., and Riener, R., 2012, "Towards more effective robotic gait training for stroke rehabilitation: a review," Journal of NeuroEngineering and Rehabilitation, 9(1), p. 65.

[23] Veličković, T.D. and Perat, M.V., 2005, “Basic principles of the neurodevelopmental treatment,” Medicina, 41, pp. 112-120.

[24] Jezernik, S., Colombo, G., Keller, T., Frueh, H., and Morari, M., 2003, "Robotic Orthosis Lokomat: A Rehabilitation and Research Tool," Neuromodulation: Technology at the Neural Interface, 6(2), pp. 108-115, doi: 108-115. 10.1046/j.1525-1403.2003.03017.x.

[25] Lane, K. W., 2007, "Hippotherapy and the Significance of Complementary Medicine: A QA with William Benda, M.D., FACEP, FAAEM," Alternative & Complementary Therapies, pp. 266-268.

[26] Uchiyama, H., Ohtani, N., and Ohta, M., 2011, "Three-dimensional analysis of horse and human gaits in therapeutic riding," Applied Animal Behaviour Science, 135(4), pp. 271-276, doi: 10.1016/j.applanim.2011.10.024.

[27] Garner, B., and Rigby, B., 2015, "Human pelvis motions when walking and when riding a therapeutic horse," Human Movement Science, 39, pp. 121-137, doi: 10.1016/j.humov.2014.06.011.

[28] Benda, W., McGibbon, N., and Grant, K., 2003, "Improvements in Muscle Symmetry in Children with Cerebral Palsy After Equine-Assisted Therapy (Hippotherapy)," The Journal of Alternative and Complementary Medicine, 9(6), pp. 817-825, doi: 10.1089/107555303771952163.

[29] Beinotti, F., Correia, N., Christofoletti, G., and Borges, G., 2010, "Use of hippotherapy in gait training for hemiparetic post-stroke," Arquivos de Neuro-Psiquiatria, 68(6), pp. 908-913, doi: 10.1590/s0004-282x2010000600015.

[30] Debuse, D., Gibb, C., and Chandler, C., 2009, "Effects of Hippotherapy on People with Cerebral Palsy from the Users' Perspective: A Qualitative Study," Physiotherapy Theory and Practice, 25(3), pp. 174-192.

[31] Govender, P., Barlow, C., and Ballim, S., 2016, "Hippotherapy in occupational therapy practice," South African Journal of Occupational Therapy, 46(2).

[32] Copeland-Fitzpatrick, J., 1997, "Hippotherapy and Therapeutic Riding: An International Review," Proceedings of the Ninth International Therapeutic Riding Congress, pp. 1-15.

[33] Benoit, H., 2011, “Designing, Constructing, and Testing a Second-Generation Prototype Mechanical Hippotherapy Horse,” Master’s Thesis, Baylor University, Waco, TX.

[34] “Hippotherapy”, Carlisle Academy Integrative Equine Therapy & Sports, accessed March 20, 2020, http://carlisleacademymaine.com/therapy-services/hippotherapy.

[35] Fleck, C., 1992, “Hippotherapy: Mechanics of human walking and horseback riding,”, Rehabilitation with the aid of the horse: A collection of studies. B. Engel, and J. Benjamin, eds., Barbara Engle Therapy Services, Durango, Colorado, pp. 153–176.

[36] Faye, B., 2014, “The camel today: assets and potentials,” Anthropozoologica, 49(2), pp.167-176.

[37] Yam, B.A.Z. and Khomeiri, M., 2015, “Introduction to Camel origin, history, raising, characteristics, and wool, hair and skin: A Review,” Research Journal of Agriculture and Environmental Management, 4(11), pp.496-508.

[38] Janis, C. M., Theodor, J. M., Biosvert, B. 2002, “Locomotor evaluation in camels revisited: A quantitative analysis of pedal anatomy and the acquisition of the pacing gait,” J. Vert. Paleontol. 22(1): 110-121.

[39] Abdo, M., Haddad, S.S., Aziz, E.K., Abdeen, A. and Sabek, A., 2019, “Kinematics Biomechanical Analysis and Three Dimensional Reconstruction Diagnostic Technique of Carpal Joint during gait in One-Humped Camel (Camelus dromedarius),” Alexandria Journal for Veterinary Sciences, 60(2).

[40] Li, J., Qiu, X., Wang, Z., and Xu, P., 1993, “Experiment and Analysis of the Camel Gait,” Transactions of The Chinese Society of Agricultural Engineering, 9(3).

[41] Xu, P., Zhuang, J., and Wang, Z., 1993, “Experiment and Analysis of Camel Locomotion Characteristics on Slope,” Transactions of The Chinese Society of Agricultural Engineering, 9(4), p.2.

[42] Zhuang, J., Qiu, J., Wang, Z., Xu, P., and Luo J., 1991. “Primary Study on the Ability for Camel to Travel on Sand,” Transactions of The Chinese Society of Agricultural Engineering, 7(1).

[43] Larsson, M., and Brothers, D., 2019, “Camels in animal-assisted interventions – survey of practical experiences with children, youth and adults,” Proceedings of the International Society of Applied Ethology, Bergen, Norway, August, 2019.

[44] “About Us,” Oasis Camel Dairy, accessed February 1, 2020, https://cameldairy.com/about.

[45] van der Kruk, E., and Reijne, M., 2018, "Accuracy of human motion capture systems for sport applications; state-of-the-art review," European Journal of Sport Science, 18(6), pp. 806-819, doi:10.1080/17461391.2018.1463397.

[46] Williams, S., Schmidt, R., Disselhorst-Klug, C., and Rau, G., 2006, "An upper body model for the kinematical analysis of the joint chain of the human arm," Journal of Biomechanics, 39(13), pp. 2419-2429, http://dx.doi.org/10.1016/j.jbiomech.2005.07.023.

[47] Ziegler, J., Gatteringer, H., Reiter, A., Hormandinger, P., Muller, A., and Mitterhumer, M., 2018, "Generating realistic trajectories for robotic hippotherapy from 3D captured horseback motion," Processings of the 5th Joint International Conference on Multibody System Dynamics, Lisbon, Portugal, June 24-28, 2018.

[48] Cooper, C., "Team Toping How To – Heeler," The Team Roping Journal, last modified August 18, 2017, accessed September 11, 2019, https://teamropingjournal.com/news/team-roping-how-heeler.

[49] Starnes, K., 2011, Team Roping 101: The Complete Sport from Header to Heeler, Trafalgar Square Books, North Pomfret, Vermont.

[50] Ferguson, C., Greathouse, A., Pousson, B., Comeaux, K., and Browning, J., 2013, "The effect of transporting, scoring and roping on cortisol concentrations in acclimated roping calves," Journal of Applied Animal Research, 41(1), pp. 8-13.

[51] Moro, L., Spröwitz, A., Tuleu, A., Vespignani, M., Tsagarakis, N., Ijspeert, A., and Caldwell, D., 2013, "Horse-Like Walking, Trotting, and Galloping Derived from Kinematic Motion Primitives (kMPs) and Their Application to Walk/trot Transitions in a Compliant Quadruped Robot," Biol Cybern, 107(3), pp. 309-320.

[52] Byström, A., Roepstorff, L., Rhodin, M., Serra Bragança, F., Engell, M., Hernlund, E., Persson-Sjödin, E., van Weeren, R., Weishaupt, M., and Egenvall, A., 2018, "Lateral movement of the saddle relative to the equine spine in rising and sitting trot on a treadmill," PLOS ONE, 13(7), p. e0200534.

[53] Roberson, P., 2007, "Validation of a Three Dimensional Motion Capture System for Use in Identifying Characteristics of the Running Walk," Master's Thesis, University of Tennessee, Knoxville, Knoxville, TN.

[54] Harrison, S., Whitton, R., Kawcak, C., Stover, S., and Pandy, M., 2010, "Relationship between muscle forces, joint loading and utilization of elastic strain energy in equine locomotion," Journal of Experimental Biology, 213(23), pp. 3998-4009.

[55] Torres-Pérez, Y., Gómez-Pachón, E.Y. and Cuenca-Jiménez, F., "Horse's gait motion analysis system based on videometry," Ciencia Y Agricultura, 13(2), pp. 83-94.

[56] Kreyszig, E., 2011, Advanced Engineering Mathematics, John Wiley and Sons, Hoboken, NJ.

[57] "Plug-in Gait Reference Guide," Vicon Documentation, last modified August 10, 2017, accessed January 20, 2020, https://www.vicon.com/downloads/documentation/plug-in-gait-product-guide.

[58] BYSTRÖM, A., RHODIN, M., Von PEINEN, K., WEISHAUPT, M., and ROEPSTORFF, L., 2010, "Kinematics of saddle and rider in high-level dressage horses performing collected walk on a treadmill," Equine Veterinary Journal, 42(4), pp. 340-345.

[59] Clayton, H., 2016, "HORSE SPECIES SYMPOSIUM: Biomechanics of the exercising horse1," Journal of Animal Science, 94(10), pp. 4076-4086.

[60] Back, W., MacAllister, C., van Heel, M., Pollmeier, M., and Hanson, P., 2007, "Vertical Frontlimb Ground Reaction Forces of Sound and Lame Warmbloods Differ From Those in Quarter Horses," Journal of Equine Veterinary Science, 27(3), pp. 123-129.

[61] Robilliard, J., Pfau, T., and Wilson, A., 2007, "Gait characterisation and classification in horses," Journal of Experimental Biology, 210(2), pp. 187-197.